A REMOTE MAGNETOELASTIC SENSOR WITH ANTIBODY AS A PROBE TO

DETECT SALMONELLA TYPHIMURIUM

Except where reference is made to the work of others, the work described in this
dissertation is my own or was done in collaboration with my advisory
committee. This dissertation does not include proprietary, restricted
or classified information.

_____
Rajesh Guntupalli

Certificate of Approval:

_____
Zhong Yang Cheng
Assistant Professor
Materials Engineering

_____
Bryan A. Chin, Chair
Professor
Materials Engineering

_____
Jong Wook Hong
Assistant Professor
Materials Engineering

_____
Dong-Joo Kim
Assistant Professor
Materials Engineering

_____
Tung-shi Huang
Assistant Professor
Nutrition and Food Sciences

_____
George T. Flowers
Interim Dean
Graduate School

A REMOTE MAGNETOELASTIC SENSOR WITH ANTIBODY AS A PROBE TO

DETECT SALMONELLA TYPHIMURIUM

Rajesh Guntupalli

A Dissertation

Submitted to

the Graduate Faculty of

Auburn University

in Partial Fulfillment of the

Requirements for the

Degree of

Doctor of Philosophy

Auburn University, Alabama
May 10, 2007

A REMOTE MAGNETOELASTIC SENSOR WITH ANTIBODY AS A PROBE TO

DETECT SALMONELLA TYPHIMURIUM

Rajesh Guntupalli

_____
Signature of Author

_____
Date of Graduation

VITA

Rajesh Guntupalli, son of Ramaswamy and Vijaya Lakshmi Guntupalli, was born on August 30th, 1978 in Gottipadu, India. He graduated from BVSR High School, Ongole, India in March 1994 and Intermediate school from Vikas Junior College, Guntur in March 1996. He joined Nagarjuna University, Guntur, India in August 1997 and graduated with a Bachelor of Technology in Mechanical Engineering in May 2001. He entered doctoral program in Materials Engineering at Auburn University in January 2002.

DISSERTATION ABSTRACT

A REMOTE MAGNETOELASTIC SENSOR WITH ANTIBODIES AS A PROBE TO

DETECT SALMONELLA TYPHIMURIUM

Rajesh Guntupalli

Doctor of Philosophy, May 10, 2007
(B. Tech, Nagarjuna University, 2001)

161 Typed pages

Directed by Bryan A. Chin

Every year millions of people around the globe suffer from foodborne illnesses as a result of the ingestion of food products contaminated with pathogens. Foodborne illnesses not only result in suffering and permanent injury but also loss of productivity due to hospitalization. Traditional methods such as enzyme linked immunosorbent assay (ELISA) and fluorescence methods are widely used in bacterial detection. However these methods are time consuming, expensive and require trained personnel. Hence, it is desirable to develop real-time detection devices that can be used for the identification of contaminated food products.

This study presents the results of an investigation designed to develop a real time wireless biosensor for the detection of *Salmonella typhimurium*, the bacterial species responsible for *Salmonellosis*. This new biosensor technology consists of a wireless, magnetoelastic transducer and an immobilized species specific antibody monolayer. A

time varying magnetic field was then used to actuate the platform into mechanical resonance and a pickup coil used to measure the resulting resonance frequency. The characteristic resonance frequency of a magnetoelastic sensor is inversely proportional to its length and mass, so the capture of the target organism onto the surface of the sensor causes a mass increase and, hence, a decrease in the fundamental resonance frequency of the magnetoelastic sensor. Different sizes of sensor strips were used in the study, so as to study the effect of size on the sensitivity of the biosensor. The sensor response was studied in liquid media (water, milk and apple juice) containing graded concentrations of *S. typhimurium*. The dissociation constant, (K_d) and binding valencies were calculated using a Hill Plot. Binding assays of tests conducted in water showed a K_d values of 435± 76 cfu/ml with a binding valency of 2.3 ± 0.02 in a 2×0.4mm dimension sensor, where fat free milk and apple juice samples showed K_d's of 1389 ± 142 and 310 ± 101 cfu/ml, respectively. The binding valency for fat free milk was found to be 1.9 ± 0.03 and that for apple juice was 2.3 ± 0.02. These similar values of both K_d and the binding valency clearly suggest consistent performance of the sensors even in the presence of different surrounding media. Confirmation of bacterial binding to the sensor antibody was achieved through Scanning Electron Microscopy (SEM) studies of the sensor samples.

Style manual or journal used   Sensors and Actuators B

Computer software used   Microsoft Office XP and Microcal Origin 6.0

ACKNOWLEDGEMENTS

I would like to express my sincere gratitude to Dr. Bryan A. Chin for his expert guidance, support and persistent encouragement throughout my study period. It is a privilege to work under Dr. Chin with his extensive knowledge and genuine concern for his students. I would like to emphasize that his influence on me was not only in acquiring scientific knowledge but also as a person.

I received utmost support from my committee members Dr. Z-Y. Cheng, Dr. T. S. Huang, Dr. Jong Wook Hong and Dr. Dong-Joo Kim and thank them whole heartedly. I owe my deepest gratitude to Dr. Vitaly Vodyanoy for providing me with training and use of equipments. I would also like to express my thanks and appreciation to Dr. William C. Neely, for his thoughtful questions and suggestions at my defense.

Special mention goes to Ramji, Ben, Hu, L. C. Mathison, Helen, Mike and Anna. I would like to thank my friends (Viswaprakash, Rajeev, Nanda, Atresh and Shakib) for their constant motivation and valuable discussions. My sincere appreciation and thanks are due to Dr. Nilmini, whose suggestions and timely help have made a difference.

Finally, the author would like to dedicate this dissertation to his parents (Mrs. Vijaya Lakshmi and Mr. Ramaswami) and brothers (Mr. G. L. N. Prasad and Krishna) without their love and blessings, it would not have been possible to learn many things in science as well as in general aspects of life and throughout my life. I am grateful to god for giving me all the opportunities in professional and personal life.

TABLE OF CONTENTS

LIST OF TABLES

LIST OF FIGURES

1 INTRODUCTION

1.1 Introduction to biosensors

The ever increasing need for simple, rapid and continuous *in situ* monitoring methods for a broad range of areas has led to the growing popularity of biosensors in recent years. Biosensors may be regarded as a modern alternative to conventional detection techniques due to their high degree of sensitivity, selectivity and versatility for field deployment. A biosensor such as the one shown in Figure. 1-1 is defined as a self-contained, integrated device capable of providing quantitative or semi-quantitative analytical information; that includes a biological sensing element in direct contact with a transducer [1]. The biological recognition elements play a crucial role in determining the sensitivity and selectivity of the detection technique. The detection of the analyte by the receptor is by way of a specific interaction that generates a chemical or physical perturbation. These perturbations can be converted into a measurable effect, for example a shift in the frequency (piezoelectric/magnetoelastic sensors) or refractive index (surface plasmon resonance/fiber optic sensors). Because of their technical and economical advantages, such as faster response time, reduced sample preparation times, ease of operation, lower instrumentation and transportation costs, biosensors are now being used in a wide variety of fields such as food industries, toxic gas environments,

detection of liquid contamination, clinical diagnostics, agriculture and also in the fight against bio terrorism [2-8].
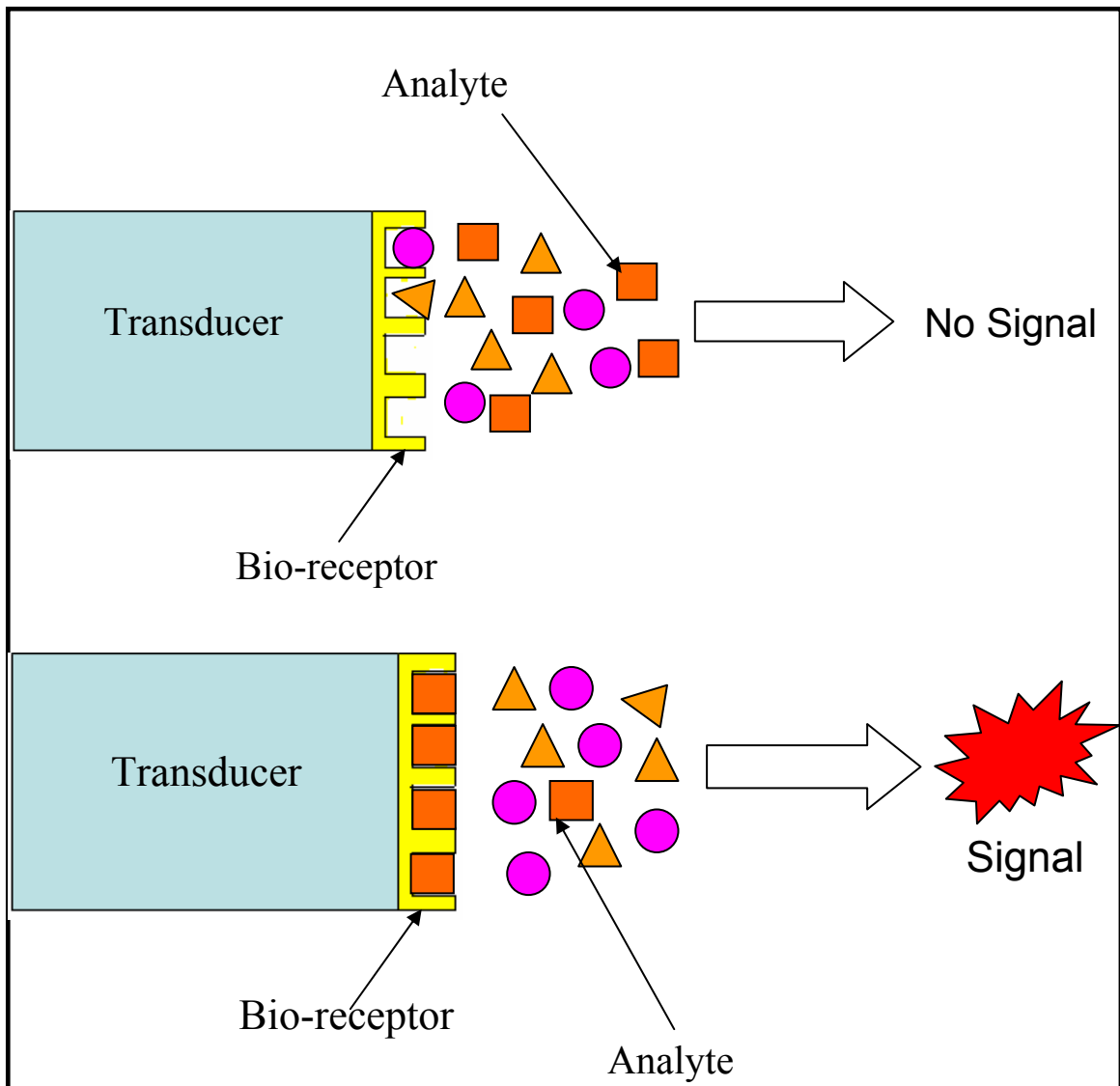
Figure 1-1: Biosensor structure

1.2   The Bio-recognition Element

In the current study antibodies were used as the bio-recognition element. The vertebrate immune system has evolved several ways to protect the organism from invasions of foreign bodies and infections by bacteria, viruses or other micro-organisms, all of which may be referred to as "antigens". The two main responses of the immune system to the presence of a foreign organism are the cellular immune response and the humoral immune response. Antibodies belong to the immunoglobulin proteins (Igs). Five main types of immunoglobulins are produced by mammals, namely IgA, IgD, IgE, IgG and IgM. Of the five types, IgG represents approximately 75% of the Igs in blood plasma [9]. IgG is the smallest antibody of its class with a molecular weight of 150 kDa and is the easiest to produce and extract from blood serum. The stability of antibodies along with their solubility in aqueous solutions and their high tolerance to a wide range of pH concentrations, make them the ideal candidate for the biological sensing element in biosensors. They denature reversibly and hence are easy to isolate and purify. The presence of several different chemical groups on the antibody surface also makes it relatively easy to functionalize them with markers such as enzymes, fluorescent dyes or radioactive labels [10].
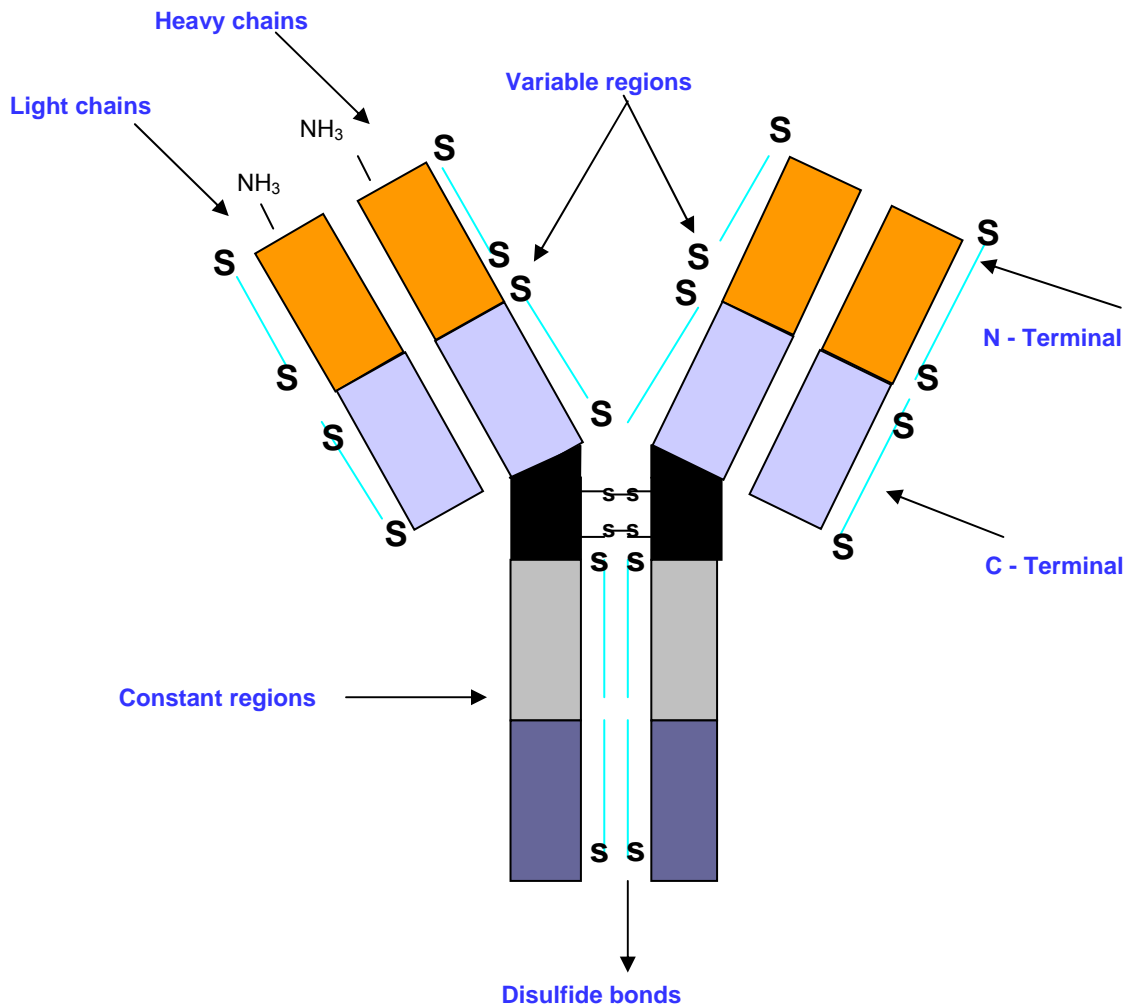
Figure 1-2: Antibody structure

IgGs are chiefly composed of four chains of polypeptides, which in turn consist of
two identical light (L) chains and heavy (H) chains that are linked together by disulfide
bonds (S), hydrogen bonds, salt bridges and Vander Waals forces. Each L chain consists
of 220 amino acids and each H chain consists of 440 amino acids. The four chains are

further divided into variable and constant regions. The constant chains CH1 and CH2 are linked through a hinge, which is mainly responsible for the flexible nature of the antibody structure. The variable regions of the heavy chains and the light chains comprise the binding sites of the antibody, although technically only parts of the variable regions actually bind to the antigen. The "Complementary Determining Regions" (CDRs 1, 2 and 3) are also known as the hyper-variable regions. The term "paratope" refers to the group of amino acids on the antibody that are crucial for binding to the antigen, and there is a complementary region on the antigen called the "epitope". Antibodies have been in use as probes for some time in biosensor technologies [11, 12] and prior research performed at the Auburn University's Detection and Food Safety (AUDFS) has successfully demonstrated the effectiveness of antibody-antigen based acoustic wave devices for the detection of foodborne pathogens [13, 14].

1.3   Introduction to Food Borne Pathogens

Currently, there are more than 250 known food borne diseases caused by pathogenic microorganisms such as viruses, bacteria and fungi [15]. Foodborne diseases result from the ingestion of the contaminated food products such as ready-to-eat (RTE), unprocessed or under processed food products and beverages.

Although there are several possible sources of food contaminations, including poisonous chemicals, heavy metals, fungi, viruses and bacteria, the major causative agents are bacteria. Table1-1 gives information about the major sources of contamination, the agents responsible for the contamination of food products and the resulting diseases. Figure1-3 summarizes the number of foodborne disease cases per 100,000 population in 2005 for 10 states (Connecticut, Georgia, Maryland, Minnesota,

New Mexico, Oregon, Tennessee, California, Colorado, and New York) in the United States.

Table 1-1: Major sources of contamination, agents responsible for contamination of food products and resulting diseases [16].

Bacterial Species	Infected area	Sources of contamination	Symptoms of illness
Salmonella	Intestinal tracts of animals and humans.	Meat, poultry, fish and eggs.	Diarrhea, nausea, chills, vomiting and fever.
Staphylococcus aureus	Nose, throat, skin and open wounds.	Meat and seafood salads, sandwich spreads and high salt foods.	Nausea, vomiting and diarrhea. No fever.
Listeria monocytogenes	Intestinal tracts	Milk, soft cheeses, vegetables.	Mimics meningitis.
Enteropathogenic E. coli	Feces of infected humans.	Meat and cheeses.	Diarrhea, abdominal cramps, no fever.
Clostridium perfringens	Gastrointestinal tracts of animals and humans.	Meat and poultry dishes, sauces and gravies.	Cramps and diarrhea. Usually no vomiting or fever.
Campylobacter jejuni	Animal reservoirs and foods of animal origin.	Meat, poultry, milk, and mushrooms.	Diarrhea, abdominal cramps and nausea.
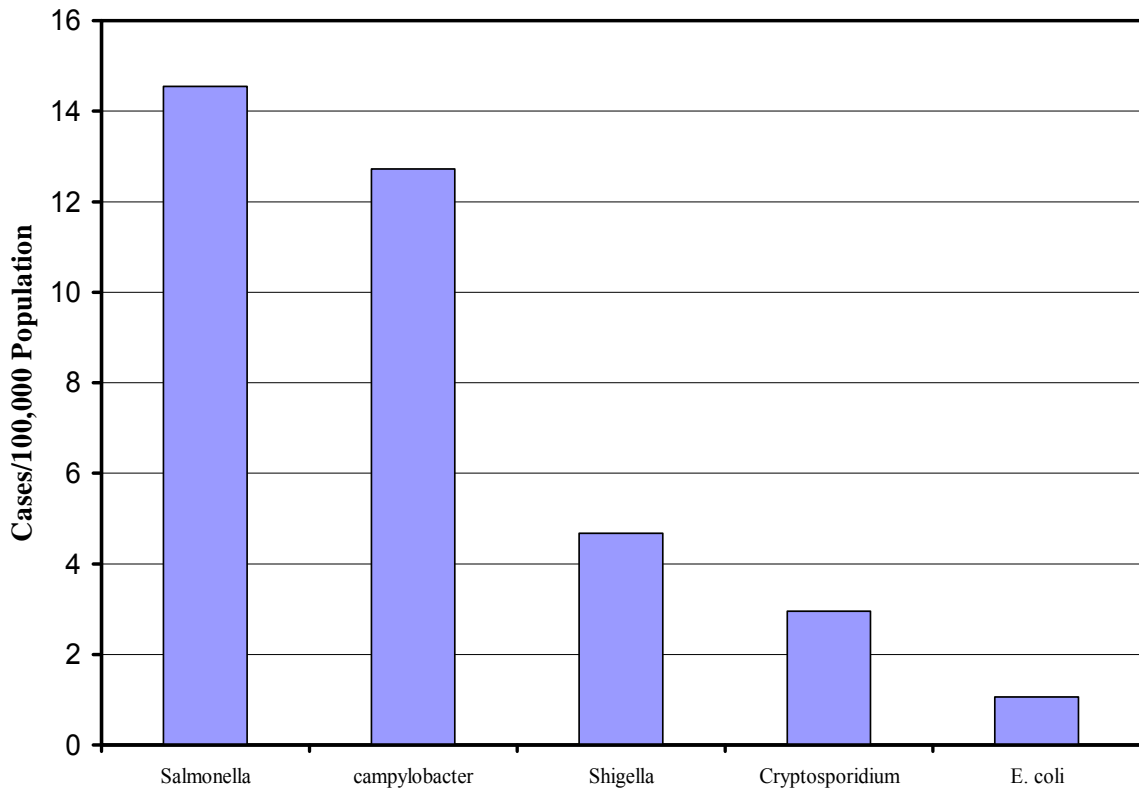
Figure 1-3: Number of foodborne disease cases per 100,000 population in 2005 for 10 states (Connecticut, Georgia, Maryland, Minnesota, New Mexico, Oregon, Tennessee, California, Colorado, and New York) in the United States of America [17].

1.3.1 Salmonella typhimurium

The first strain of *Salmonella* was reported in 1884 by T. Smith and Daniel E. Salmon [18], who dubbed it *Salmonella cholerasius*. Since then, more than 2000 distinct types of *salmonella* species have been discovered [19]. The *salmonella* species most commonly found in the United States are *Salmonella enteridis* and *Salmonella typhimurium*. This research focused on the detection of *Salmonella typhimurium*, the primary source of *Salmonellosis*. *S. typhimurium* is a rod-shaped, gram-negative enterobacteria that affects the abdomen, causing infection, diarrhea and pain [19] .

This research was designed to develop a new sensor technology that would be capable of capturing and detecting the presence of *S. typhimurium* in poultry products with a high specificity and sensitivity. There are several existing sensor technologies for the detection of *S. typhimurium* [20-23], of which the most commonly used are technologies based on piezoelectric or optical methods. These techniques, however, are either expensive or complicated and time-consuming. Thus, an ideal sensor platform would be fast, reliable, inexpensive, simple to use and, most importantly, be capable of making accurate measurements in liquid media.
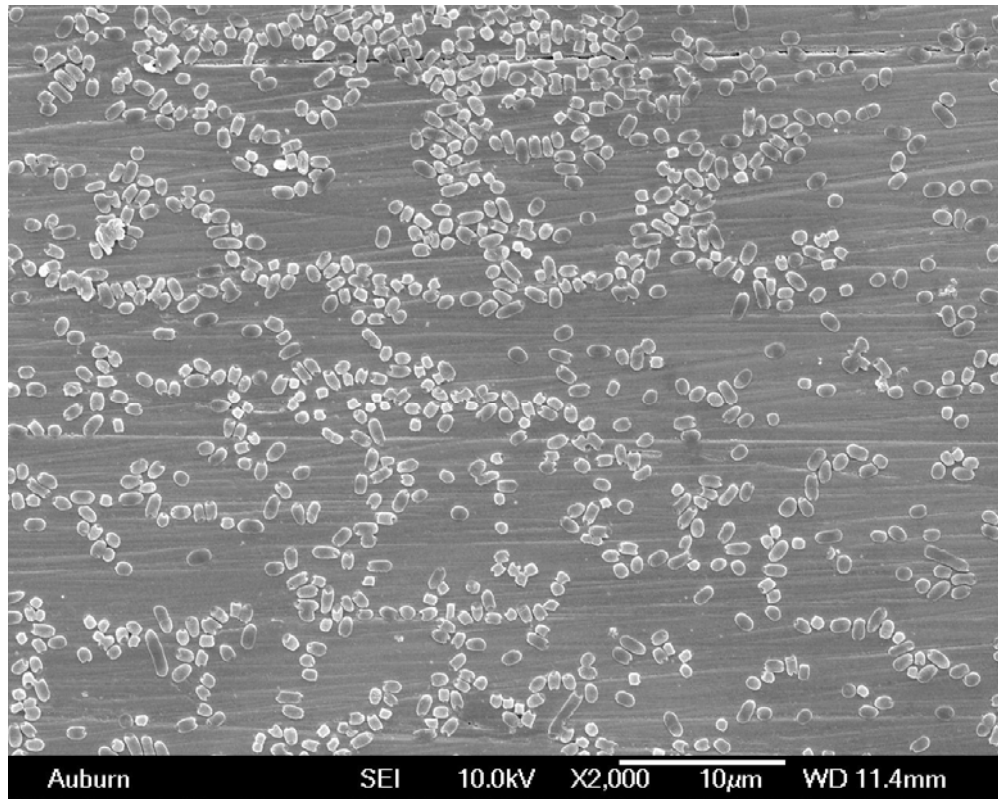
Figure 1-4: Scanning Electron Micrograph of *S. typhimurium* cells.

1.4 Transduction Element

Most conventional biosensor systems are unable to function in sealed environments. Hence, there is a need for an inexpensive and sensitive sensor platform that can operate in such conditions. This research established a new application of magnetoelastic materials as a biosensor platform for the detection of *S. typhimurium* that is capable of resolving many of the problems experienced with existing biosensor technologies. Magnetostriction is a property of soft amorphous ferromagnetic materials that undergo a shape change in the presence of a magnetic field; the magnetic energy of the material is converted into mechanical energy in the form of a change in the shape.

When a magnetoelastic material is subjected to a magnetic field, the magnetic domains in the material tend to align, causing a shape change in that material. In a time varying magnetic field, the resulting shape changes in the material can produce oscillations along its length. Applying a magnetic field actuates the sensor and the response can be detected using a non-contact pick-up coil. The response of the magnetoelastic sensor can then be converted into a frequency. Each sensor has a natural resonance frequency that is inversely proportional to its length and this natural resonance frequency shifts to a lower value as a result of any mass loading on the sensor. These frequency shifts can be measured remotely and related to the mass of the analyte attached. Because of this unique advantage, numerous magnetoelastic materials applications have been proposed, including the detection of pH, humidity, temperature, viscosity, and stress etc. [24-26]. A biosensor can be produced by coupling a suitable bioprobe to a magnetoelastic sensor platform.
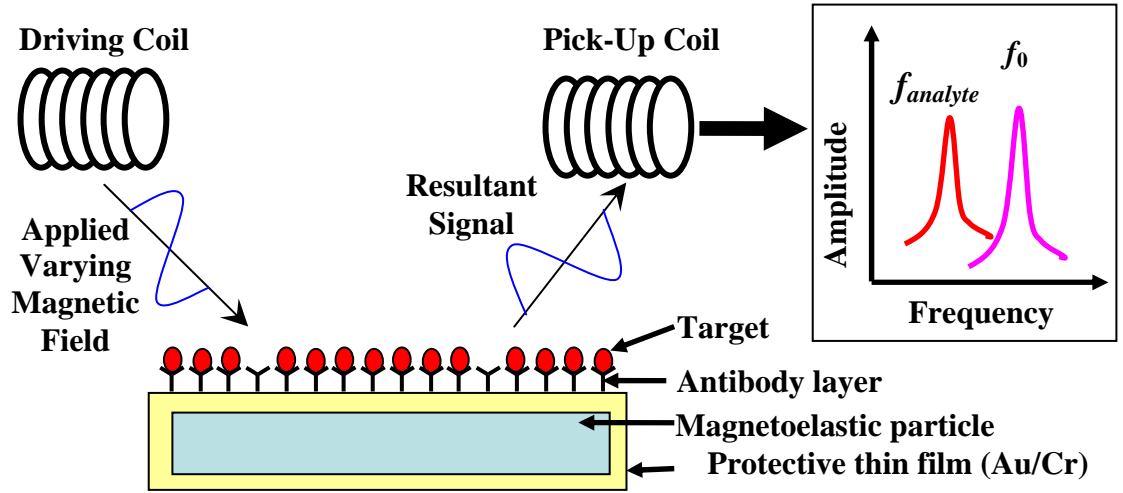
Figure 1-5: Schematic drawing illustrating the wireless nature of magnetoelastic biosensors and the basic principle for detecting bacterial cells. The fundamental resonance frequency of the biosensor is f_0 without cell binding. Upon binding of cells the resonance frequency decreases to $f_{analyte}$ due to the increased mass of cells bound to the antibody that has been immobilized on the sensor surface.

Magnetoelastic material oscillates along its length in the presence of a varying magnetic field. These oscillations along the y- direction can be represented as [27]:

$$\rho_s \frac{\partial u_y}{\partial t^2} = \frac{E}{2(1-\sigma^2)} \frac{\partial u_y}{\partial y^2} \tag{1-1}$$

The solution to this first order differential equation yields the resonance frequency as

$$f_n = \sqrt{\frac{E}{\rho(1-\sigma^2)}} \cdot \frac{n}{2L} \tag{1-2}$$

Where,

f_n – Resonance frequency of the sensor, ρ – Density of the sensor material,

11

E – Elastic modulus of the sensor, σ – Poisson's ratio, L – Length of the sensor,

n - Mode of oscillation.

The above equation is for the nth mode of oscillation. Substituting n=1 gives the relation

for the fundamental resonance frequency:

$$f_0 = \sqrt{\frac{E}{\rho(1-\sigma^2)}} \cdot \frac{1}{2L} \qquad (1\text{-}3)$$

In equation (1-3), if E, σ, L, are constants then

$$\Rightarrow f_0 \alpha \sqrt{\frac{1}{M}} \qquad (1\text{-}4)$$

From the above equation it is evident that the frequency is inversely proportional

to the square root of the mass.

$$\Rightarrow \frac{\Delta f}{\Delta m} = -\frac{f_o}{2M} \qquad \text{(Here, Δm<<<M)} \qquad (1\text{-}5)$$

Where, M – Mass of the sensor, Δm – mass attached on the sensor surface, Δf – change in

resonance frequency.

The above equation (1-5) gives the relationship between the mass that is

uniformly attached on the sensor surface and the resulting shift in the resonance

frequency of the magnetoelastic sensor.

1.5   Research Objectives

The primary objective of this research was to develop a robust and inexpensive biosensor technology for the detection of bacterial pathogens by using magnetoelastic particles. The antibody against *S. typhimurium* was used as the probe to investigate the capabilities of the methodology.   This new sensor technology could be used in place of existing technologies like ELISA [28] and other sensor technologies such as surface acoustic wave devices [13] or fiber optic sensors [21].

To achieve the main objective, this research was subdivided into three sections.

1. Fabrication of micro sensors with magnetoelastic material

In the development of sensor technology, fabrication plays a major role. In order to achieve good corrosion resistance and suitable sensor surface for antibody immobilization magnetoelastic sensors were diced and sputtered with thin layers of protective films. In this research METGLAS® 2826MB alloy was used as the sensor platform.

2. Characterization of the bio-recognition element

(i) Immobilization of bio-recognition element

In order to build an effective biosensor, it is desirable to have an effective technique for probe immobilization. The probe (antibody) immobilization technique should be both reliable and reproducible. In this study the application of a Langmuir – Blodgett (LB) technique for the immobilization of antibody monolayers was established.

(ii) Specificity

Immobilized bioprobe should be specific towards the analyte (*Salmonella typhimurium*). To investigate the specificity characteristics, biosensor was exposed to *Salmonella* species and other antigens such as *Listeria monocytogenes* and *E. coli*. Measurement of the bound bacterial cell densities on the sensor surface provided information on the specificity of the antibodies towards *Salmonella typhimurium*.

(iii) Longevity

For all practical applications, it is essential to evaluate the effectiveness of biosensor technology in different testing conditions. The current study investigated the stability of polyclonal antibody immobilized magnetoelastic sensor platform at three different temperatures (25, 45 and 65 °C).

3. Study of the probe analyte interactions.

In this study, antibody immobilized magnetoelastic biosensors were exposed to target analytes in different environments. Biosensors were exposed to graded concentrations of the target analyte in static conditions and as well as in the flow through mode. To simulate real world applications, magnetoelastic sensors were exposed to the target analyte in the presence of non specific bacterial species such as *Listeria monocytogenes* and *E. coli*. Magnetoelastic sensors were also tested in food products such as fat free milk and apple juice.
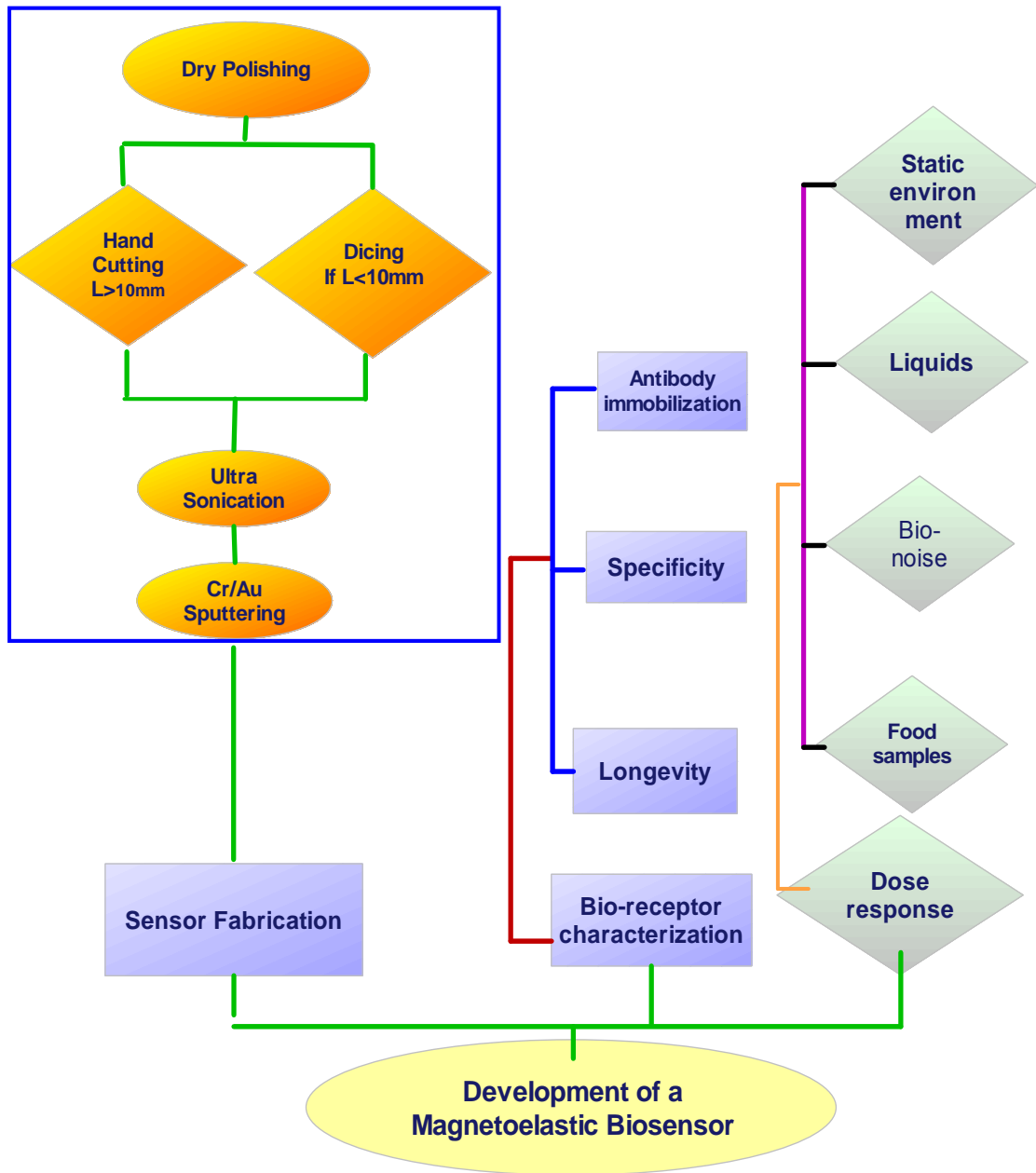
Figure 1-6: Experiment Flow Chart

2 LITERATURE REVIEW

2.1 Background

In the United States alone, human cases of foodborne illnesses are estimated to have an economic impact of about 2-6 billion dollars annually [29]. The estimated cases of human illness due to foodborne microbial pathogens are between 6.5 million to 33 millions annually, and account for up to 9000 deaths. Contamination of animal products such as red meat, poultry, eggs, seafood and dairy products [29] are the most common causes of human related food poisoning. Although more than 250 different foodborne pathogens are present in the environment [30], 91% of foodborne outbreaks were accounted for by bacterial contamination [31, 32]. Pathogens such as *Salmonella sp., Escherichia coli, Listeria monocytogenes, Staphylococcus aureus, Campylobacter jejuni,* and *Bacillus cereus* are reported to be the main sources of bacterial contamination in the food products [33].

Daily consumables including tomatoes, eggs, milk, beef, chicken, orange juice, cheese and other ready–to-eat (RTE) food products such as hot dogs and salami are particularly susceptible to bacterial contamination. There have been reports of illnesses due to bacterial contamination of pasteurized milk [34-36], tomatoes [37], eggs [38, 39], orange juice [40], milk [35, 41-43], chicken [44-47], ground beef [48] and

cheddar cheese [49]. Table 2-1 summarizes the reported cases of illnesses in the United States due to various food contaminations and the respective causative bacterial species. Table 2-2 summarizes the foodborne illnesses caused by the top six bacteria each year and provides information about their infectious doses.

Table 2-1: Salmonella outbreaks in various food products in the USA.

Source	Serover	Number of illnesses	Year	Reference
Tomatoes	*S. braenderup; S. javiana*	561	2004	[37]
Orange Juice	*S. muenchen*	207	1999	[40]
Ground Beef	*S. typhimurium*	31	2004	[48]
Milk	*S. typhimurium, S. Newport*	150, 181	1960-2000	[35, 41-43]
Eggs	*Salmonella. enteritidis*	182,060	2000	[38, 39]
Cheddar Cheese	*S. heidelberg*	25,000	1976	[49]

Table 2-2: Infectious doses for different species [50]

Bacteria	Estimated cases/year	Deaths/year	Infectious Dose (cfu/ml)
Salmonella	3,840,000	4000	10^4 to 10^7
E. coli O 157:H7	725,000	400	10^1 to 10^2
Campylobacter jejuni	4,000,000	511	400 to 10^6
Listeria monocytogenes	1,767	485	400 to 10^3
Staphylococcus aureus	1,513,000	1,210	$> 10^6$
Clostridium perfringens	10,000	100	$> 10^8$

2.2 Traditional Methods for Detecting Bacterial Contamination

Bacterial detection using traditional methods such as Enzyme-linked Immunosorbent Assay (ELISA) is time consuming (up to 72 hours to confirm results), expensive and requires skilled personnel. Multiple tests are needed to obtain a definitive answer that confirms the presence of a target analyte. Conventional methods also require test sample pre-enrichment, selective enrichment and serological confirmation [51-54] .

New technologies such as Polymerase Chain Reactions (PCR) offer better sensitivity but require even longer analysis times, pure test samples, hours of processing time and the employment of skilled personnel [55, 56]. In addition to these problems, conventional pathogen detection techniques need test samples to be brought into the laboratory, which often leads to other issues such as sample degradation during transportation and the extra costs and time involved.

Currently, new technologies are being developed to address these issues and extensive research is being conducted, both in academia and in industrial biotech labs. Smart, handheld detection technologies using different sensing platforms, coupled with probes ranging from enzymes and chemicals to molecular probes such bacteriophages and DNA, have seen tremendous success in improving the sensitivity and the rapidity of foodborne pathogen identification.

2.3   Biosensor Technology

Classification of biosensors

Classification of biosensors is essentially based either on the type of bio-recognition elements (e.g. enzymes, lipid layers, antibodies, or DNA) used to capture the target analyte or on the physical transducers employed (e.g. electrochemical transducers such as amperometric, potentiometric, and conductometric transducers; acoustic wave devices based on Thickness Shear Mode resonators, Surface acoustic waves, and Flexure plate waves and optical sensors that utilize Surface Plasmon resonance, fiber optics and wave guides) to detect changes in device characteristics due to analyte binding. A high-quality biosensor can selectively bind the target analyte even in the presence of interferants and should also be robust enough to withstand environmental perturbations.
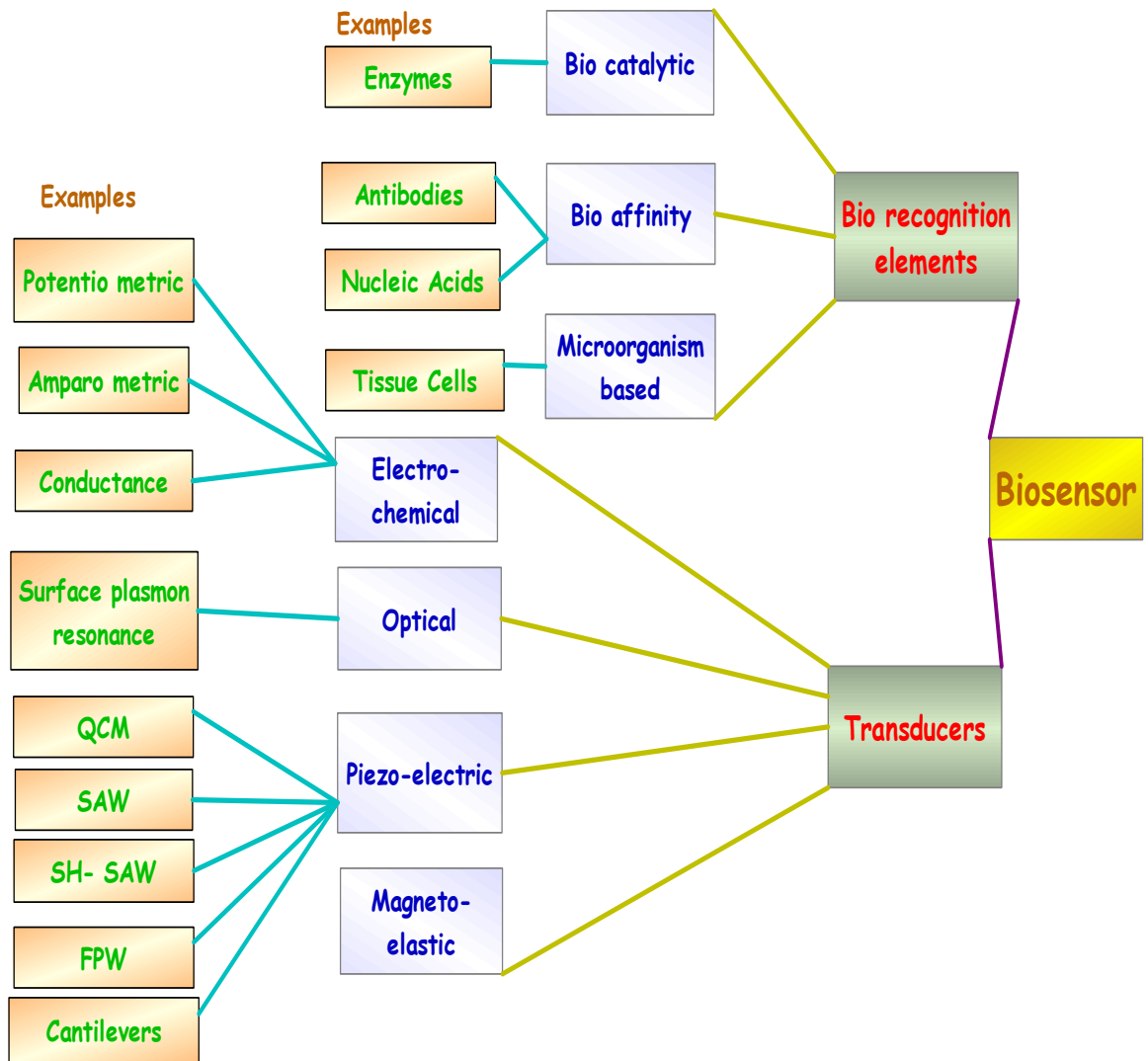
Figure 2-1: Schematic representation of biosensor classification.

2.3.1 Classification based on the bioreceptor/biological sensing element

Biosensors can be classified into three groups based on the characteristics of their receptors, namely protein, nucleic acid and cell-based biosensors. For example, immunoassay biosensors make use of the specific binding between an antibody and its antigen, while nucleic acid biosensors utilize the affinity of complementary single-stranded DNA (ssDNA) to form double-stranded DNA (dsDNA). Whole cell biosensors, on the other hand, examine the effects of an analyte on an intact microorganism. The focus of this research is on protein-based biosensors since they are the most well-studied and popular, however a brief consideration is also given to studies of the other two kinds of biosensors.

2.3.1.1 Protein-based biosensors

The vast diversity of proteins with their myriad functions has lead to their widespread use in biosensors. Enzymes and antibodies belong to protein family. Enzymes catalyze nearly all chemical reactions and antibodies provide defense against infections, most importantly act as receptors that are essential for specific cell-cell interactions.

2.3.1.1.1 Enzymes

Enzymes serve as the catalysts in biological systems and they determine many of the patterns of chemical transformations. They are responsible for the mediation of one form of energy into another. The catalytic power of enzymes, coupled with their high specificity of action, make them the most extraordinary molecules in biological systems. Enzyme-based biosensors commonly operate in either indirect or direct detection modes. For indirect detection, biosensors rely on changes in an indicator or reactant to generate

the recognition signals, while in direct detection the enzyme sensors can detect changes in the products, or intermediates, such as nicotinamide adenine dinucleotide (NAD) [57]. Oxidases, which catalyze the oxidation of compounds using oxygen, are usually co-immobilized with oxygen-sensitive luminescent materials such as polycyclic aromatic hydrocarbons [58-60], porphyrins [61], or transition metal complexes [62-64]. Successful applications that monitor pH changes to reveal the presence of metabolites such as penicillin, creatinine [65], heavy metals [66] and the chlorinated herbicide atrazine [67] have also been well documented.

2.3.1.1.2 Antigens/antibodies

Antibodies are produced by the immune system in response to the presence of antigens. Antigens can be living foreign organisms such as viruses, or bacteria, could be proteins, polysaccharides, lipids, or even dust. Antibodies are proteins that bind to the specific antigen with high affinity and thus negate the destructive mechanism of the invading antigens. The inherent specificity of antigen-antibody reactions, combined with the use of sensitive physical transducers, contributes to the superior selectivity and sensitivity of the new types of immunosensors that are being developed. Immunosensors, are generally used in one of four ways: direct assay, competitive assay, binding inhibition assay, and sandwich assay.

In a direct assay, the antigens are usually incubated with excess amounts of immobilized antibodies [68, 69]. Hence, the antigen could be a fluorescent compound that is then monitored using fluorescence-based methods [69]. In a competitive assay, analytes are labeled with chemicals such as Cy5 or fluorescein (FITC) [70-72]. On incubation, both the analyte and the labeled derivative compete for the limited binding

sites of the antibodies. As the amount of labeled derivative bound is inversely proportional to that of the unlabeled analyte present in the sample, the signal decreases with increasing analyte concentration. In a binding inhibition assay the antigens are immobilized, with the antibodies usually being labeled in same way [73, 74]. In a sandwich assay, antibodies to the analytes are first immobilized to a sensor, after which it is incubated with the analytes [75]. Next, a secondary labeled antibody that recognizes the analytes is added. On binding to the analyte of interest, a color change occurs and the intensity of the color obtained is directly proportional to the amount of antigen present.

2.3.1.2   Nucleic acid-based biosensors

The two types of nucleic acid-based biosensors use either deoxyribonucleic acid (DNA) or ribonucleic acid (RNA). However, as the latter degrades easily, most such sensors use DNA as the sensing element. Although the hydrogen bonds that hold the two strands of the DNA together are relatively easy to break, they are still strong enough to provide good stability on the biosensor platform. In such sensors, a single stranded DNA is immobilized on the receptor or transducer, and then allowed to interact with its labeled DNA complement. Thiazole orange or ethidium bromide act as labels [76-78] and are used as fluorescent dyes for detection purposes.

2.3.1.3   Cell-based biosensors

Cell based biosensors using cytoplasmic membranes have also been reported, for example. for the detection of lactate [79]. The inducible promoter of a reporter gene of *E. coli* that encodes for a bioluminescent protein has also been used for the detection of heavy metals [80] and toxic organic compounds [81]. Microorganism based sensors mainly use tissue cells [82, 83] and other living or mutant organisms [84] as receptors.

23

Cell based sensors offer many advantages, including simultaneous measurements of multiple effects, enhanced sensitivity due to internal amplification cascades and, most importantly, the sustenance capacity of whole cells [85]. Different transduction mechanisms such as measurement of cell fluorescence, metabolism, impedance, intracellular potentials, or extracellular potentials may be employed to detect changes due to the interaction of the microorganisms with their target analytes. Although whole cell-based biosensors are more rapidly fabricated, they are more difficult to maintain, as the cells or organisms must be kept alive with constant monitoring and supplication of nutrients, and the metabolic waste that is generated must be removed otherwise the cells die.

2.3.2 Transducers

The transducer is the second important functional unit of a biosensor, and is responsible for translating the recognition event into a measurable signal. This measurable signal maybe in the form of a change in electrical potential (potentiometric), vibrational frequency (Piezoelectric devices such as the Quartz Crystal Microbalance or Surface Acoustic Wave devices), reflectance (Surface Plasmon Resonance) or magnetic flux (Magnetoelastic). Electrochemical transducers include potentiometric devices that measure cell potential at zero current, amperometric devices where a reducing potential is applied between the cell electrodes and the cell current is measured, and conductometric devices where the conductance of a cell is measured by an alternating current bridge method. For quantitative measurements, electrochemical sensors can be used to detect metal ions and non-metals. Some of the advantages offered by electrochemical sensors include their high sensitivity, small size, low cost, versatility and capacity for stand-alone

operation. Optical transducers incorporate optic fibers or metal films coated on prisms, allowing for greater flexibility and miniaturization. Absorption spectroscopy and surface plasmon resonance spectroscopes are both examples of the types of techniques typically used in optical transducers. Optical sensors have also found many applications in the measurement of pH, oxygen, carbon dioxide, and ions. Piezo-electric devices function by generating a voltage potential from a vibrating crystal. The amount of mass that is adsorbed on the surface of the piezo-electric sensor alters the resonance frequency of the crystal, and these changes in frequency are then measured by the incorporation of suitable oscillatory circuits.

2.3.2.1 Electrochemical transducers

2.3.2.1.1 *Potentiometric Transducers*

Conventional potentiometric sensors consist of a reference electrode, which is inert and a working electrode, which is the ion-selective electrode. The potential difference between the working electrode and the reference electrode depends on the concentration of the target analyte [86-88]. Working electrodes are immobilized with a bio-recognition layer or an ion selective membrane, which can specifically react with the analyte of interest. When the bio-recognition layer interacts with the target analyte, a change in potential results from the ion accumulation or depletion which is directly related to the analyte concentration.

The Nernst relation describes the relationship between changes in potential and the level of analyte (a_i) activity

$$E = E_0 + \frac{RT}{nF} \ln a_i \qquad (2\text{-}1)$$

Where, E_0 is the standard potential, a_i is the activity of the analyte, R is the gas constant, F is the Faraday constant, T is the temperature in K, and n is the total number of charges on the ion.

Potentiometric sensors have been employed for measuring enzyme activity [89] in catalysis, monitoring organophosphates using a pH electrode [81, 90, 91], tracking the concentration of heavy metal ions through measurement of the associated inhibitory enzyme activity [92], monitoring the urea contamination in milk [93], and measuring levels of *Y. pestis* and *Bacillus globigii* spores [94] and *S. typhimurium* [95].

The primary advantage of these devices is their wide dynamic range of detection (10^{-6} - 10^{-1} mol/L) along with their suitability for continuous monitoring applications. In spite of these advantages, however these devices are limited by their low sensitivity, and poor selectivity, as they are vulnerable to false signals due to interferants.

2.3.2.1.2 *Amperometric Transducers*

Amperometric biosensors consist of a pair of reference and working electrodes, with the working electrode operating at a fixed potential with respect to the reference electrode. The concentration of the target analyte is determined by the current generated by the oxidation or reduction reactions at the working electrode surface. The current produced at the working electrode is linearly proportional to the concentration of the product of the chemical reaction, which in turn is related to the concentration of the target analyte.

The following chemical reaction exemplifies a typical reaction that takes place at the surface of the working electrode of a enzyme based amperometric biosensor. The

concentration of target analyte can be estimated by the O_2 or H_2O_2 concentration detected.

$$\text{Analyte} + O_2 \text{ --------------> } \text{Product} + H_2O_2$$
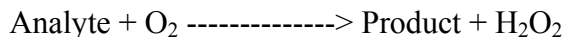
These transducers offer many advantages, such as higher reproducibility, low cost and the ease with which they can be modified for field testing, all of which make them a good choice for field deployment. However, their use is limited by their small dynamic range due to the rapid saturation of enzyme on the working electrode, and the interaction of interferants with the bio-recognition layer.

Amperometric sensors have found many applications such as their use in the detection of organophosphate pesticides [96], genotoxic compounds in drinking water [97], campylobacter [98], *Staphylococcus aureus* [99], *E. coli* 0157:H7 [100, 101] and *S. typhimurium* [102].

2.3.2.1.3 Conductometric Transducers

Conductometric electrodes have been used to measure heavy metals such as Ag^+, Hg^{2+} and Pb^{2+} by immobilizing butyril oxidase [103] and urease [104] on the electrode surface. Recently, conductometric biosensors have been developed to monitor the metabolic activity of *E. coli* [105]. The operating principle of conductometric sensors is that the membrane layer (e.g. an enzyme) reacts with the analyte solution, which results in a change in the net ionic charge and a consequent change in conductivity of the analyte solution. These sensors have a dynamic range of 1-100 μM. The main advantage of such sensor systems is the high reproducibility of their measurements.

27

2.3.2.2   Piezoelectric Transducers

The direct piezoelectric effect was discovered by the Curie brothers in 1880. A year later, in 1881, the converse piezoelectric effect was illustrated. When a voltage is applied to a piezoelectric crystal, the crystal deforms reversibly due to the lattice strain caused by the effect. Thus, under suitable conditions, the piezoelectric effect provides a coupling between electrical circuit and the mechanical changes in the crystal lattice. Piezoelectric devices such as the quartz crystal microbalance (QCM), otherwise known as thickness shear mode (TSM) resonators work, on this principle of converse piezoelectricity.

2.3.2.2.1 *Surface acoustic wave (SAW) sensors*

SAW devices have found many applications as chemical sensors for a wide range of purposes, including the detection of gas and vapor concentrations [106, 107], relative humidity [108-111], and ion concentrations [112-114].
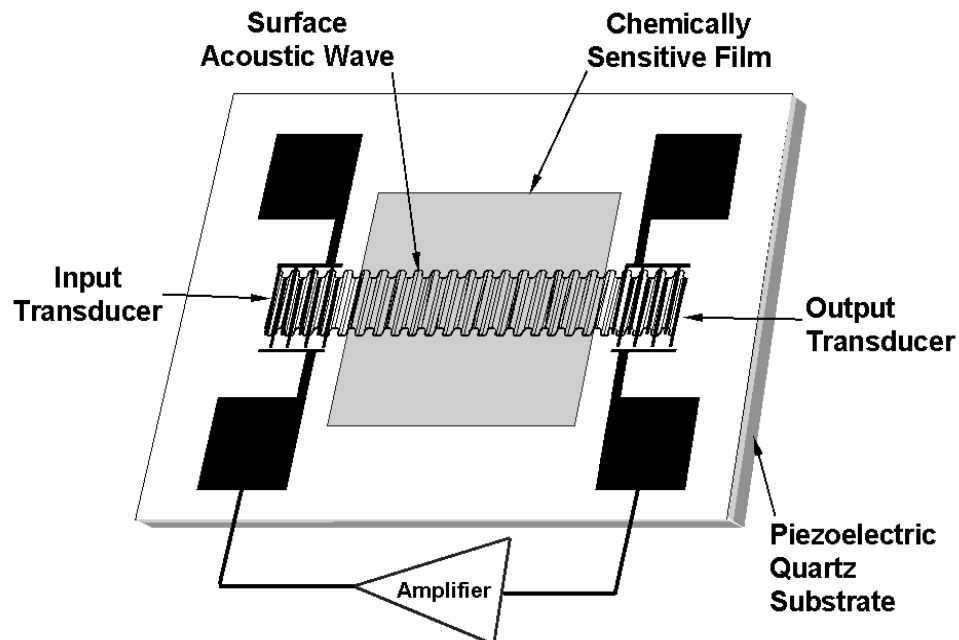
Figure 2-2: Schematic of a surface acoustic wave delay-line chemical sensor.

SAW devices usually consists of ST-cut quartz substrates with two gold/titanium-interdigitized transducers (IDTs) deposited on the surface. The operating frequency is approximately 97 MHz, with a delay path between the IDTs of approximately 1 cm. Chemical detection is achieved by depositing a thin sorptive coating in the SAW delay path. When an analyte is adsorbed onto the sensor surface, changes occur in the fundamental resonance frequency of the resonator. By measuring these changes in the resonance frequency, it is possible to measure the amount of analyte that is adsorbed by the chemically interactive layer. Although SAW devices function well in the air/gas environment they perform poorly in liquids due to dampening of the acoustic wave, resulting in a non-specific signal from the sensor.

The mass adsorbed by the chemically interactive layer at the sensor surface and the changes in the resonance frequency of the sensor are given by the following equation [115]

$$\frac{\Delta v}{v_0} \cong -c_m f_0 \Delta\left(\frac{m}{A}\right) = \frac{\Delta f}{f_0} \tag{2-2}$$

Where v_0 is the unperturbed wave velocity, f_0 is the unperturbed wave oscillation frequency, Δv and Δf are the changes in the wave velocity and oscillation frequency, respectively, c_m is the coefficient of mass sensitivity (substrate dependent), and $\Delta(m/A)$ is the mass change per unit area for the device.

2.3.2.2.2 *Shear-Horizontal Surface Acoustic Wave (SH-SAW) and Love Wave Devices*

Shear horizontal surface acoustic wave (SH-SAW) devices have been in use for liquid phase chemical and biological detection for some years [116, 117]. Lithium tantalite is often used as a substrate material for SH-SAW device fabrication [118, 119]. When an SH-SAW device is electrically excited by an RF signal, the resultant acoustic wave travels between the pair of interdigital transducers (IDTs) along the surface of the device. Adding a waveguide layer to the SH-SAW improves the device sensitivity by lowering the acoustic shear wave velocity compared to the substrate, and also isolates the IDTs from the liquid analytes [120]. Silicon dioxide, silicon nitride and polymers are used as waveguide materials.
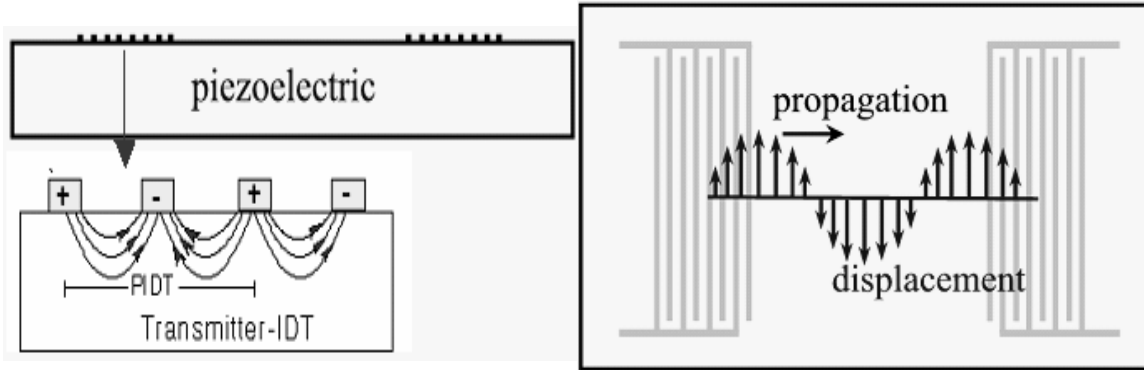
Figure 2-3: Schematic of a shear- horizontal surface acoustic wave delay-line chemical sensor. (Courtesy: R. W. Cernosek)

Higher operating frequencies enable these devices to offer better sensitivities and packaging of these sensors is easy as only one surface of the sensor is used for detection. However, due to difficulties in electronics design, these devices have not yet fully realized their commercial potential.

The response of an SH-SAW device to an analyte depends upon many parameters, including changes in the mass on the device surface, changes in the viscoelastic properties and changes in the film conductivity. Changes in the acoustic wave velocity related to shifts in the SH-SAW device oscillation frequency are described by the following equation [121, 122]

$$\frac{\Delta v}{v_0} \cong -c_m f_0 \Delta\left(\frac{m}{A}\right) + 4c_{ve}\frac{f_0}{v_0^2}\Delta(hG) - \frac{K^2}{2}\Delta\left(\frac{\sigma_s^2}{\sigma_s^2 + v_0^2 C_s^2}\right) \tag{2-3}$$

where v_0 is the unperturbed wave velocity, Δv is the change in wave velocity, C_m and C_{ve} are the coefficients of mass sensitivity and elasticity of the substrate respectively, (m/A) is

31

the change in mass per unit area, f_0 is the operating frequency of SAW device, h is the coated film thickness, G' is the shear modulus, K^2 is the electromechanical coupling coefficient, and σ_s is the sheet conductivity of coated film. C_s is the capacitance per unit length of the SAW substrate material.

2.3.2.2.3 *Thickness Shear Mode (TSM) Resonator*

Thickness Shear Mode (TSM) resonators have been actively used in applications such as blood characterization, organic vapor sensing, monitoring of biofilm growth under different flow conditions, liquid property measurements and bacterial pathogen detection [123-129]. Thickness shear mode (TSM) resonators are usually constructed from AT- cut quartz crystals which are deposited with metal electrodes, usually gold, on both sides of the disk atop a chromium interlayer. Any voltage potential across the electrodes results in strain in the quartz crystal. The mass sensitivity of a TSM resonator is around 1 ng/cm^2 in air and 5 ng/cm^2 in a liquid. TSM resonators have a good Q-value (quality factor) in both air and liquid media, due to the shearing mode being along the thickness of the resonator. The classical Saubery Equation gives the relationship between the frequency shift and change in the mass on the surface of a TSM resonator [115]:

$$\Delta f = \frac{-[2f_0{}^2 \Delta m]}{A(\rho_g \mu_g)^{1/2}} \tag{2-4}$$

where Δf = frequency shift, f_0 = resonant frequency of the fundamental mode of the crystal, Δm = mass change per unit area (g/cm^2), A= piezo-electrically active area, ρ_g = density of quartz, and μ_g = shear modulus of quartz

AT-cut quartz crystals have zero first order temperature coefficients at room temperature and the low range resonance frequency (5 MHz) operation of these devices makes the electronics easy to design for TSM resonators. However, due to the low frequency of operation the sensitivity is low compared to that of other SAW devices.

2.3.2.2.4 *Flexural plate wave (FPW) devices*

Flexural plate wave (FPW) devices are used as sensors for gas chromatography, biochemical detection and pressure measurements [130-135]. FPW device fabrication begins with the deposition of a membrane layer (silicon nitride, silicon dioxide, oxy-nitride, aluminum nitride, and diamond) onto a silicon substrate, followed by the sputtering of a piezoelectric material (e.g. Zinc oxide) onto the membrane. Finally, metal electrodes (IDTs) are patterned on to the membrane layer followed by backside etching of the silicon wafer to release the line in the IDTs. The membrane layers are much thinner than the acoustic wave length.

The membrane movement can be either a shear wave propagation or normal to the surface. Subtle variations at the surface of the membrane can change the wave propagation velocity and damp the acoustic vibration [136].

The flexure plate wave sensor oscillation frequency can be expressed as [137]:

$$f = \frac{1}{\lambda}\sqrt{\frac{B}{M + \delta\rho}}$$ (2-5)

where λ is the acoustic wave length, B is the plate flexural rigidity, M is the mass per unit area of the plate, δ is the $1/e$ – distance of evanescent wave, and ρ is the liquid density.

FPW devices offer advantages such as high sensitivity, and easy electronics design due to their low operating frequencies. However, the commercial viability of FPW devices is limited by operation difficulties in rigorous environments due to their fragile membrane films.

Membrane Perimeter 2 mm×6 mm

Metal ground Plane (0.2 -0.5µm)
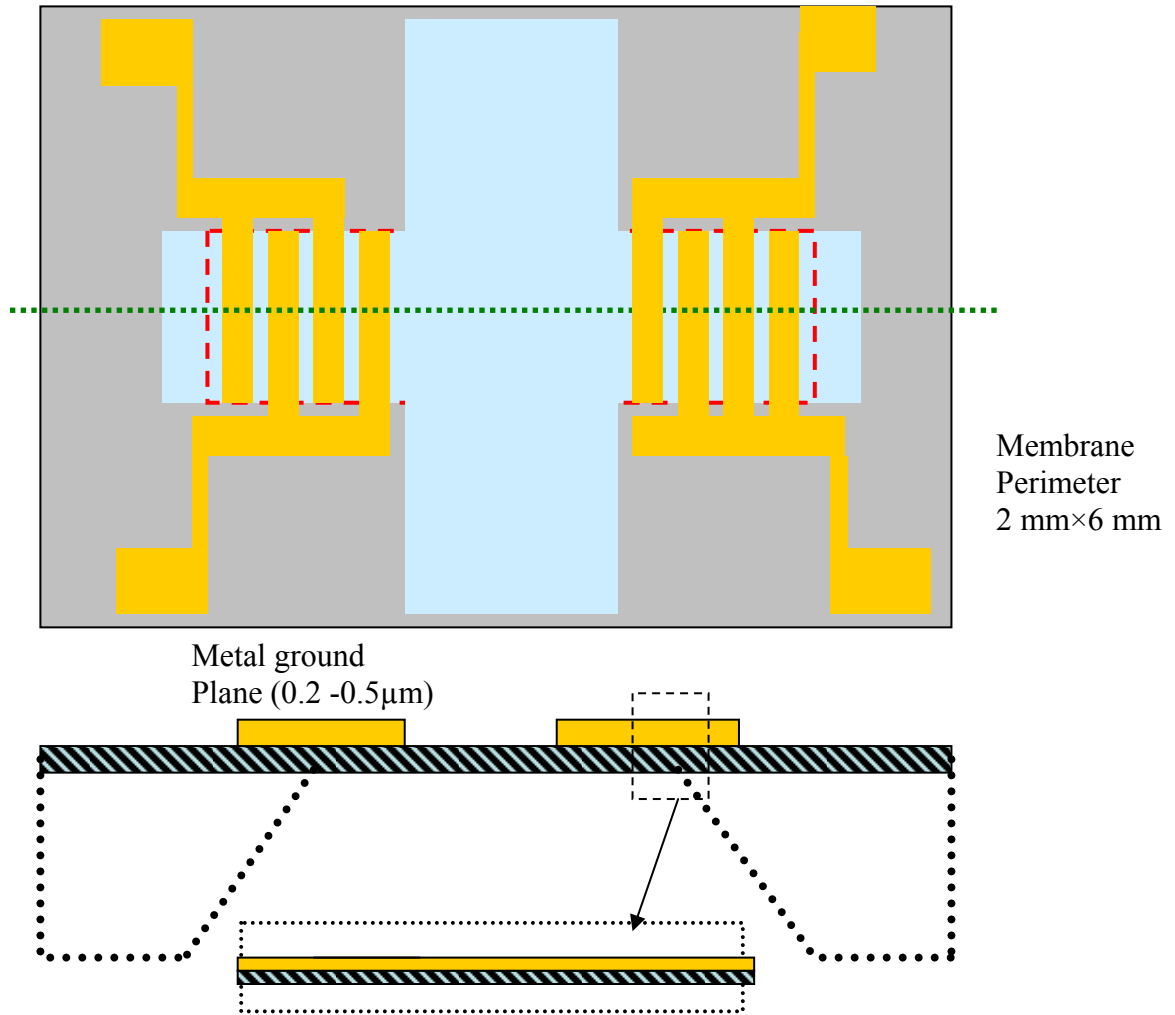
Figure 2-4: Schematic of a Flexural Plate Wave (FPW) chemical sensor.
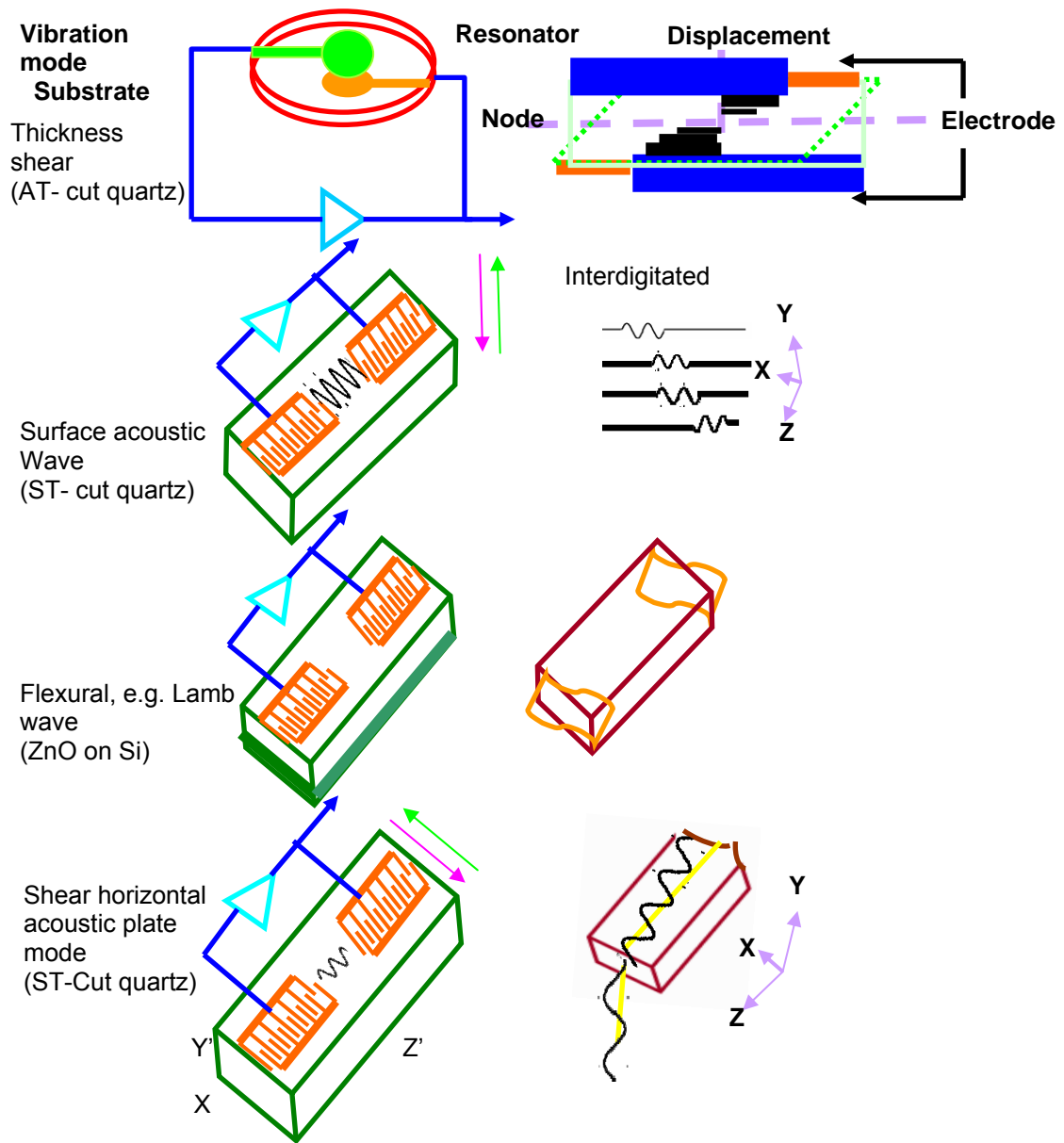
Figure 2-5: Piezoelectric devices and their deformation in electric fields. (Arrows represent the direction of particle motion)

2.3.2.3 Optical biosensors

Rapid advances in fabrication, material design, signal generation and detection, and vastly improved optoelectronics [138] have led to the extensive use of optical sensors for the detection of a wide range of substances. After immobilization of a suitable probe on the optical sensing surface, the detection of the target analyte can be achieved by measuring the resulting change in the fluorescence, luminescence, rotation or refractive index. Immobilization of an appropriate probe enhances the sensitivity of these devices. Extensive research has been reported on bacterial detection using different optical techniques, including monomode dielectric waveguides [139, 140], surface plasmon resonance [141-145], ellipsometry [146, 147], resonance mirrors [148] and interferometers [149].

2.3.2.3.1 Surface Plasmon Resonance

Surface plasmon resonance (SPR) has begun to be used as a transduction mechanism in biosensors. SPR has a multi layer design consisting of a prism surface made of quartz or glass, a thin noble metal film (e.g. gold) bio-recognition layer and a target analyte. SPR is a physical phenomenon that occurs when a plane polarized light strikes a thin metal film (~50nm) under conditions of total internal reflection (TIR), when the evanescent wave interacts with free oscillating electrons in the metal film at the prism surface [150]. The surface plasmon resonance angle depends on many factors, such as the wavelength of the incident light, the refractive index of the medium, the properties of the metal film that is deposited on the prism surface and the temperature [151].

Optical transducers offer many advantages, in particular the speed and reproducibility of the measurements and are now being used for affinity and microbial-

36

based biosensors [152]. However, their disadvantages include the high cost of the apparatus and bulkiness of equipment, both of which limit the application of optical biosensors for on-site measurements.
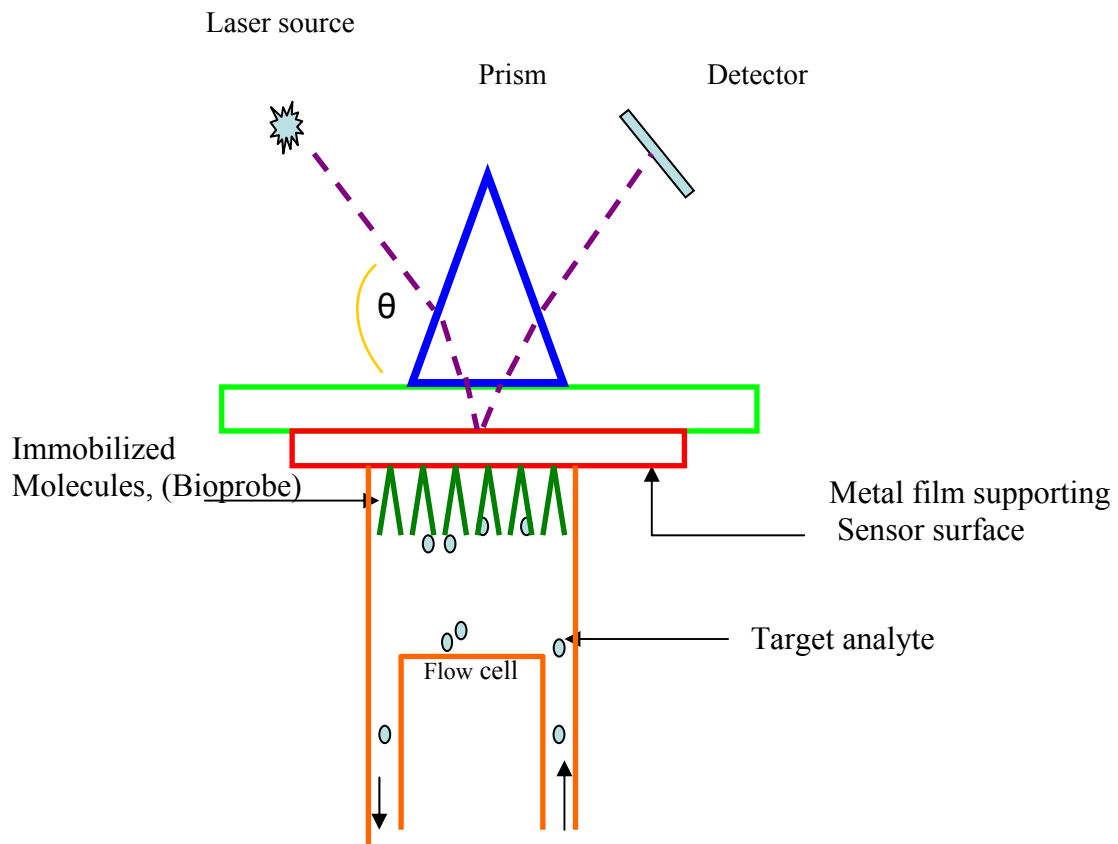
Figure 2-6: Surface plasmon resonance (SPR) schematic for bio sensing.

2.3.2.4 Magnetoelastic sensors

Magnetostriction, also known as the Joule effect was first observed by James Joule in 1842 in nickel [153]. Magnetoelastic materials undergo a shape change in the presence of a magnetic field due to the reorientation of the magnetic domains with the applied external magnetic field.

Magnetoelastic materials are amorphous ferromagnetic alloys. Due to the magnetoelastic nature of the amorphous magnetoelastic alloy, the sensor exhibits a physical resonance when it is subjected to a time-varying magnetic field, causing it to emit a magnetic flux. This flux can then be monitored remotely without the need for direct physical connections.
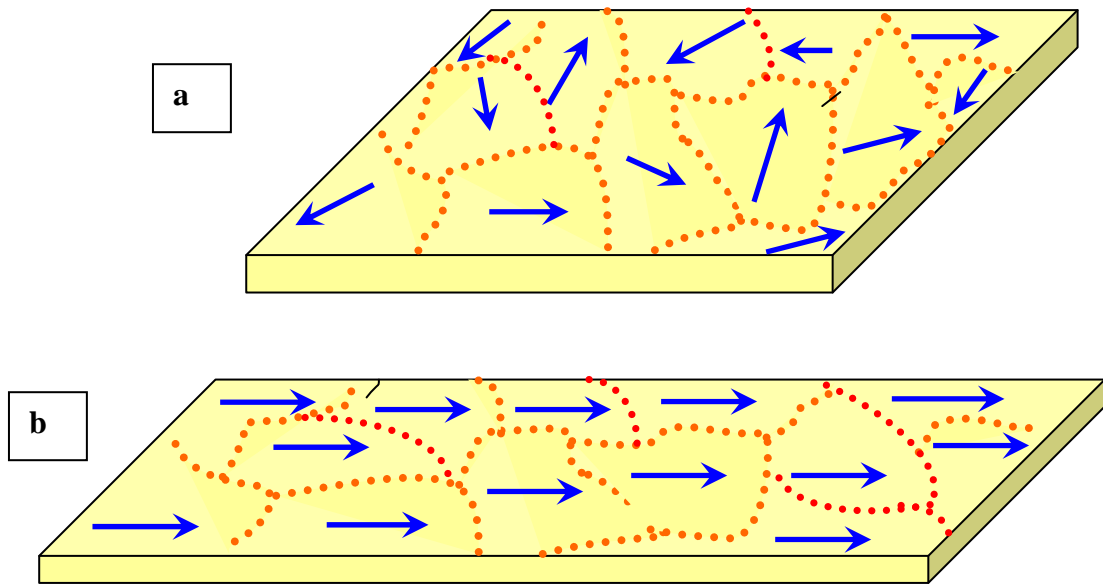
Figure 2-7: Behavior of magnetoelastic material (a) with no magnetic field; (b) in the presence of a magnetic field.

Existing biosensor transducers offer wide ranges of applications and advantages like high sensitivity and selectivity, but lack the capability for the remote detection of analytes. Magnetoelastic transducers have the potential to address this issues, allowing actuation and data acquisition to be carried out from a remote location. Consequently, magnetoelastic sensors can be used to detect bacterial contaminations in sealed containers and conducting liquids. Magnetoelastic materials have already been used to develop both environmental and chemical sensors [24-26, 154-160]. The research reported here successfully established the effectiveness of magnetoelastic sensors for bacterial detection by employing a magnetoelastic transducers coupled with the use of an antibody as the bioprobe.

2.4 Sensor attributes

The choice of an appropriate sensor depends upon several fundamental characteristics, all of which are essential for the successful detection of the target analyte. The chief sensor attributes that need to be considered before selection of an ideal sensor are:

Sensitivity:

Sensitivity generally refers to the lowest quantifiable entity of the target analyte that the sensor is capable of detecting in a sample. It may be expressed in various forms, such as units of particles or mass per unit air volume (particles/liter or mg/m^3).

Selectivity:

Selectivity of a sensor refers to its ability to detect only the analyte of interest, even in the presence of other non-specific analytes. Although most sensors show a response to some degree for non-specific analytes, it is possible to minimize this non-

specific interaction by careful choice of the biorecognition element to be deployed on the sensor.

Longevity:

Longevity refers to the sensor's capacity to detect the analyte of interest even after prolonged storage. The longevity of the sensor can be enhanced by the application of robust biorecognition elements that are capable of withstanding rigorous environmental conditions, such as high humidity and/or temperature and vibrations.

Wide dynamic range of detection:

The dynamic range of a sensor refers to the range of input physical signals that can be converted to electrical signals by the sensor. Signals that are larger or smaller than this range generally cause unacceptably large inaccuracies. This span, or dynamic range, is usually specified by the sensor supplier as the range over which other performance characteristics described in the product data sheets are expected to apply.

Quick response time:

In modern biosensors, the rapidity of their response to the presence of the analyte of interest is a key characteristic that will define the success or failure of a biosensor on the field.

Robustness in rugged environmental conditions:

This characteristic of the sensor is applicable to both the biorecognition element and the transducer component of the biosensor, both of which must be able to withstand the shock, vibration, exposure to harsh weather conditions and even extreme effects such as an electromagnetic pulse.

Noise:

Successful sensors should enjoy a high signal to noise ratio. Higher noise results in lower resolution of the sensor signal, which in turn affects the sensitivity.

Portable and user friendly:

The ability to miniaturize a biosensor system is essential for easy deployment in the field. A biosensor that is small and can operate as a stand alone device with minimum power requirements is ideal for use in war zones or in disaster areas, where ease of operation with few limitations often plays a pivotal role in the choice of a suitable biosensor.

Low cost:

This attribute of the sensor is often crucial factor that must be considered before any commercialization of biosensor is possible. The viability of most business plans that aim to commercialize a lab device to bring a new product to the market depends on this characteristic.
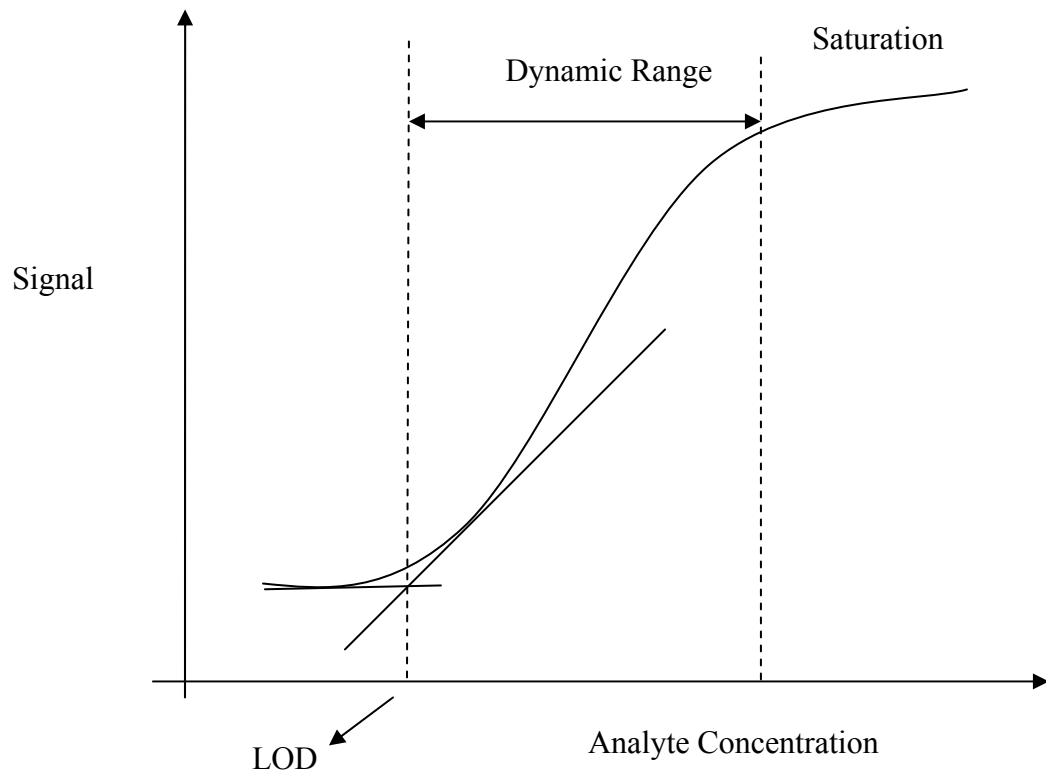
Figure 2-8: Sensor calibration curve.

LOD: Limit of Detection

3 EXPERIMENTAL PROCEDURES

3.1 Sensor Platform

METGLAS® 2826MB alloy (Conway, SC) obtained from Honeywell International was used as the sensor platform for this study. The composition of this alloy is $Fe_{40}Ni_{38}Mo_4B_{18}$ and its theoretical value of saturation magnetostriction is 12 ppm. To increase the mass sensitivity, sensors were mechanically polished using fine grit paper to reduce the thickness from 30μm to 15μm and to decrease the initial mass. Magnetoelastic strips were constructed using an auto controlled, micro dicing saw and the diced sensors were then ultrasonically cleaned in methanol (100 %) for 20 minutes to remove the organic and inorganic debris left by the dicing process. To improve the environmental stability and the bioactivity of the biosensors, thin layers of chromium (50nm at 100 W DC power) and gold (100 nm at 200 W RF power) were sputtered onto the surfaces of the magnetoelastic particles using a Denton™ (Moorestown, NJ) high vacuum RF sputtering system. The sensors were rinsed in hexane before the monolayer deposition and finally air dried and stored at ambient temperature in a dessicator until needed. Table 3-1 and Table 3-2 explain the physical and magnetic properties of METGLAS® 2826 MB alloy respectively.

Table 3-1: Physical Properties of METGLAS® 2826MB [161].

Density (gram/cc)	7.90
Tensile Strength (GPa)	1-2
Elastic Modulus (GPa)	100-110
Thermal Expansion (ppm/°C)	11.7
Crystallization Temperature (°C)	410
Continuous Service Temp. (°C)	125
Vicker's Hardness (50g load)	740
Lamination Factor (%)	>75

Table 3-2: Magnetic Properties of METGLAS® 2826MB [161].

Saturation Induction (Tesla)	0.88
Maximum D.C. Permeability (μ): Annealed	800,000
Maximum D.C. Permeability (μ): As Cast	> 50,000
Saturation Magnetostriction (ppm)	12
Curie Temperature (°C)	353

3.2   Antibodies

Rabbit polyclonal antibody (1.0 mg/ml) (Product# ab13634) to *Salmonella* was purchased from Abcam Inc (Cambridge, MA) and immobilized on the magnetoelastic biosensors using the Langmuir – Blodgett (LB) film technique.   The functional performance of the biosensors was evaluated with a graduated series of bacterial suspensions.

3.3   *Salmonella typhimurium* Cultures

S. typhimurium (ATCC 13311) obtained from the American Type Culture Collection (Rockville, MD) was confirmed for identity and propagated by the Department of Life Science at Auburn University.   One pure colony of *Salmonella typhimurium* from a subculture plate was inoculated into 25 ml of NZY and incubated at 37 ^{0}C in a shaker (200 rpm) for 18 hours. Following inoculation, the culture was gently mixed for homogeneity and transferred into 50-ml sterile tubes that were then centrifuged (Allegra 21R centrifuge, Beckman Coulter; S4180 rotor) at 5500 rpm for 10 minutes, and the supernatant decanted. The cells were washed by resuspension in 25 ml of distilled water and centrifuging (same conditions), followed by decanting the supernatant once more. The centrifugation with distilled water was performed twice. The suspensions were serially diluted in water (or the other experimental media, namely fat free milk and apple juice) to prepare bacterial suspensions ranging from $5x10^1$ to $5x10^8$ cfu/ml. All test solutions were prepared on the same day as the biosensor testing and maintained at 4 °C until needed.

3.4   Monolayer Deposition

The Langmuir-Blodgett (LB) technique was used for antibody immobilization on the magnetoelastic sensors. Antibody monolayers were deposited using an LB film balance KSV 2200 LB, (KSV Chemicals, Finland). This system comprises a Wilhelmy-type surface balance (sensitivity range 0-100 mN/m), a teflon trough of dimensions 45×15 cm^2, and a teflon barrier (0-200 mm/min) driven by a variable speed motor, all of which are encased in a laminar flow hood. To minimize any variations that may arise due to vibrations, the trough is mounted on a marble table and protected by interposing rubber shock absorbers. Subphase temperature (20 ± 0.1 ^{o}C) control is achieved by circulating water through a quartz tube coil at the bottom of the trough.   In this experiment the magnetoelastic sensors were submerged into the deionized water (DD H$_2$O) in the LB trough. A monolayer from the antibody suspension was formed by allowing 100 µl of the antibody solution (1 mg/ml) to run down a wetted glass rod that was partially submerged into the subphase (deionized water).   When the antibody suspension reached the air $-$ water interface, it forms a monolayer due to surface forces [162]. After spreading, the monolayer was allowed to equilibrate and stabilize for 10 min at 20 °C.

The monolayers were then compressed using a computer controlled compression barrier at a rate of 30 mm/min until the pressure reached 22 mN/m, after which, the pressure was held constant and vertical antibody film deposition was carried out at a rate of 4.5 mm/min. Multiple monolayers of antibody were obtained by successive dipping of the sensors through the monomolecular film deposited at the water-air interface. Seven monolayers containing antibodies were transferred onto the surface of the magnetoelastic

sensor in this way. Only one surface of the magnetoelastic sensor was coated with the antibody. The relative coverage of the antibody film on the substrate was measured by calculating the transfer ratio, which is the ratio of the area of the monolayer that has been removed during the dipping cycle to the area of the substrate to be immobilized. A representative set of transfer ratios reported in Table 3-3. It is apparent from the transfer ratios that immobilization of monolayers onto the magnetoelastic sensors occurred only during the upward motion of the substrate.

Table 3-3: A representative set of transfer ratios for antibody monolayer deposition using LB film method.

Monolayer	Direction	Transfer ratio
1	Up	0.277
2	Down	0.061
3	Up	0.124
4	Down	-0.001
5	Up	0.108
6	Down	-0.012
7	Up	0.109

MONOLAYER APPARATUS
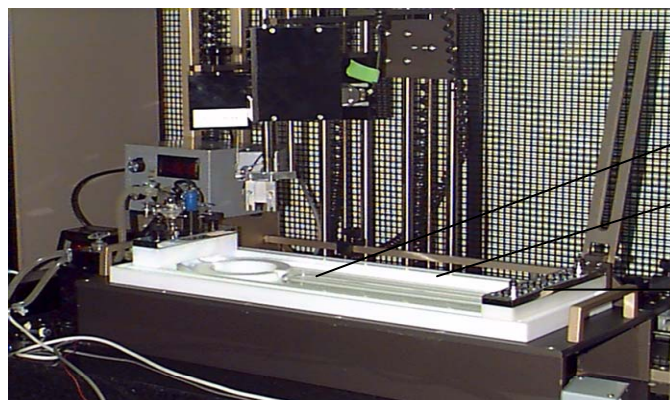
Teflon trough

Quartz tube for circulating water

Variable speed Teflon barrier

Monolayer Formation

Barrier

Monolayer trough

Compression
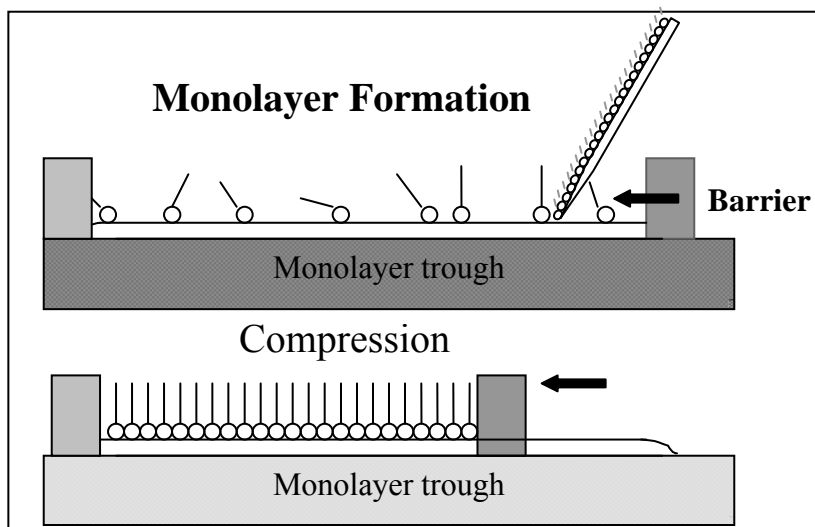
Monolayer trough

Figure 3-1: KSV 2200LB Langmuir-Blodgett System (KSV-Chemical, Finland) used for deposition of monolayer with controlled architecture. Multilayers were obtained by successive dipping of the sensors through the monomolecular film deposited at the water-air interface on the Langmuir-Blodgett trough.

3.5 Scanning Electron Microscopy Imaging

The magnetoelastic sensors were examined using Scanning Electron Microscopy (SEM) after the antibody – antigen reactions. Images were taken at different concentrations of bacterial solutions, ranging from 10^3 to 10^9 cfu/ml. After the testing, the magnetoelastic sensors were immersed in 10 ml of deionized water in a petri dish for 15 seconds in order to dissolve the salts and debris on the sensor surface which had accumulated during the testing. The sensors were then placed into a petri dish containing 1 ml of Osmium Tetra oxide (OsO_4) for 45 minutes. The vapor from OsO_4 stains the bacterial cell walls, thus indicating the structural integrity of the bound bacterial cells. After exposure to the OsO_4 vapor the sensors were mounted on aluminum studs with a double sided carbon conductive tape. The sensor aluminum stud assembly was sputtered with 50nm gold using a PELCO sputter coater, SC-7, and the JEOL 7000F SEM was used to image the sensor surface. The images were taken at an accelerating voltage of 10 KV, a working distance of 11.1 mm, an aperture size of 3, and a current of 54 μA. SEM images of the bacterial cells on the sensor surface were captured digitally using the imaging system of the Scanning Electron Microscope (SEM).   The number of bound bacterial cells in each micrograph was counted and mass of the total bacterial cells on the sensor surface was estimated.
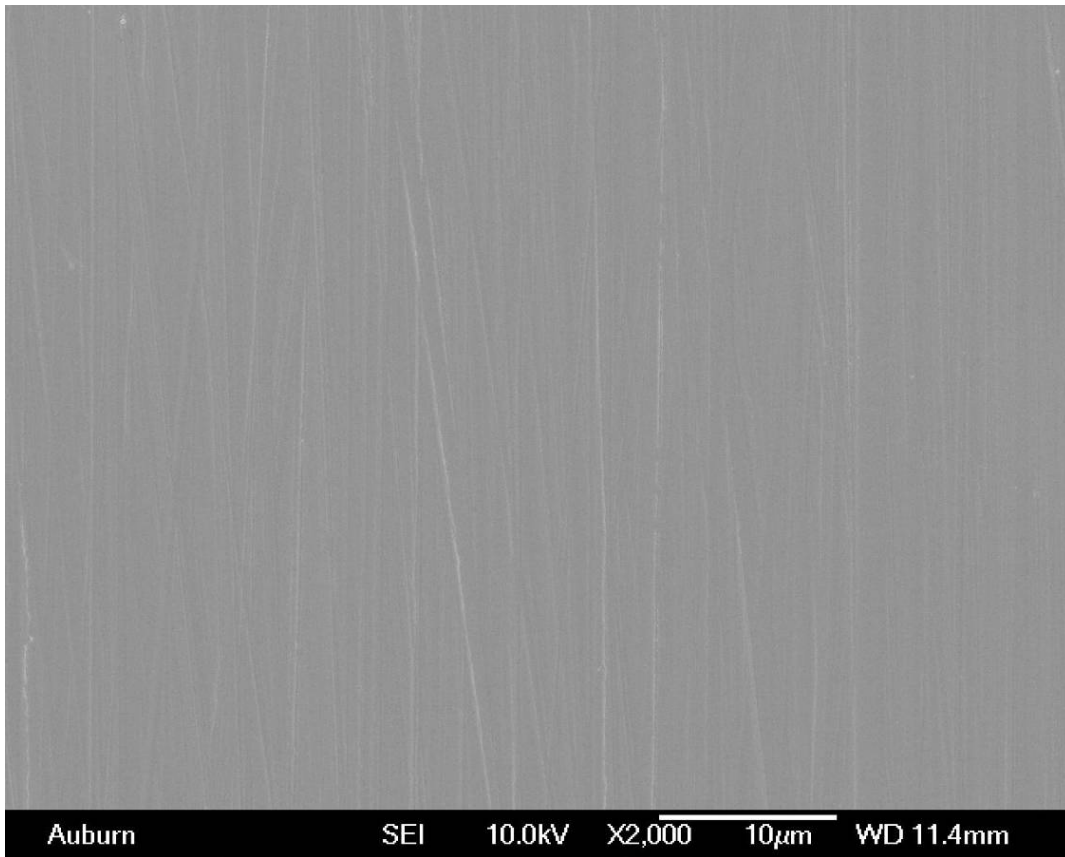
Figure 3-2: Scanning electron microscope image of a polished sensor surface sputtered with gold.
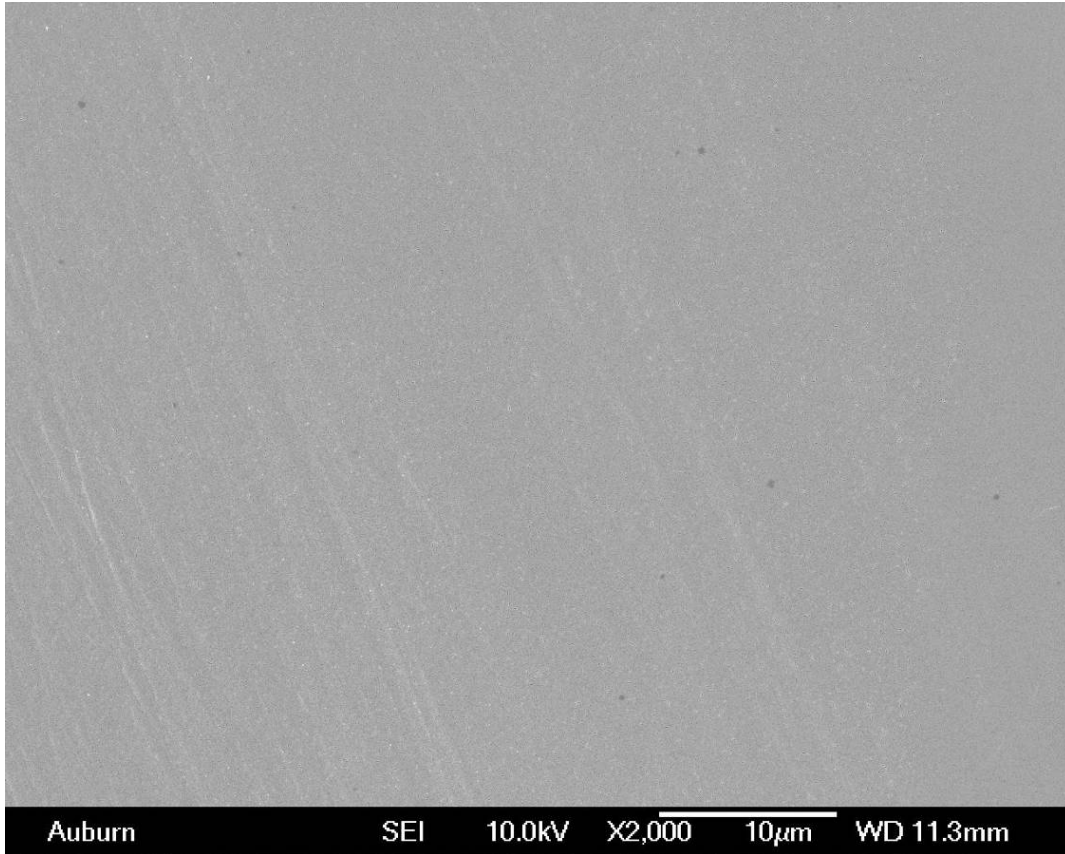
Figure 3-3: Scanning electron microscope image of a polished sensor surface after antibody immobilization.
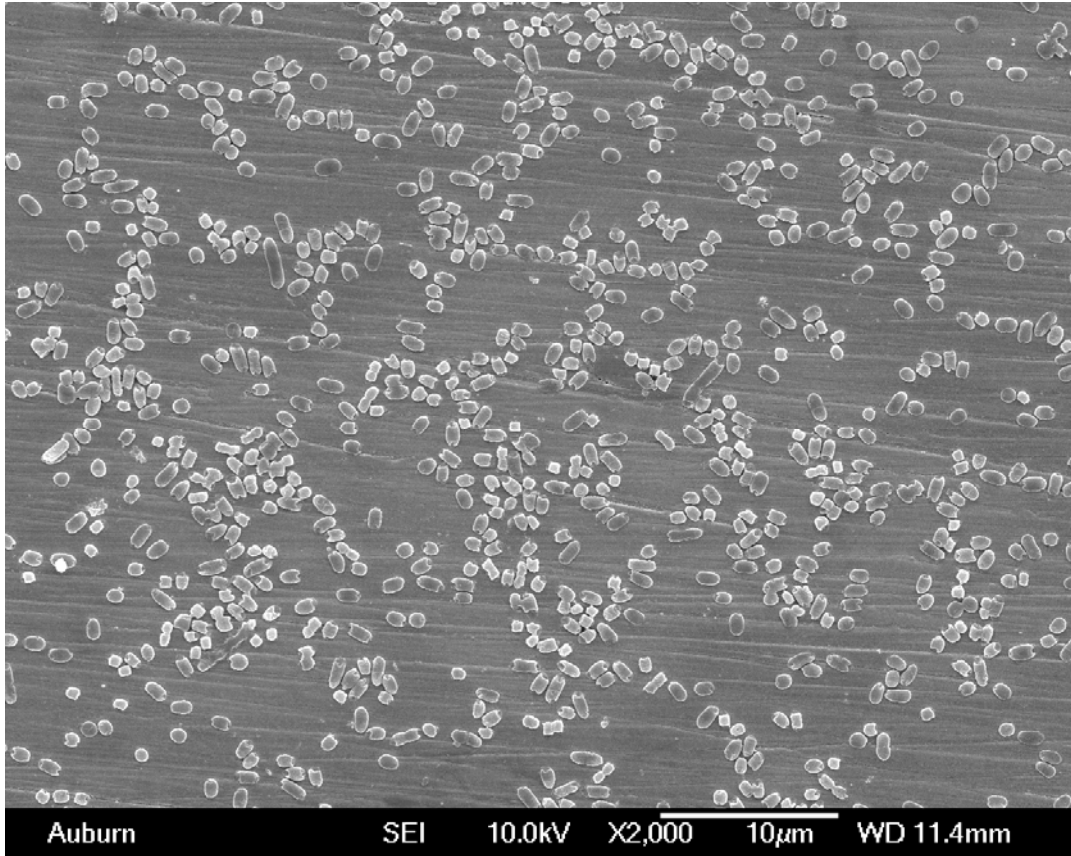
Figure 3-4: SEM image of *S. typhimurium* bound to a magnetoelastic sensor surface immobilized with an antibody film after exposure to a 5×10^8 cfu/ml concentration of bacterial solution.
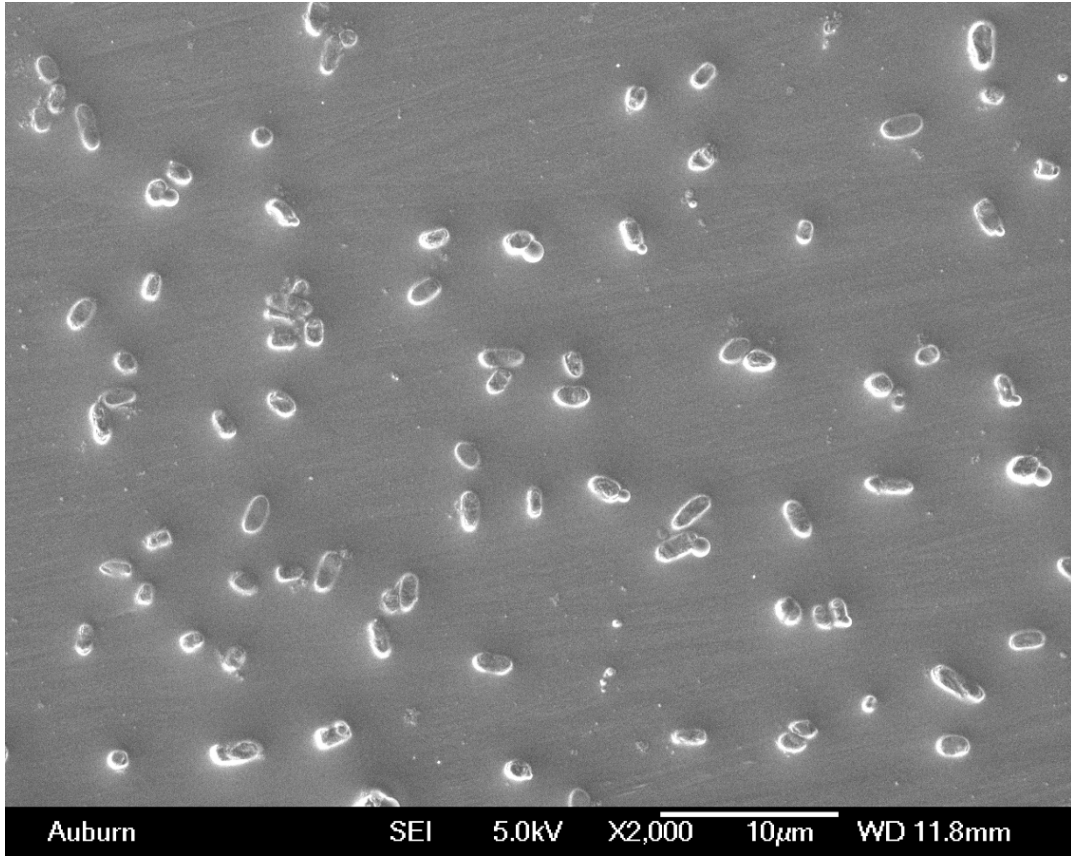
Figure 3-5: SEM image of *S. typhimurium* bound to a magnetoelastic sensor surface immobilized with an antibody film after exposure to a 5×10^6 cfu/ml concentration of bacterial solution.
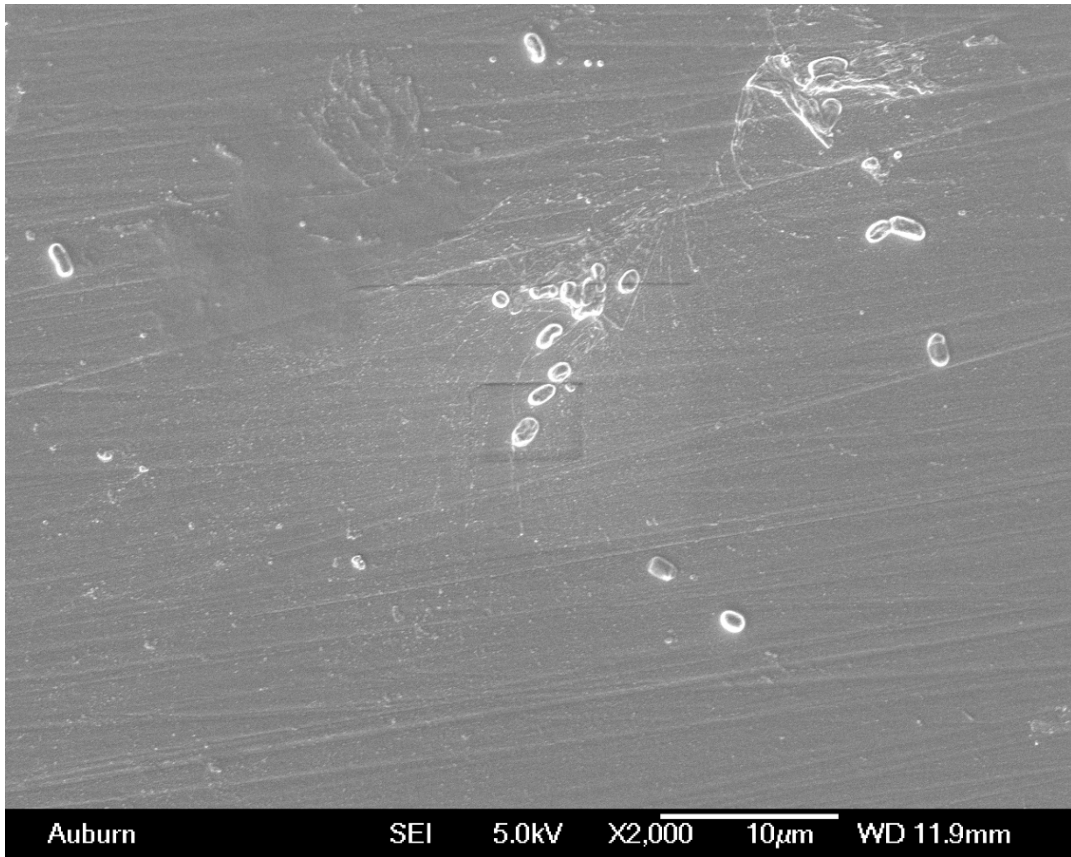
Figure 3-6: SEM image of *S. typhimurium* bound to a magnetoelastic sensor surface immobilized with an antibody film after exposure to a 5×10^3 cfu/ml concentration of bacterial solution.
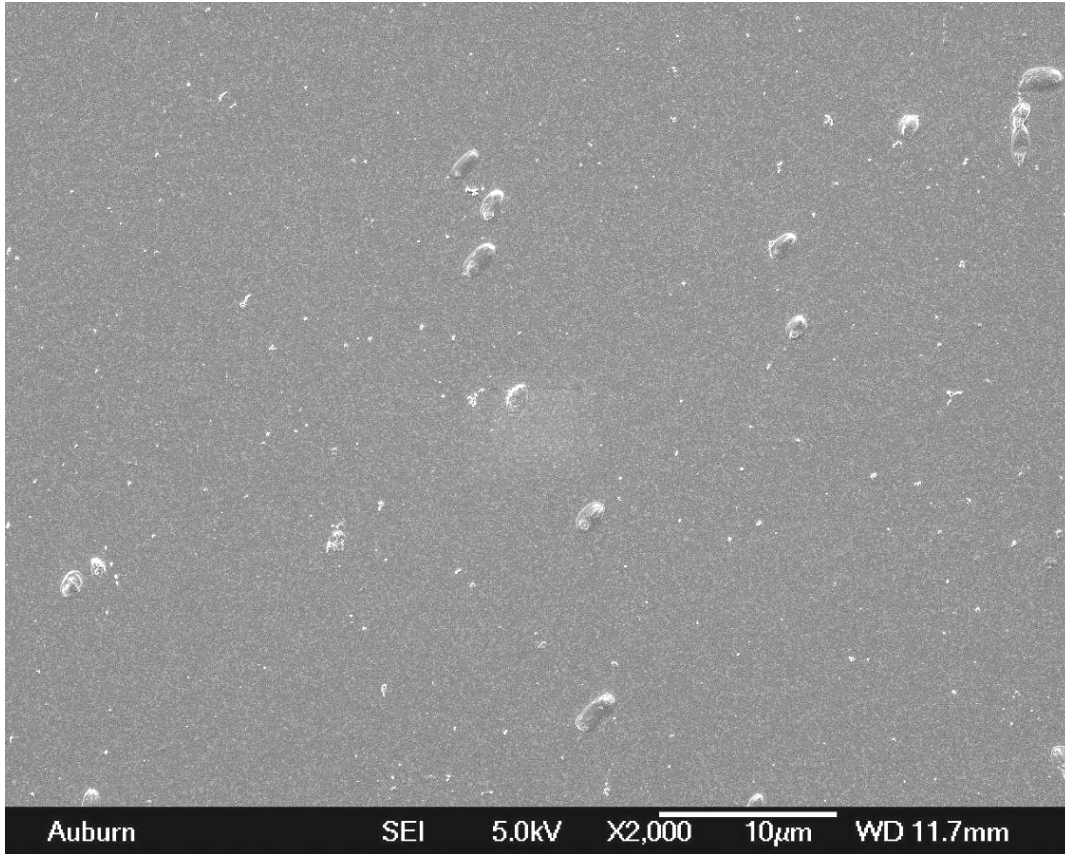
Figure 3-7: SEM image of magnetoelastic sensor surface without antibody film after exposure to a 5×10^8 cfu/ml concentration of bacterial solution.

3.6   Bacterial Density Calculations from SEM Images
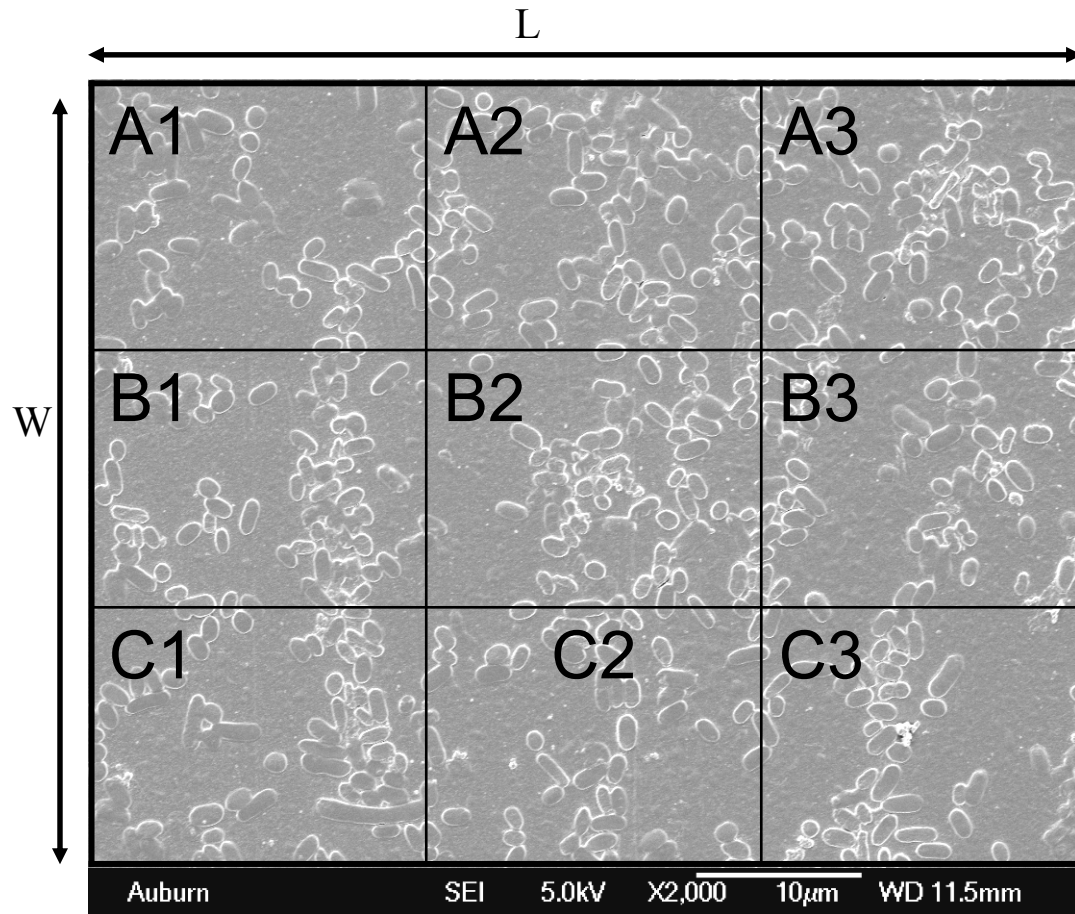
Figure 3-8: SEM image of a magnetoelastic sensor surface after immunoreaction with 5×10^8 cfu/ml concentration of *S. typhimurium*. An overlay grid is shown to illustrate the bacterial counting technique on the sensor surface.

Area of the SEM picture (A) $= L \times W$ μm^2

Total number of bacteria on the SEM surface (n) = A1+A2+A3+B1+B2+B3+C1+C2+C3

The distribution density D of *S. typhimurium* cells on the biosensor surface can be theoretically calculated as,

$$D = n / A \tag{3-1}$$

where, A is the actual area of the SEM image and "*n*" is the number of cells within the SEM image area.

The actual physical density of *S. typhimurium* cells can be obtained from the SEM images by counting the number of cells bound on the sensor surface and dividing this by the area of the surface. Several SEM pictures were taken on different areas of the biosensor surface and an average bacterial coverage density for each sensor surface was then calculated.

3.7 Calculation of Bound Bacteria Density Using Measured Frequency Shift

During the testing process, the temperature, humidity and other related parameters were kept constant, so the resonance frequency shift was the result of the increase in mass due to the analyte (*Salmonella typhimurium*) that was bound to the sensor surface. Since the increase in mass was very small compared to the initial mass of the sensor, according to the measured resonant frequency shift, Δf, the additional mass, Δm, due to bacteria binding could be determined from the following equation (3-2).

$$\Delta m = -2\Delta f M / f \tag{3-2}$$

For example, for a sensor with the dimensions of 5mm×1mm×15μm, the fundamental resonance frequency could be determined from Equation (1-3). Using a Young's modulus value, E, of 110 GPa for the magnetoelastic material, a Poisson's ratio, σ, of approximately 0.3, and a magnetoelastic alloy density, ρ, of 7.9g/cm^3 [161] the calculated fundamental resonance frequency of the biosensor was 428 kHz. The sensor's natural mass (with no bacteria attached) was measured as 5.925 x 10^{-4} gm. Thus, the additional mass Δm due to bacteria binding can be calculated from equation (3-3):

$$\Delta m = -2769 \Delta f \tag{3-3}$$

Where Δf is the frequency shift in Hz, and Δm is the additional mass in Pico grams (pg).

Since the mass of each *S. typhimurium* cell is about 2 pg, the number of *Salmonella typhimurium* cells "n" bound on the sensor's surface can be theoretically determined:

$$n = \Delta m / 2 \tag{3-4}$$

The density of *S. typhimurium* cells on the biosensor surface can then be calculated from equation (3-4) (i.e. *n*/A).

3.8   Description of the Measurement Setup

Magnetoelastic materials have a characteristic resonant frequency like other acoustic resonance sensors. For rectangular-shaped, sheet magnetoelastic sensors, the frequency is based primarily on its length and mass. A mass increase due to bacteria binding to the sensor results in a lower resonant frequency. By applying an alternating

magnetic field at the mechanical resonant frequency, the material can be made to resonate.

A coil of wire known as pickup coil is used to sense the change in flux through the sensor. Since the inductance of a coil of wire changes with flux density through the coil, and since an increase in inductance results in a higher resistance (impedance) to a current change in the coil, a device that senses current change can be used to determine the resonant frequency of the magnetoelastic sensor.

A network analyzer operating in reflected impedance mode is an ideal device for sensing the resonant frequency. It applies a voltage and monitors the current in the coil. An external magnet is used to bias the magnetoelastic sensor to its point of greatest sensitivity. The network analyzer is then used to apply a small alternating voltage to the coil and monitors changes in the coil current due to the changing flux in the sensor. The network analyzer sweeps the frequency from a low starting value to a higher ending value. The resonance frequency is located by identifying the minimum in the amplitude versus frequency curve. Any change in mass due to the binding of bacteria to the sensor surface will cause a reduction in the resonance frequency.
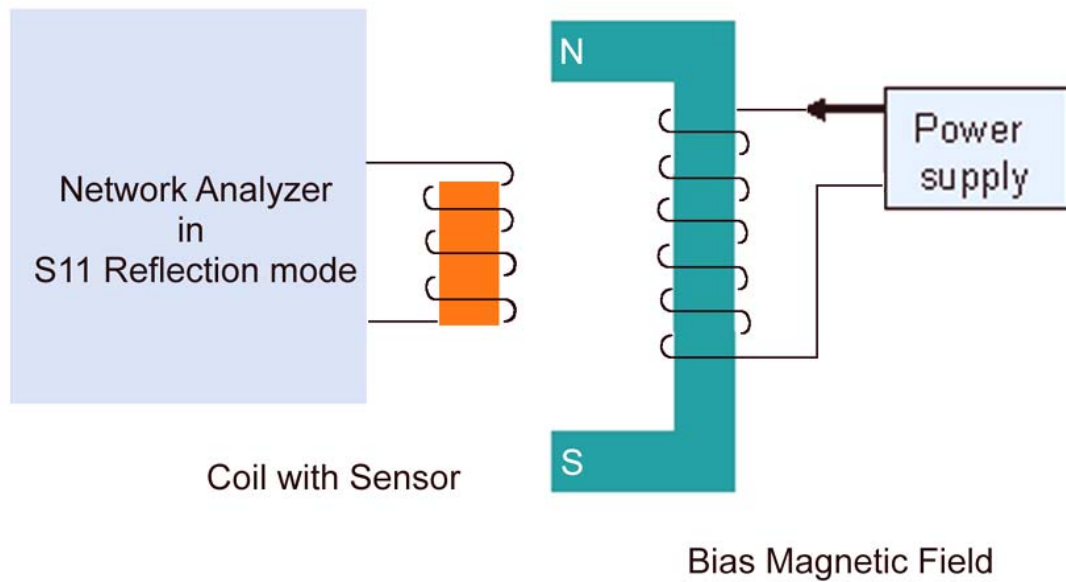
Figure 3-9: Schematic of sensor measurement set up.

3.8.1 Network analyzer measurement procedure

A network analyzer was used in this study to monitor changes in the electrical impedance with the excitation frequency (f) over a predetermined frequency range near the fundamental resonance frequency of the magnetoelastic sensor. 801 points were recorded over the frequency range with an 11.31 sec sweep time. A standard open circuit calibration was used to minimize experimental errors in the test set up. The resonance frequency of the sensors was measured using an HP network analyzer 8751A with S-parameter test set both before and after the binding of bacterial cells to the immobilized antibody on the sensor. A personal computer was used to acquire data at two minute intervals.

60
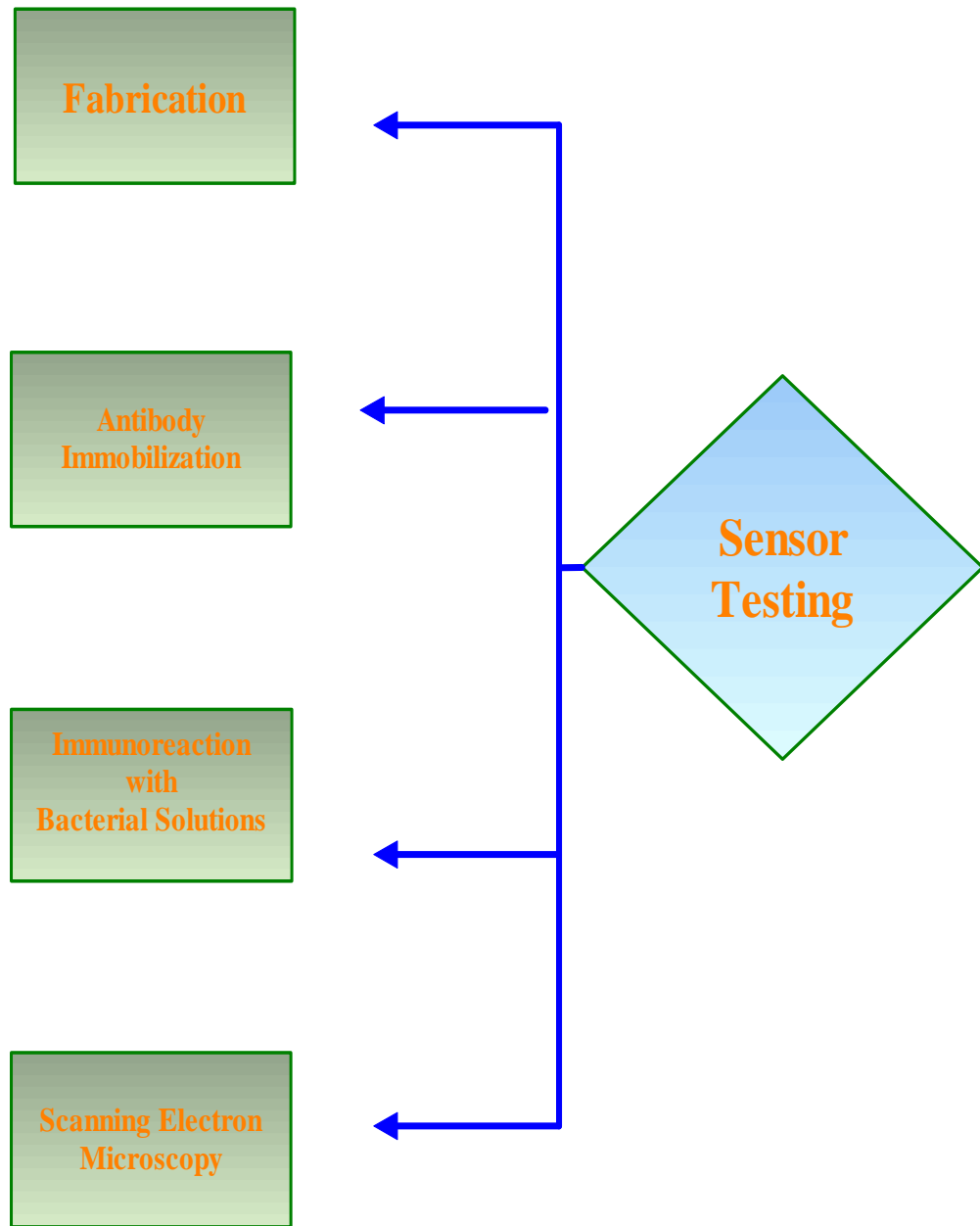
Figure 3-10: Flow chart showing the steps in sensor testing.
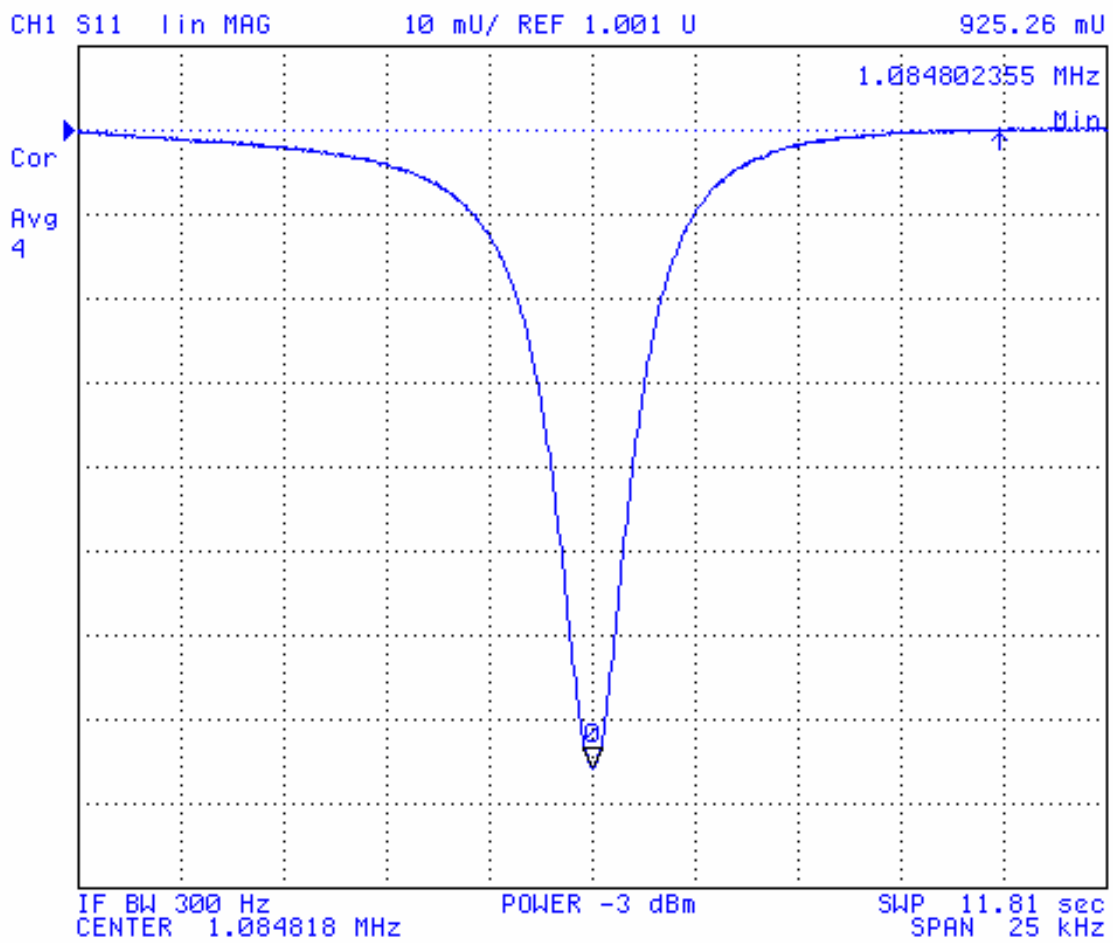
Figure 3-11: 2×0.4×0.015 *mm* size sensor frequency spectrum on network analyzer.

3.9   Hill Plot and Determination of Dissociation of Binding

The association and disassociation of an antibody and antigen in solution can be expressed by:

$$nSt \; + \; Ab \quad \underset{k_d}{\overset{k_a}{\Leftrightarrow}} \quad St_n Ab \tag{3-5}$$
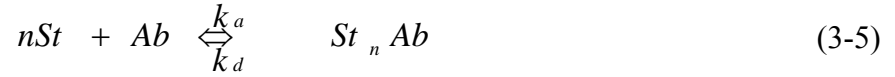
Where *St* represents the *S. typhimurium* in solution that is captured on the sensor, *Ab* represents the immobilized antibody on the sensor in solution, *StAb* is the bacteria-antibody complex, and k_a and k_d are the association and dissociation rate constants, respectively. The equilibrium constant, or the affinity (K), is given by:

$$K = \frac{k_a}{k_d} = \frac{[St^n Ab]}{[St]^n \; [Ab]} \tag{3-6}$$

$$K_d = \frac{1}{K_a} = \frac{[St]^n [Ab]}{[St_n Ab]} \tag{3-7}$$

The association in the above mixture is primarily affected by the diffusion of the bacterial cells through the solution to the sensor surface i.e, the number of bacteria cells that may come in contact with the immobilized antibody on the sensor. In contrast, the dissociation of the reaction is chiefly governed by the strength of the bonding between the bacterial cells in solution and the immobilized antibody on the sensor. This is further dependent on the type of immobilization technique used because the immobilization

63

technique establishes the single or multi site bonding between the immobilized antibody and the bacterial cells in solutions that come in contact with one another.

The association (K_a) and the disassociation constant (K_d) are calculated using a Hill plot [163]. The degree of binding can be estimated using the Hill coefficient (n), which is the slope of the Hill plot [163]. Binding valency is the reciprocal of the Hill coefficient. The Hill plot is derived by plotting log θ versus log [L], where [L] is the ligand (*S. typhimurium*) concentration and θ is given by the equation:

$$\theta = \frac{Y}{1-Y} \qquad (3\text{-}8)$$

where $Y = \Delta F / \Delta F_{max}$ [164] and F denotes the shift in frequency obtained after bacterial binding to the antibody immobilized sensor and Δf_{max} was considered as the maximum frequency shift response that can be measured before the sensor reaches saturation (i.e. saturation point). This was obtained from the sigmoid curve fitting to the sensor response data. Stronger antibody-bacterial binding is indicated by lower K_d values, which in turn imply higher sensitivity of the biosensor.

4 RESULTS AND DISCUSSION

4.1 Concentration Tests in a Static Environment

The performance of various sizes of magnetoelastic sensors was investigated in a static environment. The Sensors were immobilized with antibody as explained in the experimental section. Resonance frequency of the antibody immobilized sensor was measured before and after the exposure to bacterial solutions. The shift in resonance frequency was associated with the level of bacterial attachment.

4.1.1 Response curves

Figure 4-1 shows the frequency spectrum obtained from a 2×0.4×0.015mm biosensor before and after exposure to a solution containing *S. typhimurium* at a concentration of 1×10^9 cfu/ml. The figure shows that amplitude of frequency spectrum increases to a maximum at the resonance frequency and then decreases. The response obtained clearly shows that the resonance frequency of the magnetoelastic sensor decreases as a result of the binding of analyte (*S. typhimurium*) to the sensor surface. For these test conditions, a shift of 691 Hz was obtained.
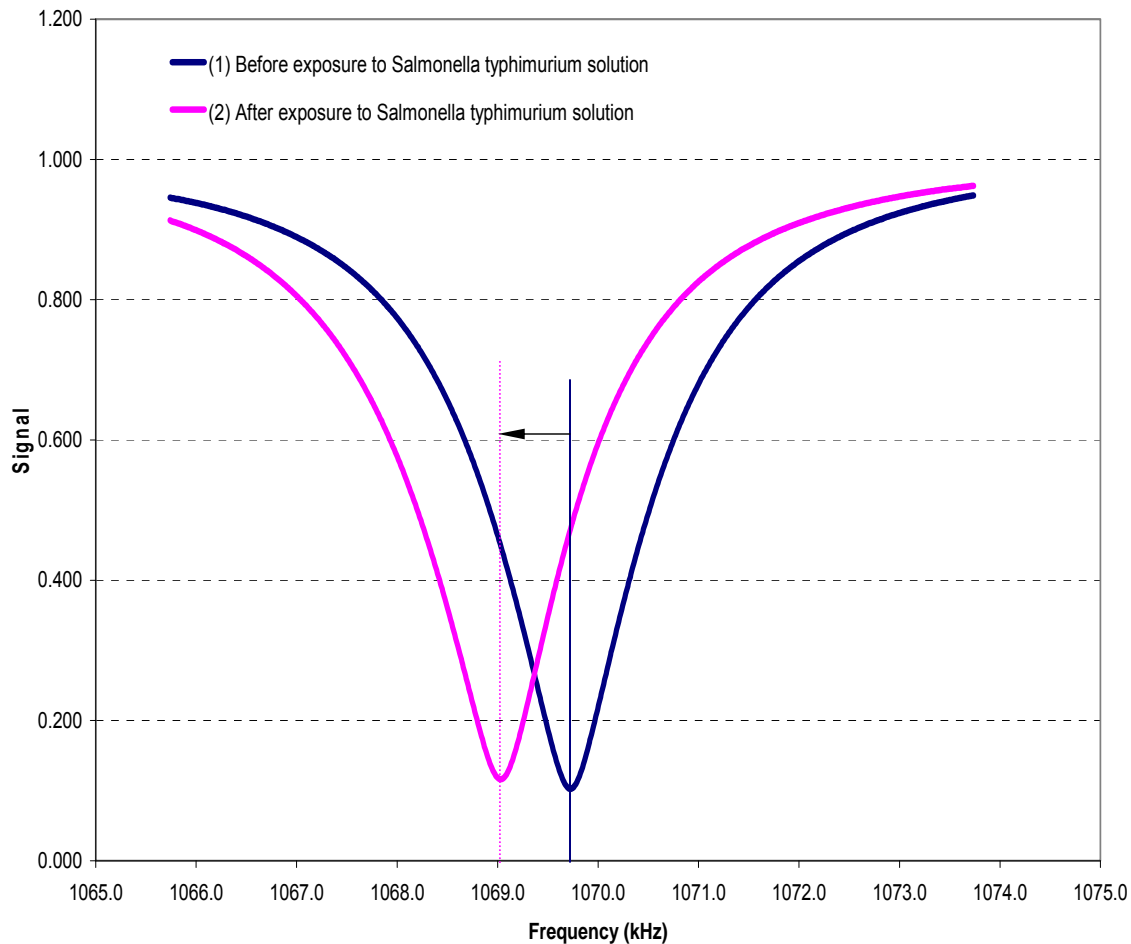
Figure 4-1: Frequency spectrum of the antibody immobilized biosensor with a size of 2 ×0.4×0.015*mm*. (1) Before exposure to *S. typhimurium* solution the resonant frequency f_0 was 1069724 Hz. (2) After exposure to a solution containing *S. typhimurium* with a concentration of 1×10^9 cfu/ml, the resonant frequency f_1 decreased to 1069033 Hz. The resonant frequency shift Δf due to the binding of analyte (*S. typhimurium*) to the sensor surface was therefore: $\Delta f = f_0 - f_1 = 1069724$ Hz -1069033 Hz $= 691$ Hz.
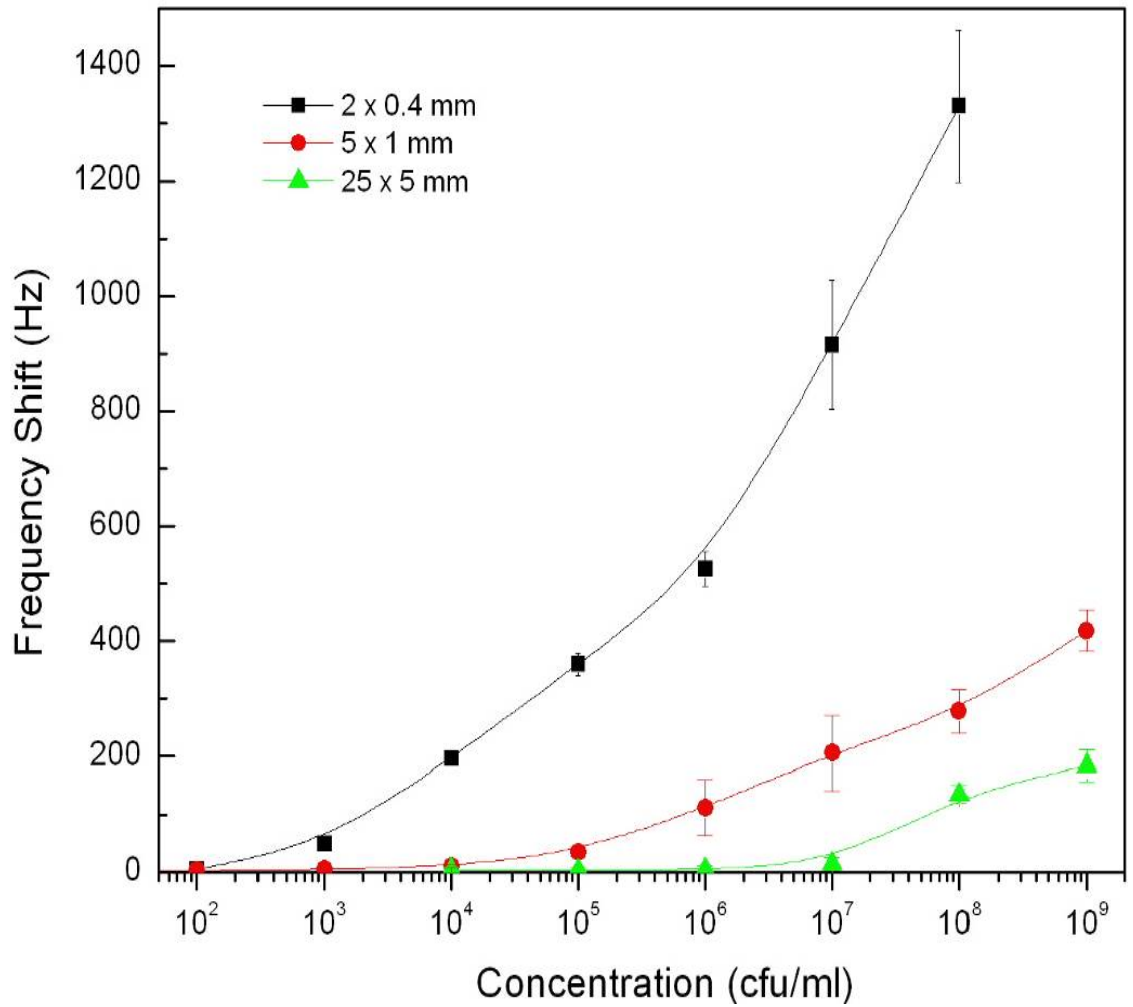
Figure 4-2: The resonant frequency shift upon exposure to solutions containing *S. typhimurium* bacteria with different concentrations ranging from 10^2 cfu/ml to 10^9 cfu/ml for 15 μm thick sensors: (1) 2×0.4mm (■), (2) 5×1mm (●) and (3) 25×5mm (▲). The detection limit is $5×10^3$, 10^5 and 10^7 cfu/ml, respectively.

4.1.2   SEM observation

In order to confirm that the frequency shifts were mainly caused by the binding of

S. typhimurium to the sensor's surface, SEM images were taken for all the sensors upon

exposure to the bacterial solutions. Figures 4-3 to 4-7 show typical SEM images for the

biosensors with a size of 5×1mm after exposure to different concentrations of *S.*

typhimurium ranging from 10^9 to 10^5 cfu/ml. The figures clearly show that exposure to

decreasing concentrations of *S. typhimurium* led to a lower density of bound bacteria on

the biosensor's surface, with consequently smaller frequency shifts. The control sensor,

which had no antibody on its surface, was subjected to the highest concentration of 10^9

cfu/ml and had almost no binding of *S. typhimurium* cells. This confirms that the *S.*

typhimurium cells bind specifically to the immobilized antibody, and that the antibody

was effectively immobilized on the sensor surface using the LB technique.
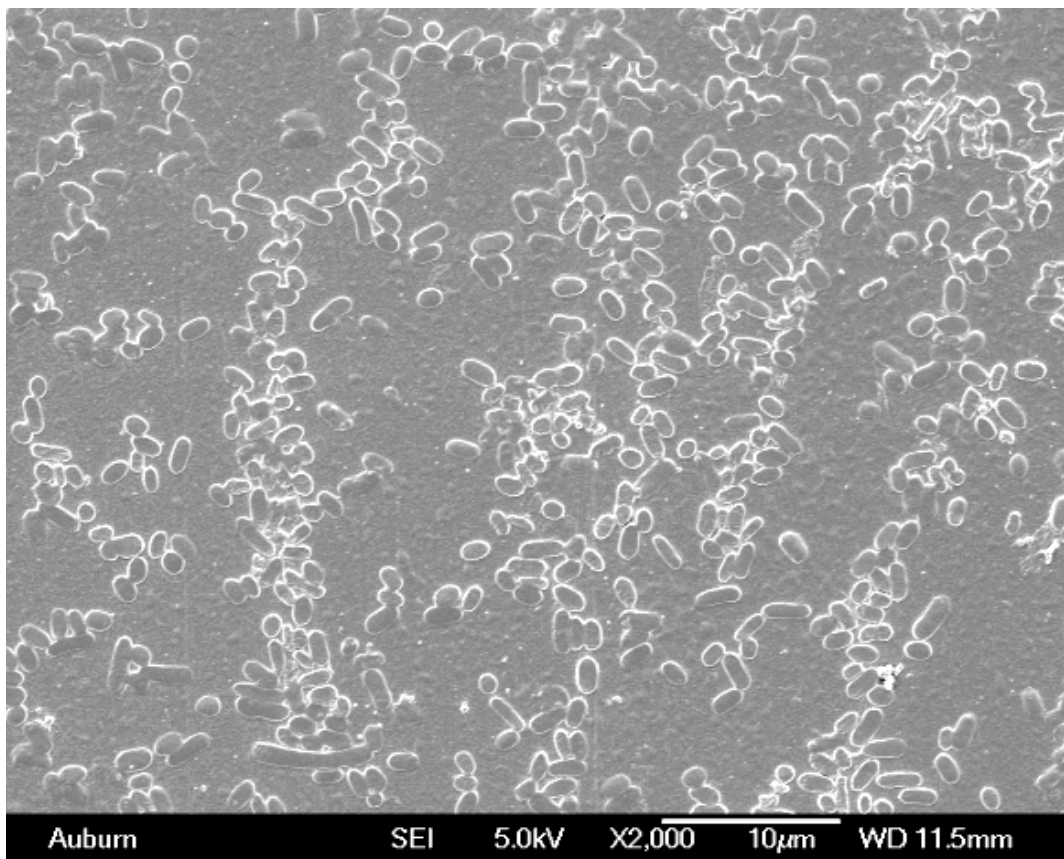
Figure 4-3: Typical SEM images of *S. typhimurium* bound to an antibody immobilized magnetoelastic resonance biosensor surface exposed to solutions containing 10^9 cfu/ml concentration of bacteria.
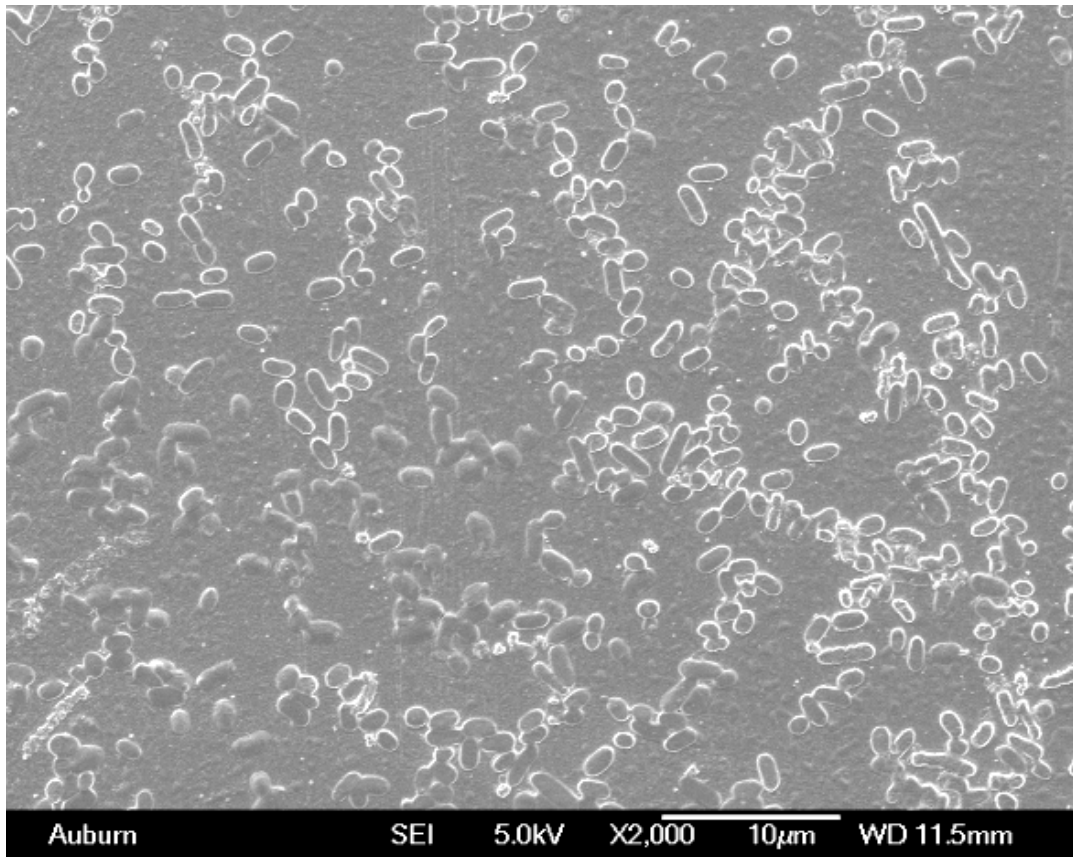
Figure 4-4: Typical SEM images of *S. typhimurium* bound to an antibody immobilized magnetoelastic resonance biosensor surface exposed to solutions containing 10^8 cfu/ml concentration of bacteria.
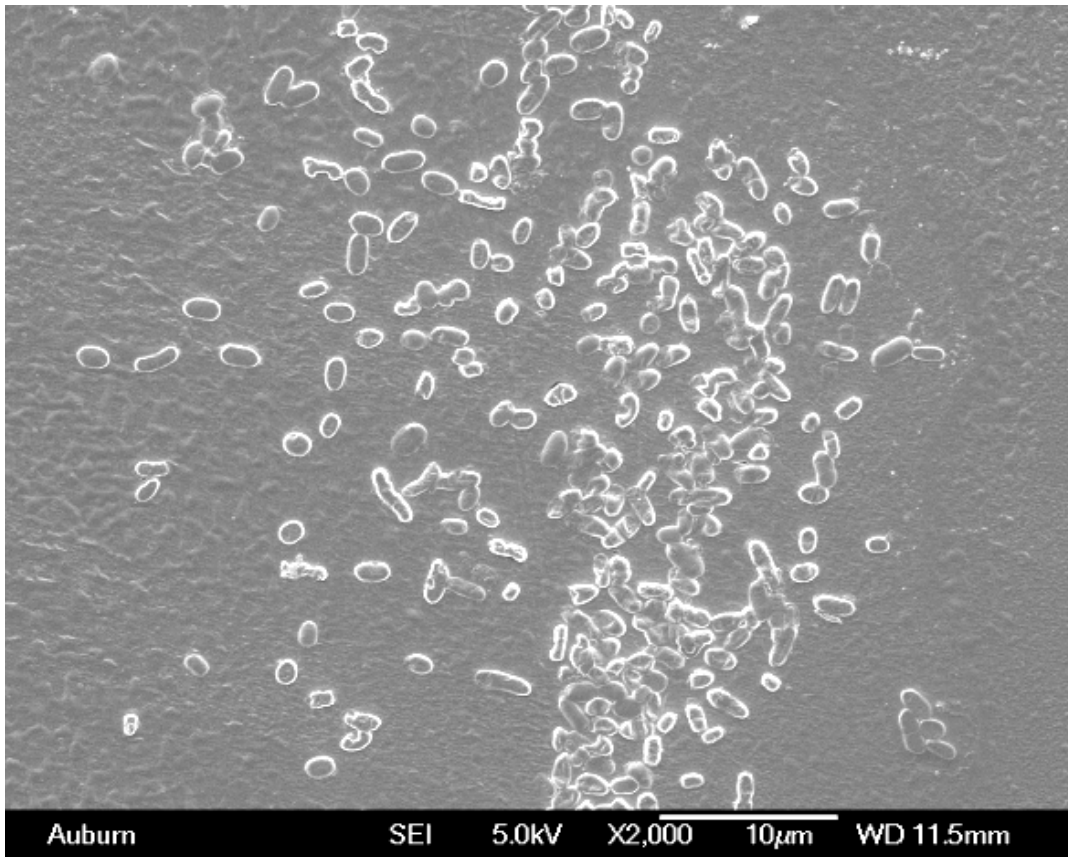
Figure 4-5: Typical SEM images of *S. typhimurium* bound to an antibody immobilized magnetoelastic resonance biosensor surface exposed to solutions containing 10^7 cfu/ml concentration of bacteria.
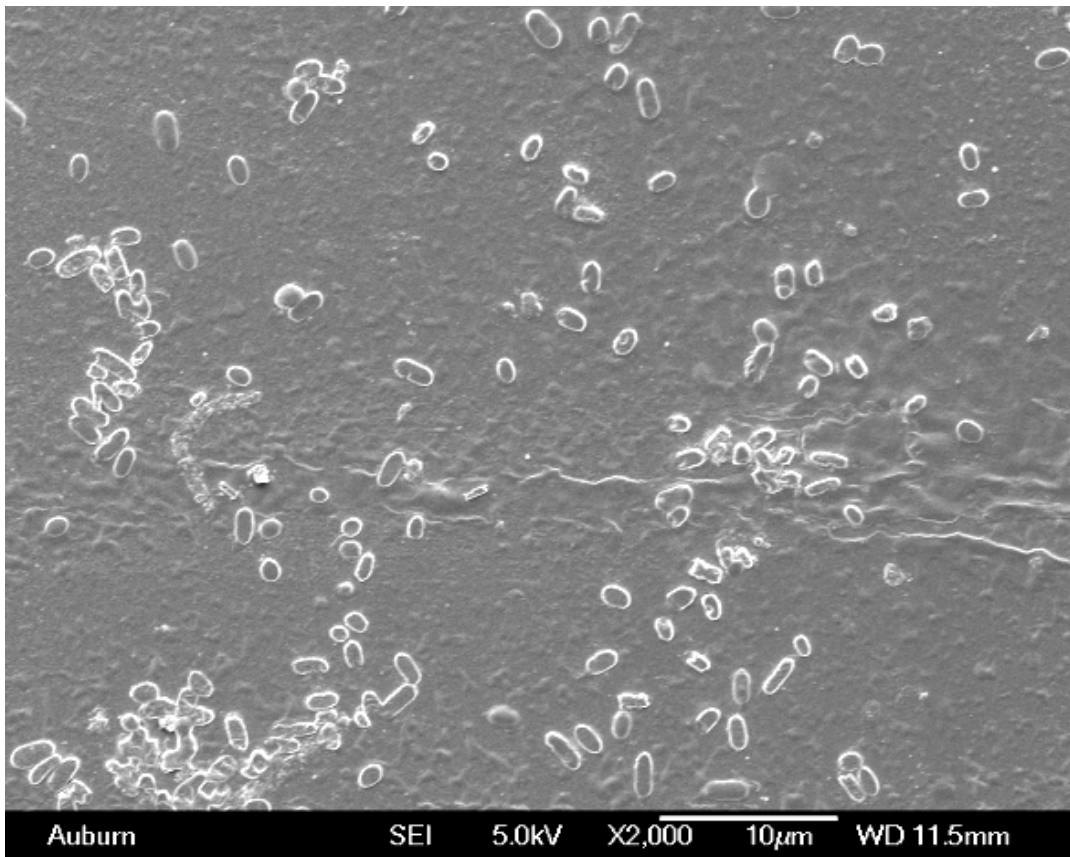
Figure 4-6: Typical SEM images of *S. typhimurium* bound to an antibody immobilized magnetoelastic resonance biosensor surface exposed to solutions containing 10^6 cfu/ml concentration of bacteria.
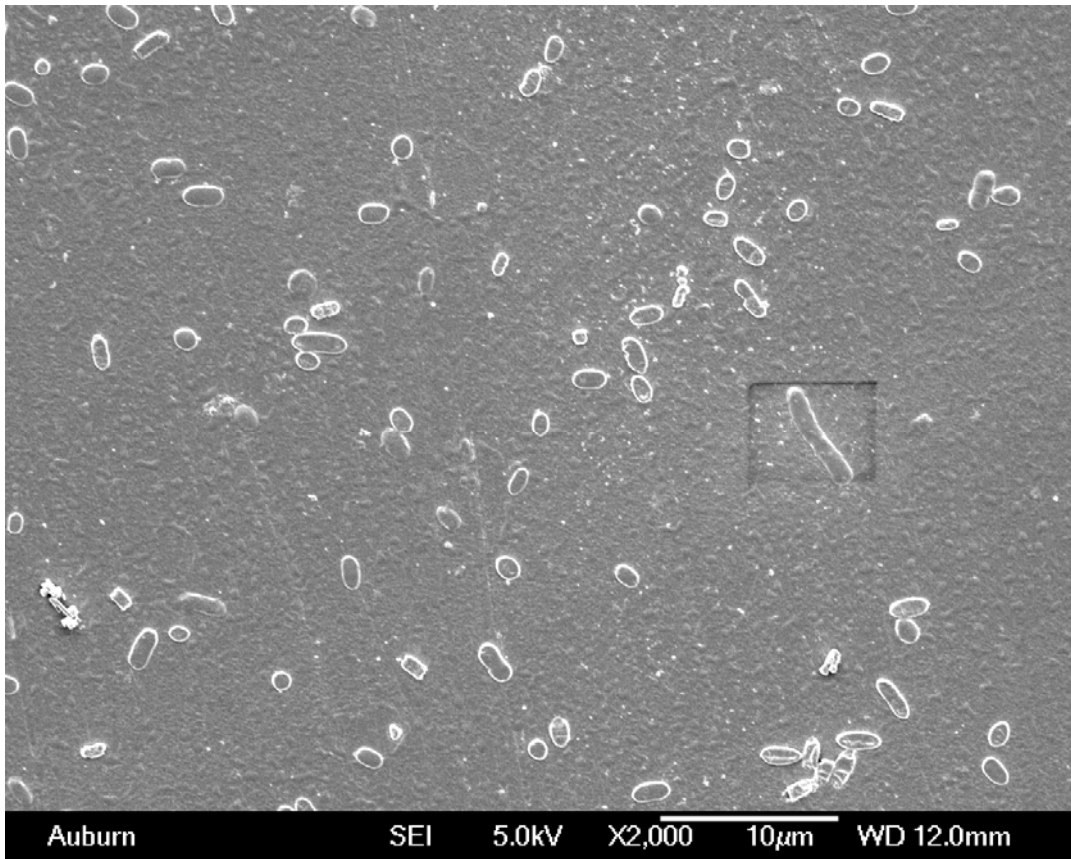
Figure 4-7: Typical SEM images of *S. typhimurium* bound to an antibody immobilized magnetoelastic resonance biosensor surface exposed to solutions containing 10^5 cfu/ml concentration of bacteria.

4.1.3 Correlation between SEM images and frequency shifts

Two different methods can be used to calculate the number of bacteria that have been captured on the surface of a magnetoelastic resonance biosensor. The first method is to calculate the area density of bacteria that attach to the sensor surface (bacteria attached per unit area) based upon the measured frequency shift of the biosensor. The second method is to directly count the number of bacteria attached to the sensor surface using SEM and statistically convert this to an area density of bacteria attached to the sensor surface. This section compares the results obtained using these two different methods.
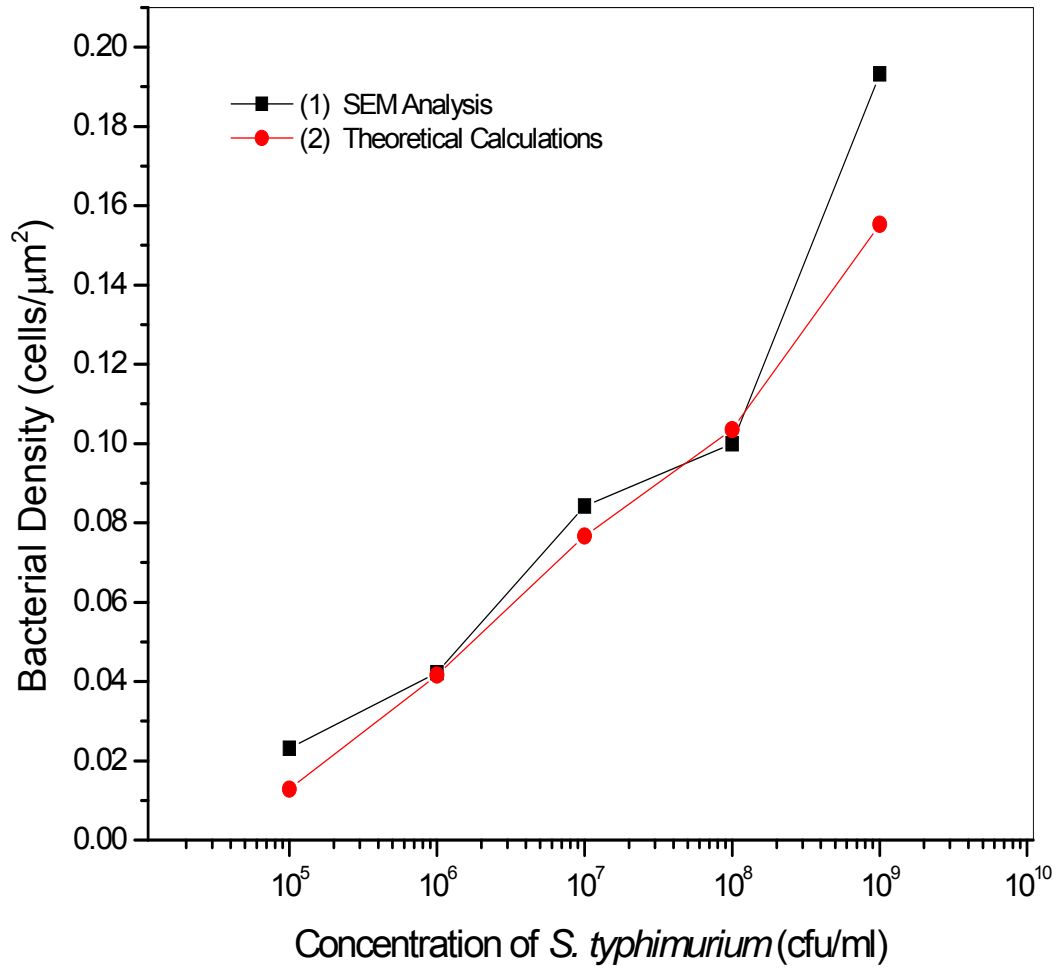
Figure 4-8: Comparison of density of captured correlation of distribution of bacterial cells and the theoretically expected values for antibody immobilized sensors with a size of 5 ×1×0.015mm. (1) Actual density of bacterial cells obtained from SEM images; and (2) theoretically expected density calculated from the measured frequency shift.

4.1.4   Discussion

In order to investigate the effect of the sensor size on the sensitivity of detection, sensors with different dimensions were prepared and exposed to various known concentration of *S. typhimurium* suspensions. Figure 4-2 shows the resonant frequency shift for three different size sensors after exposure to solutions containing *S. typhimurium* with concentrations ranging from 10^2 to 10^9 cfu/ml. The figure 4-2 clearly shows that the smaller the sensor size, the lower the detection limit, and the smaller the size, the bigger the resonant frequency shifts for the same concentration. These observations are also in good agreement with theory (equation 1-7). From the responses obtained, it can be seen that the detection limits are 5×10^3, 10^5 and 10^7 cfu/ml for sensors with the size of $2 \times 0.4 \times 0.015$ mm, $5 \times 1 \times 0.015$ mm and $25 \times 5 \times 0.015$ mm, respectively. SEM images provided visual verification that the measured frequency shifts were in fact due to the attachment of bacteria to the sensor surface. A good agreement was obtained, between the numbers of bound bacterial cells counted from SEM images and that calculated from frequency shifts.

4.2   Concentration Tests in Food Products

The performance of the magnetoelastic biosensor was investigated for the detection of *S. typhimurium* in food products such as water, fat-free milk, and apple juice. Antibody coated sensors were exposed to increasing concentrations (5×10^1 to 5×10^8 cfu/ml) of *S. typhimurium* spiked into liquid media in a flow through mode (at a flow rate of 100 μl/min for 10 minutes). The value of the resonance frequency was tracked to detect any changes due to the attachment of bacteria from the selected liquid media. Measurements were made at intervals of 2 minutes.   All sensors were tested under

identical conditions by controlling parameters such as temperature and humidity unless otherwise specified. Under identical conditions, the change in resonance frequency generated by the sensors before and after exposure to the bacterial solutions can be attributed to the increase in mass of the bound analyte (*S. typhimurium*) on the sensor surface.

4.2.1 Response curves

Figures: 4-9 to 4-11 depict the dynamic response of the magnetoelastic biosensor when exposed to increasing concentrations (5×10^1 cfu/ml through 5×10^8 cfu/ml) of *S. typhimurium* suspensions in different liquid media (water, fat free milk and apple juice). A peristaltic pump was used to flow bacterial suspension at a constant flow rate of 100 μl/min for 10 minutes, allowing 1 ml of liquid from each concentration to pass over the sensor. To simulate the real world conditions the bacterial solutions were not recycled. At higher concentrations of bacterial solutions it can be seen that the response time was approximately 120 seconds. From the experiments, it was found out that the sensors have shown a steady state response after 10 minutes. So the response at 10 minutes was taken as the resultant frequency shift for these experiments.
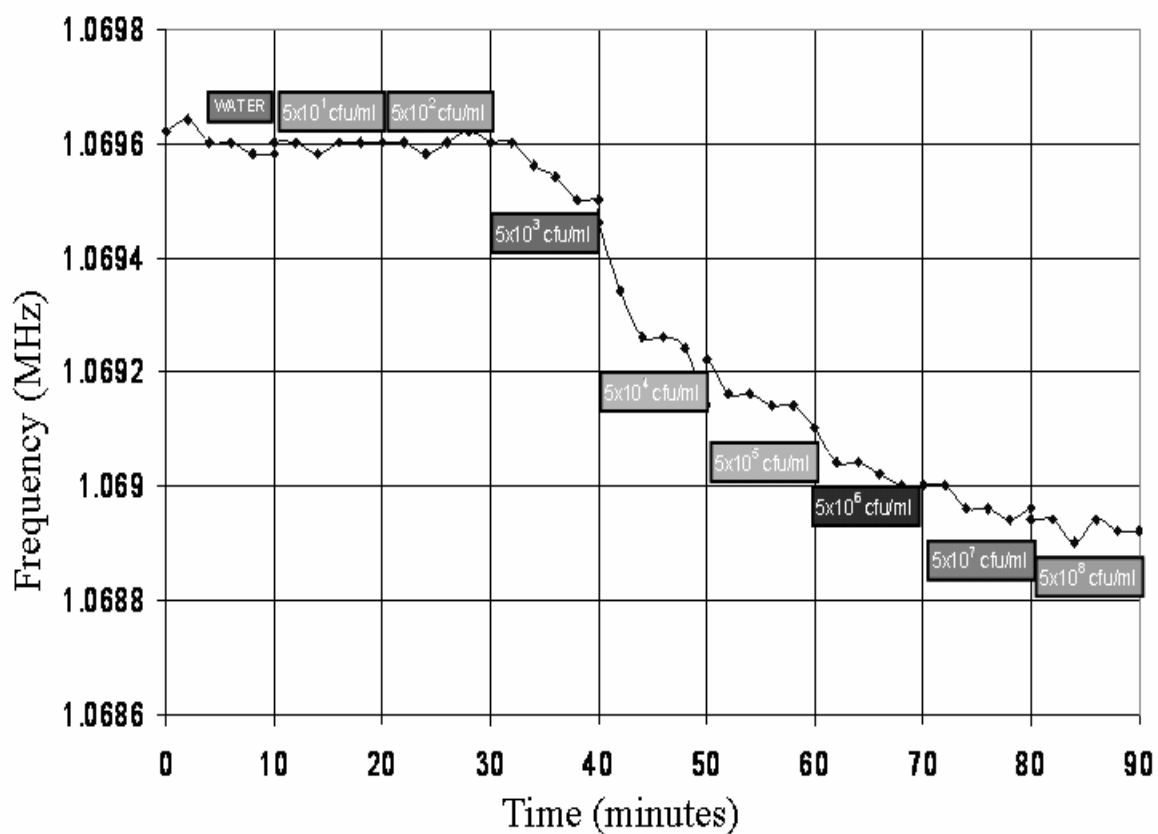
Figure 4-9: Magnetoelastic biosensor response when exposed to different concentrations (5×10^1 through 5×10^8 cfu/ml) of *S. typhimurium* suspensions in water. Water with no bacteria was used as a reference. Data was recorded at two minute intervals. Each concentration of bacterial suspension was run for 10 minutes at a flow rate of 100 µl/min.
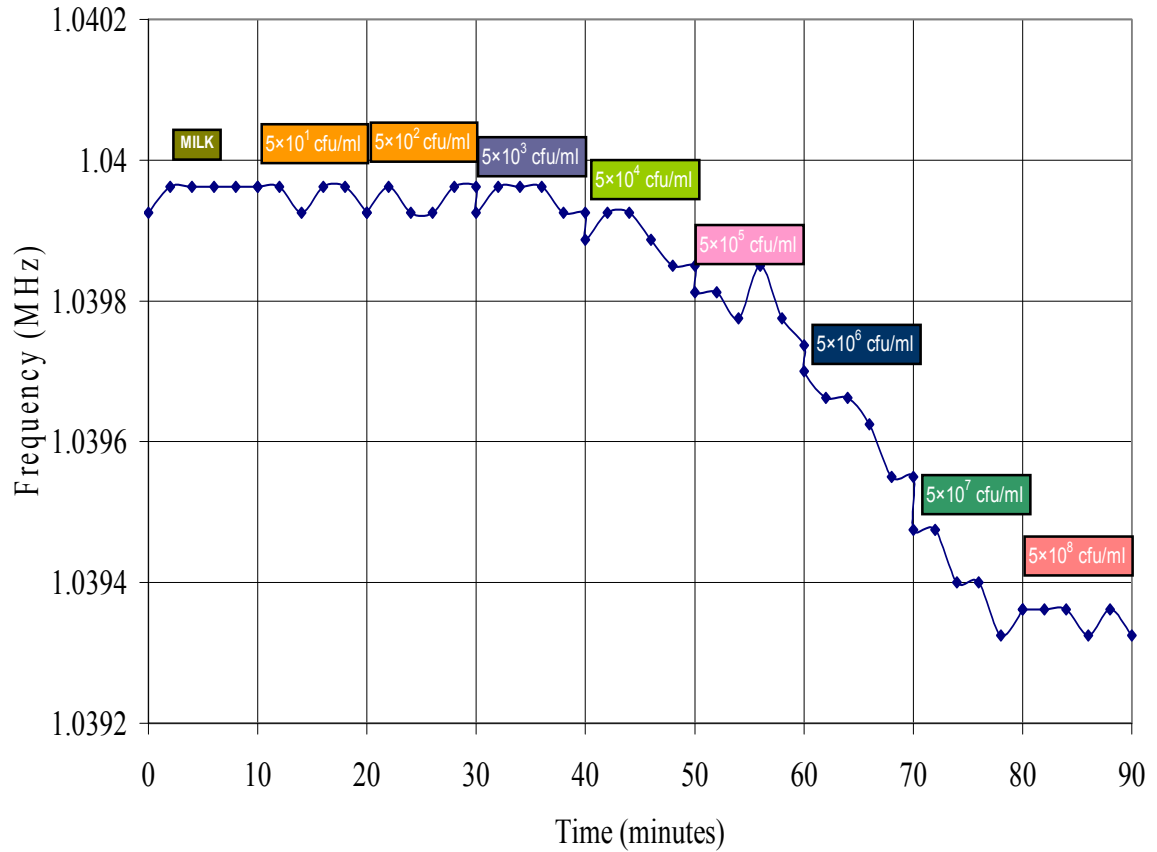
Figure 4-10: Magnetoelastic biosensor response when exposed to different concentrations (5×10^1 through 5×10^8 cfu/ml) of *S. typhimurium* suspensions in fat free milk. Fat free milk with no bacteria was used as a reference. Data was recorded at two minute intervals. Each concentration of bacterial suspension was run for 10 minutes at a flow rate of 100 μl/min.
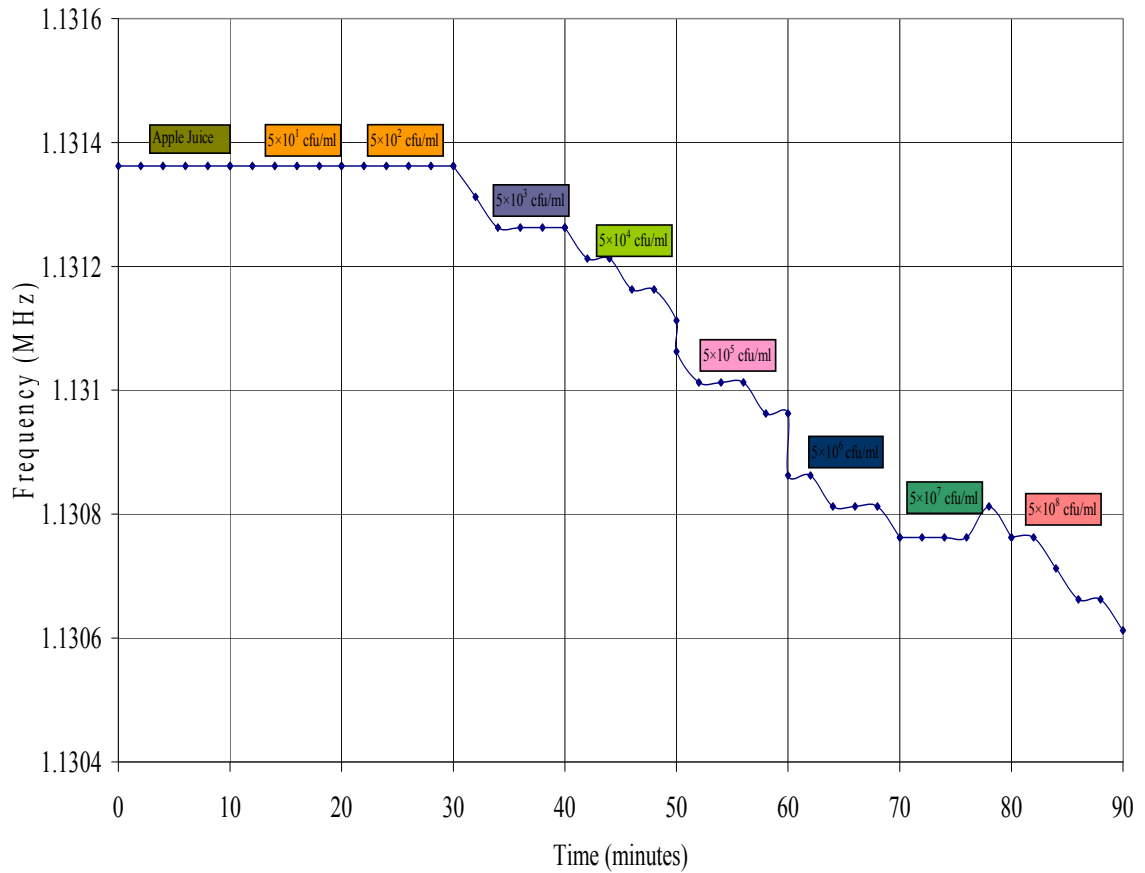
Figure 4-11: Magnetoelastic biosensor response when exposed to different concentrations (5×10^1 through 5×10^8 cfu/ml) of *S. typhimurium* suspensions in apple juice. Apple juice with no bacteria was used as a reference. Data was recorded at two minute intervals. Each concentration of bacterial suspension was run for 10 minutes at a flow rate of 100 μl/min.
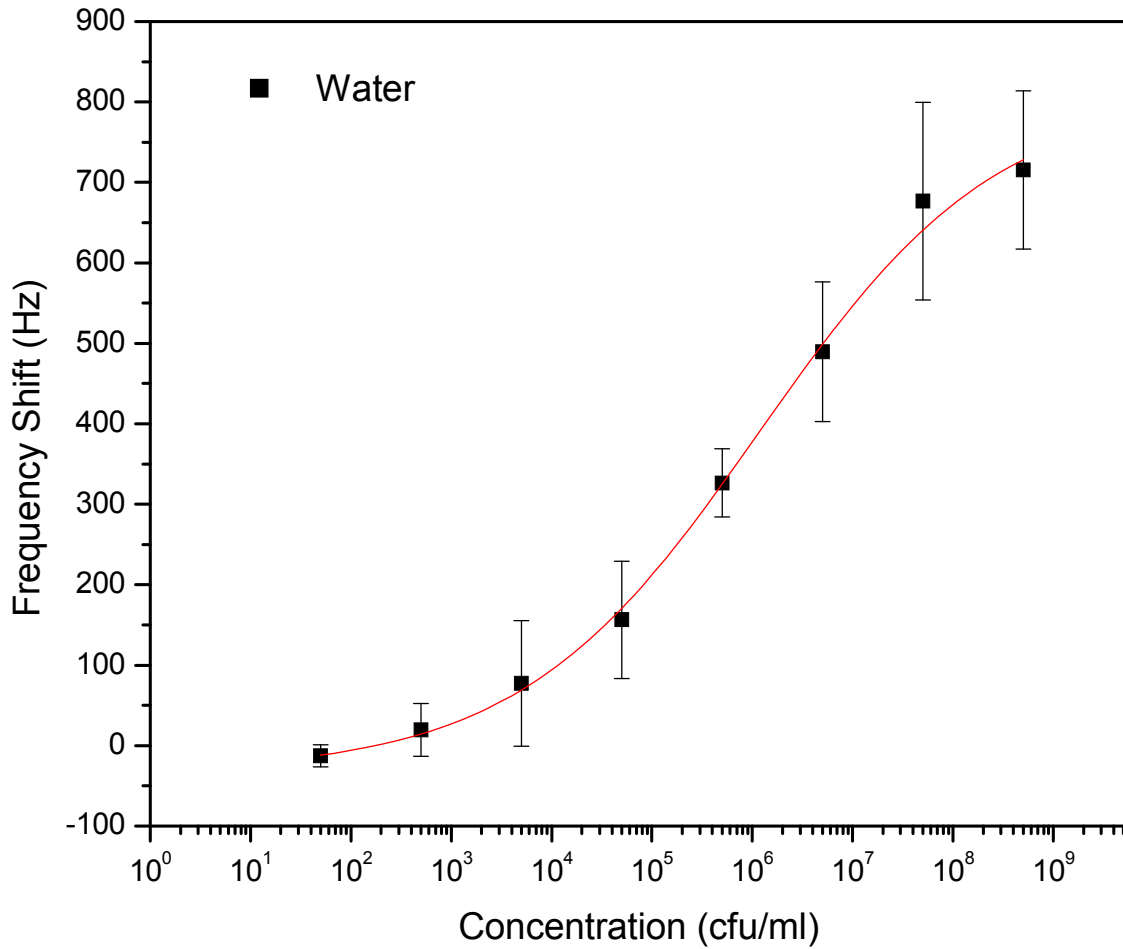
Figure 4-12: Magnetoelastic biosensor response when exposed to different concentrations (5×10^1 cfu/ml through 5×10^8 cfu/ml) of *S. typhimurium* suspensions in water. The smooth curve is a sigmoid fit of the experimental data. (R^2=0.9988 and χ^2 =0.0479). Bars represent standard deviation.
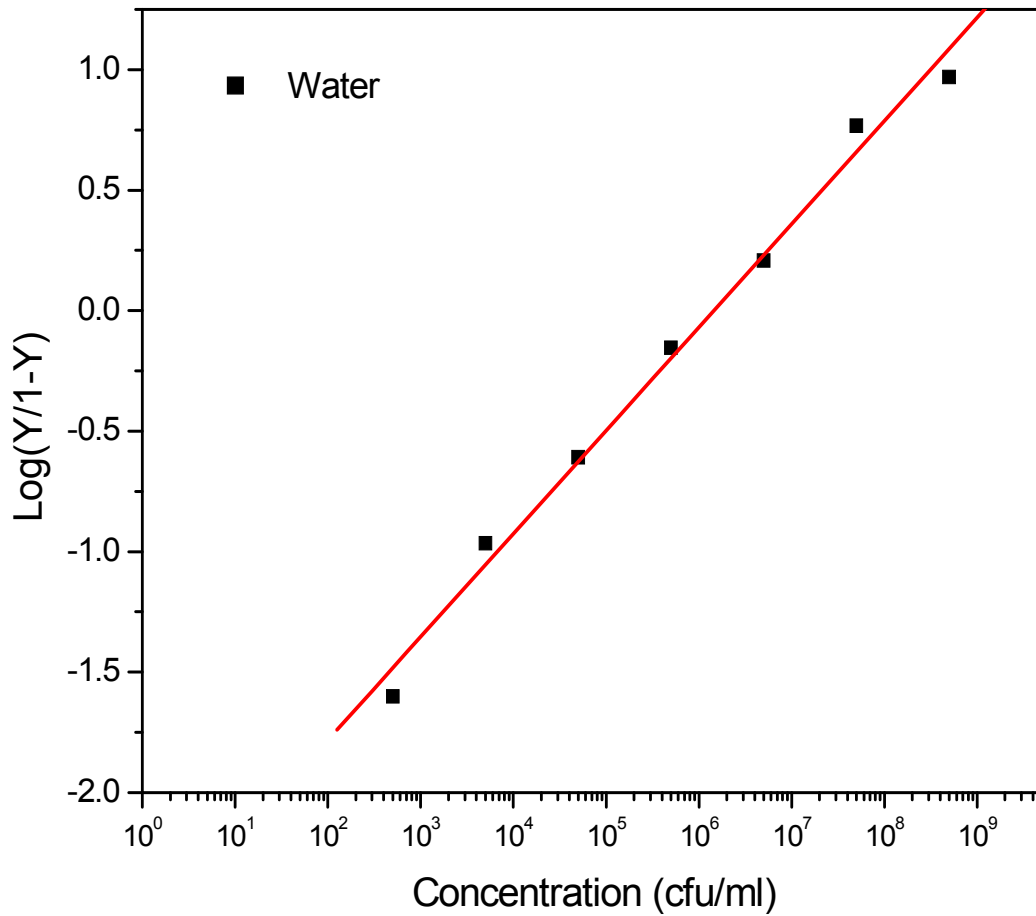
Figure 4-13: Hill plot showing the logarithmic ratio of occupied and free antibodies as a function of concentration of *Salmonella typhimurium* in water. The squares represent experimental data. The line represents the least square fit with coefficients: K_d=435 ± 76 cfu/ml and n_h=0.428 ± 0.02. (*R*=0.99, *P*<0.0001).
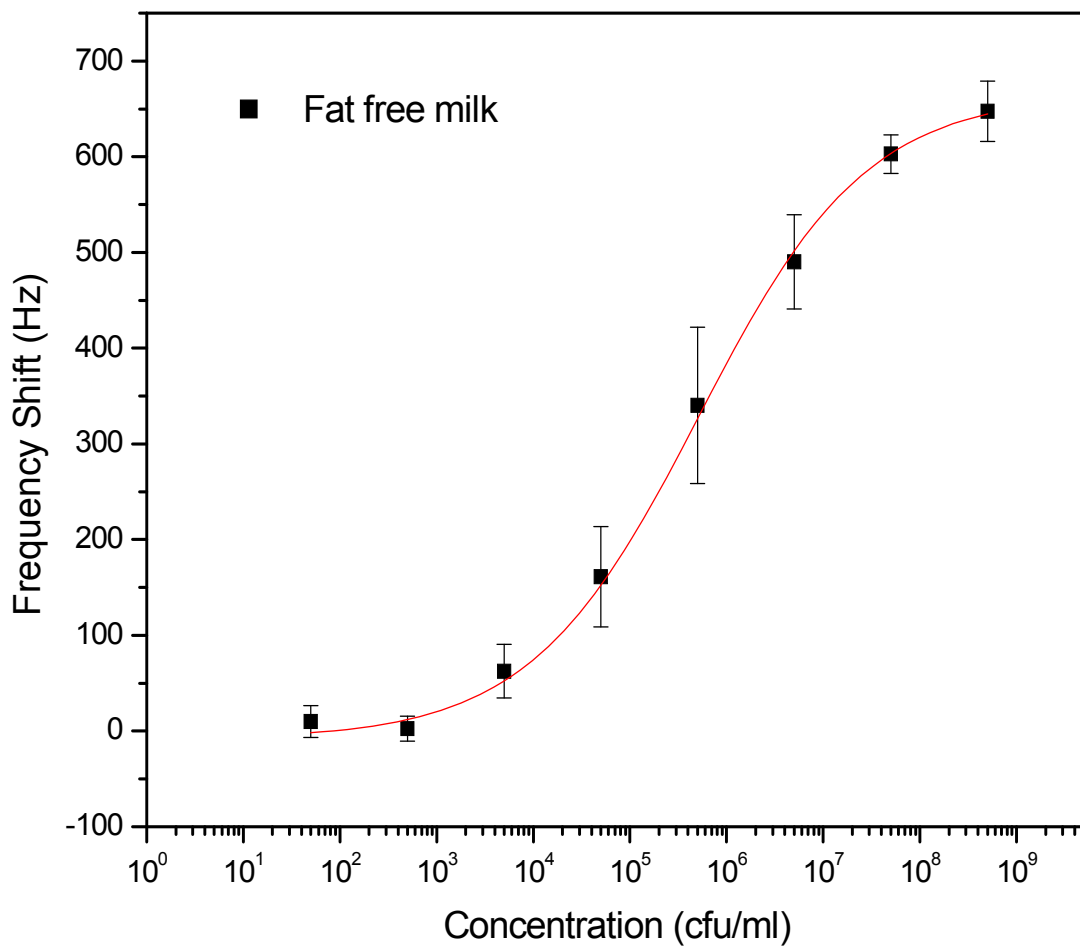
Figure 4-14: Magnetoelastic biosensor response when exposed to different concentrations (5×10^1 cfu/ml through 5×10^8 cfu/ml) of *S. typhimurium* suspensions in fat free milk. The smooth curve is a sigmoid fit of the experimental data. (R^2=0.9987 and χ^2 =0.3243). Bars represent standard deviation.
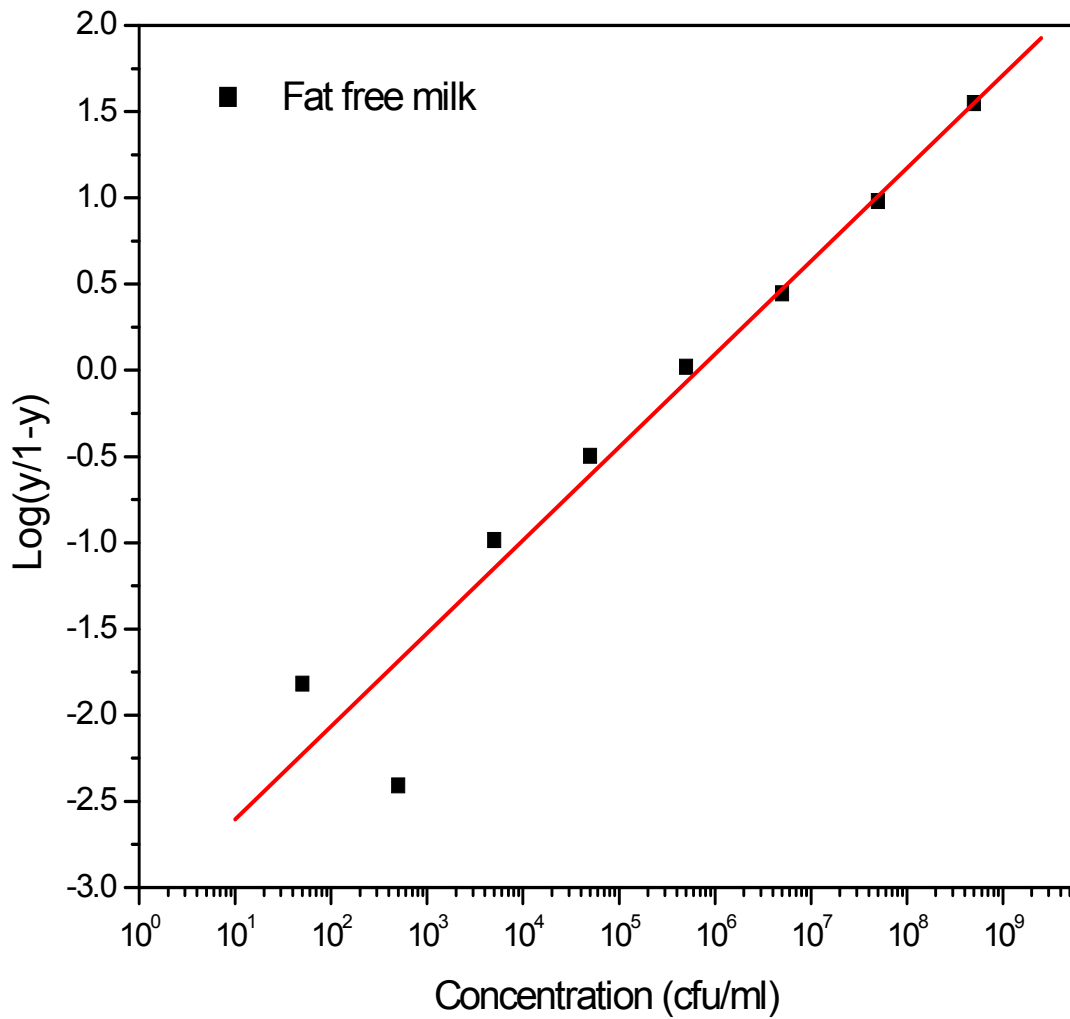
Figure 4-15: Hill plot showing the logarithmic ratio of occupied and free antibodies as a function of concentration of *S. typhimurium* in fat free milk. The squares represent experimental data. The line represents the least square fit with coefficients: K_d=1389 $\pm$ 142 cfu/ml and n_h=0.539 $\pm$ 0.02. (*R*=0.9712, *P*<0.0001).
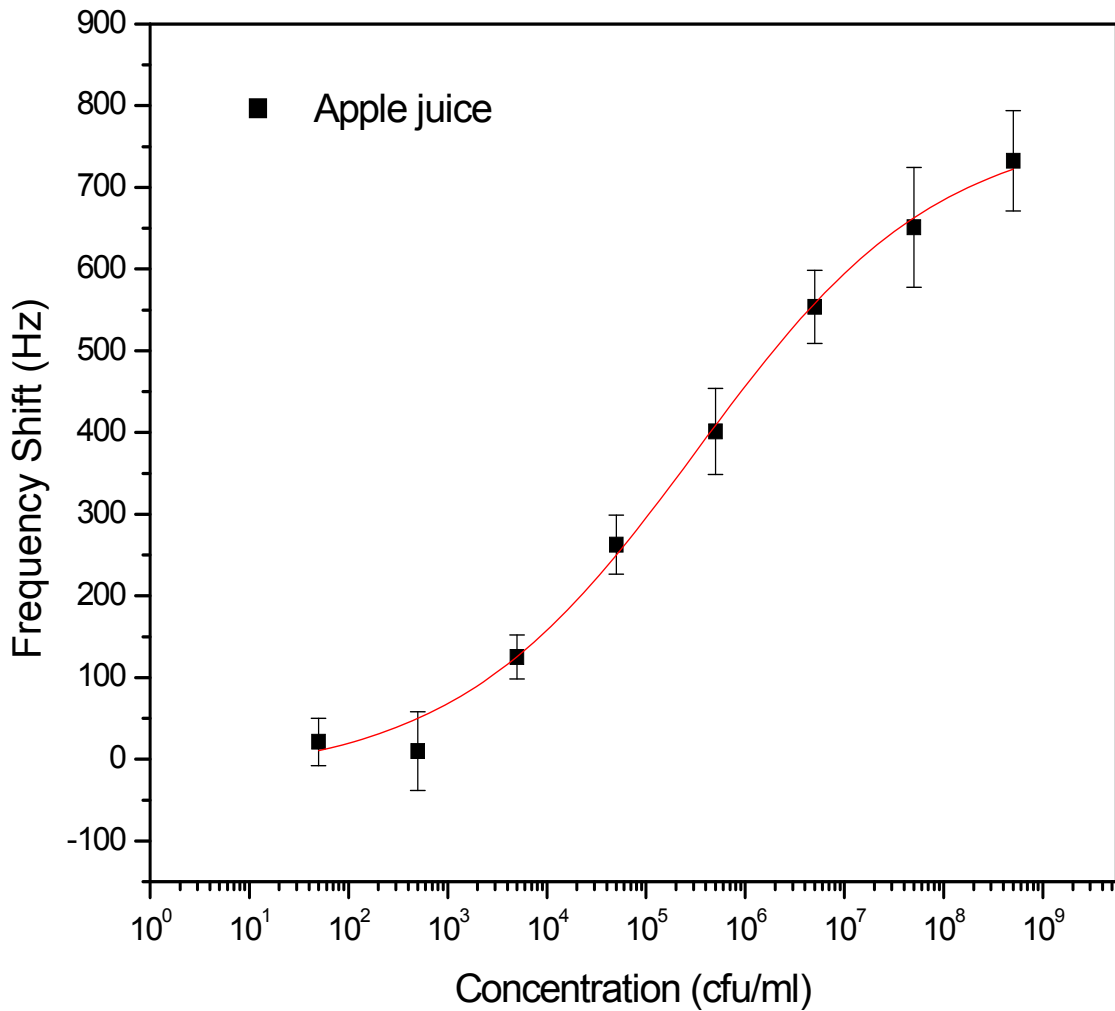
Figure 4-16: Magnetoelastic biosensor response when exposed to different concentrations (5×10^1 cfu/ml through 5×10^8 cfu/ml) of *S. typhimurium* suspensions in apple juice. The smooth curve is a sigmoid fit of the experimental data. (R^2=0.9958 and χ^2 =0.258). Bars represent standard deviation.
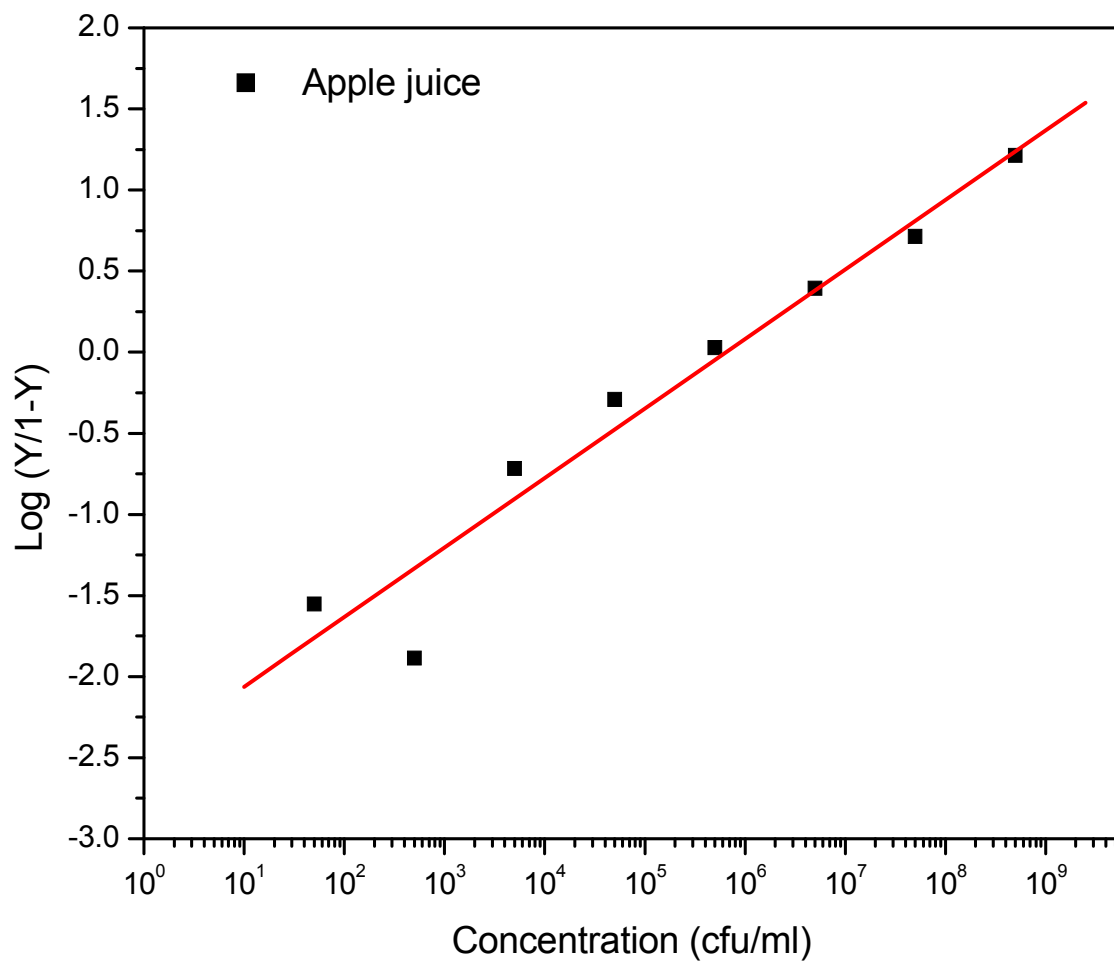
Figure 4-17: Hill plot showing the logarithmic ratio of occupied and free antibodies as a function of concentration of *S. typhimurium* in apple juice. The squares represent experimental data. The line represents the least square fit with coefficients: K_d=310 ± 101 cfu/ml and n_h=0.42876 ± 0.02. (R=0.9731, P<0.0001).
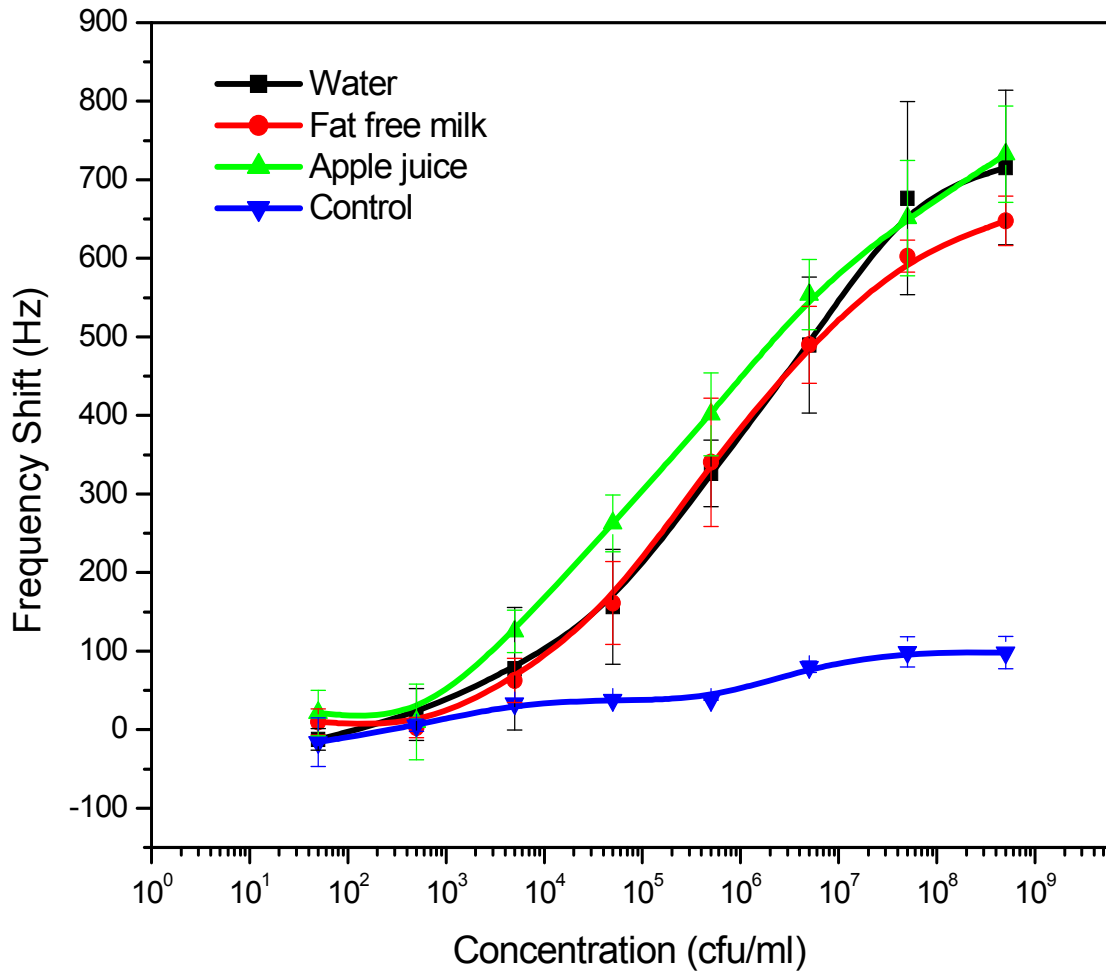
Figure 4-18: Magnetoelastic biosensor response for increasing concentrations (5×10^{1} to 5×10^{8} cfu/ml) of *S. typhimurium* suspensions in water (■- χ^{2}=0.048, R^{2}=0.99), fat free milk (●- χ^{2}=0.32, R^{2}=0.99), and apple juice (▲ - χ^{2}=0.26, R^{2}=0.99).   Control (▼ - χ^{2}=5.22, R^{2}=0.72), represents the uncoated (devoid of antibody) sensor's response.   The curves represent the sigmoid fit of signals obtained.   Each data point represents an average of five individual sensor responses.
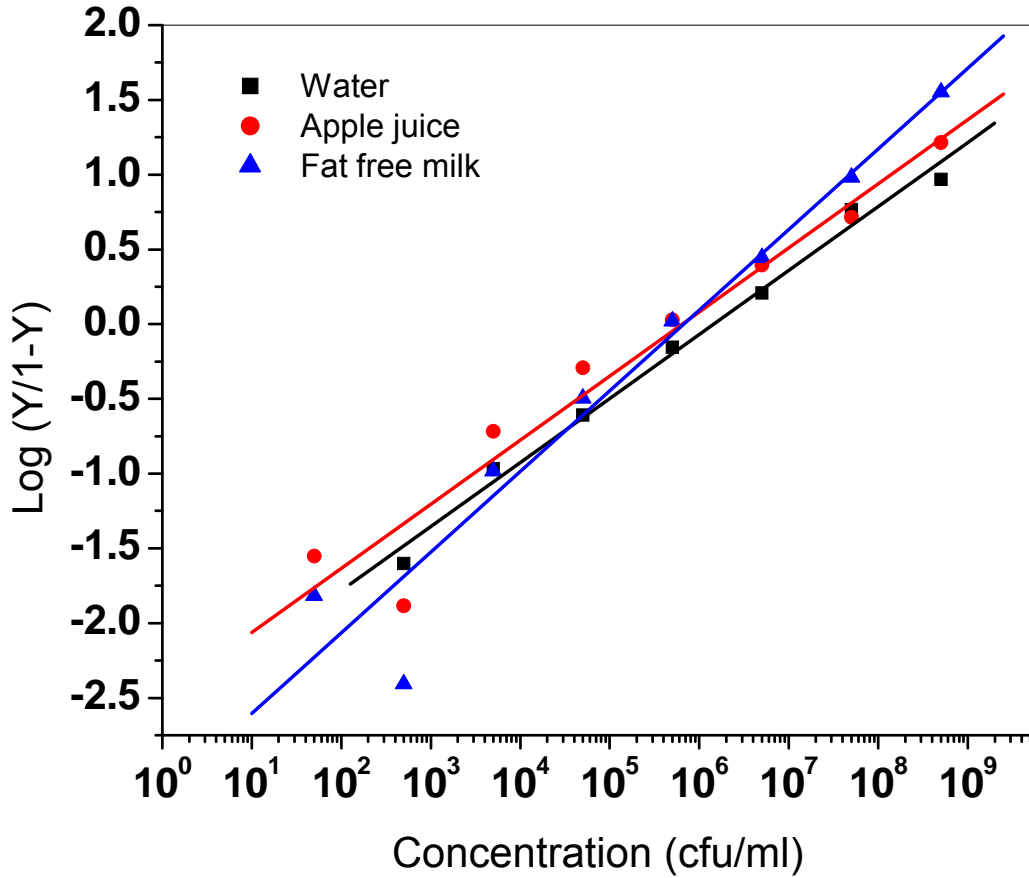
Figure 4-19: Hill plots of binding isotherms showing the ratio of occupied and free antibody sites as a function of bacterial concentrations spiked in different food samples. The straight line is the linear least squares fit to the data (Water: slope= 0.43 ±0.02, R=0.99; Apple juice: slope= 0.42 ±0.04, R=0.97; Fat-free milk: slope= 0.54 ±0.05, R=0.97)
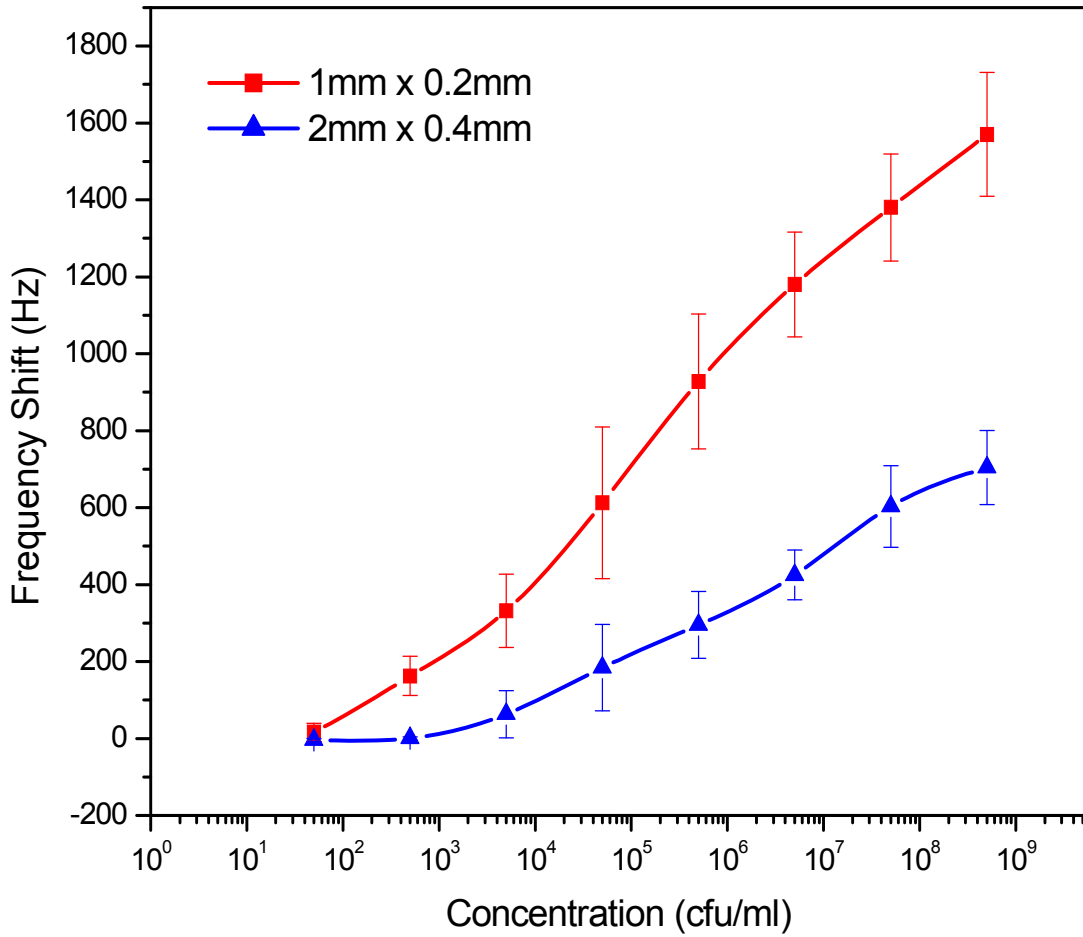
Figure 4-20: Resonant frequency shift upon exposure to solutions containing different concentrations of *S. typhimurium* for two sensors (1) 2×0.4mm, and (2) 1×0.2mm. Each concentration of bacterial solution was run for 10 minutes at a flow rate of 100 μl/min.

4.2.2 SEM observations

In order to confirm the frequency shifts caused by binding of *S. typhimurium* to the sensor with immobilized antibody, SEM micrographs were taken for all the samples after binding of *S. typhimurium*. Figure 4-21 to 4-23 shows typical SEM micrographs of the biosensor surface after exposure to *S. typhimurium* suspensions in various media. The control sensor showed only minimal capture when exposed to higher concentrations of bacteria (5×10^8 cfu/ml). Results from SEM study confirm that the observed frequency shifts are the result of capture of *S. typhimurium* cells by the immobilized antibody. The change in resonance frequency generated by the sensors before and after being exposed to bacterial suspensions can be attributed to the increase in mass of the bound analyte (*S. typhimurium*) on the sensor surface. Ten different regions of each sensor surface were examined and photographed using SEM. Sensor surface bacterial densities of 0.105, 0.075 and 0.105 cells/μm^2 were observed on the samples which were exposed to *S. typhimurium* suspensions in water, fat-free milk, and apple juice respectively at the highest bacterial concentrations. Table 4-1 summarizes a comparison between the number of bacterial cells counted from the SEM images and that calculated from the measured frequency shifts. From table 4-1 and SEM pictures it is evident that lesser number of bacterial cells were bound to the biosensor in fat free milk samples as compared other media (water and apple juice). This decrease in bacterial binding is proportional to the decrease in the value of binding valency (table 4-2) calculated from the frequency response of the sensor. Generally there is good agreement between the two methods of determining the number of cells bound to the sensor surface. The number of cells as determined from SEM measurements is an extrapolation of an average of 10

different regions on the exposed sensors. Variations in uniformity of binding from region to region and the small area viewed in making the analysis lead to an overestimation of up to 29% in the number of SEM counted cells.
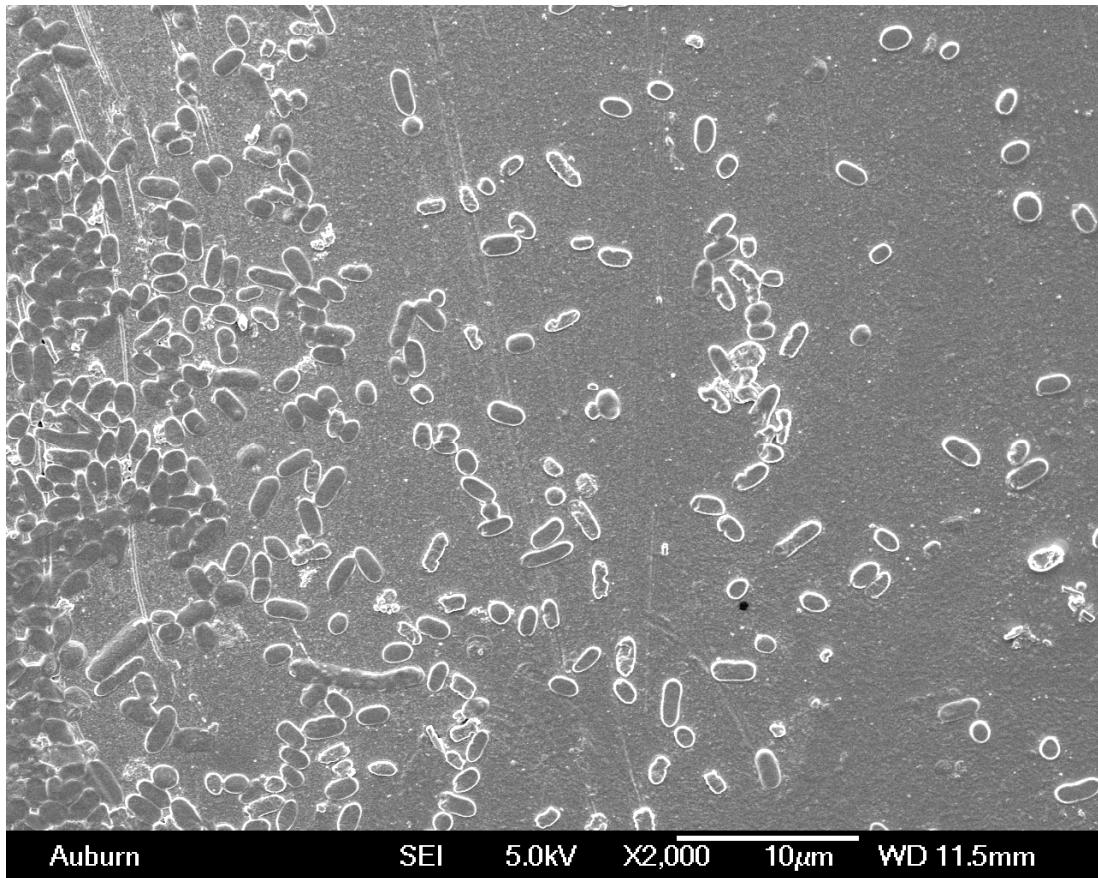
Figure 4-21: Typical SEM image of *S. typhimurium* bound to an antibody immobilized magnetoelastic sensor surface. *S. typhimurium* suspensions (5×10^8 cfu/ml) in water.

91
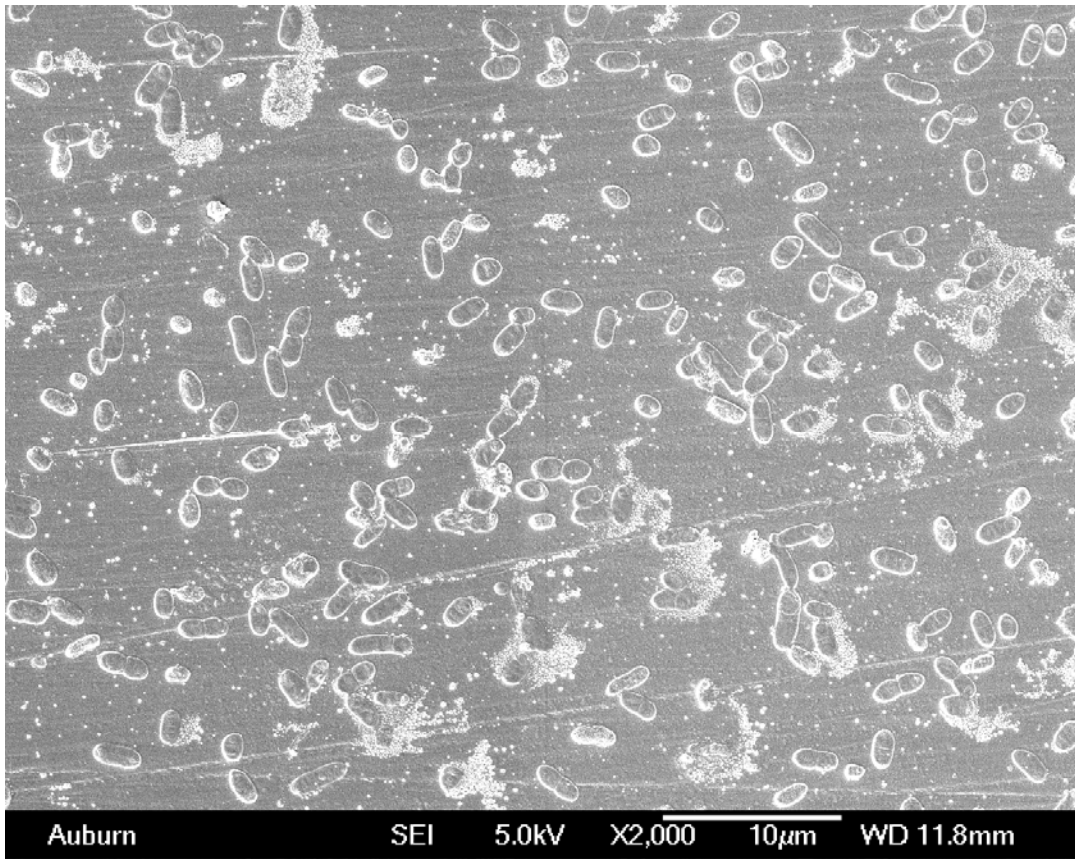
Figure 4-22: Typical SEM image of *S. typhimurium* bound to an antibody immobilized magnetoelastic sensor surface. *S. typhimurium* suspensions (5×10^8 cfu/ml) in fat free milk.
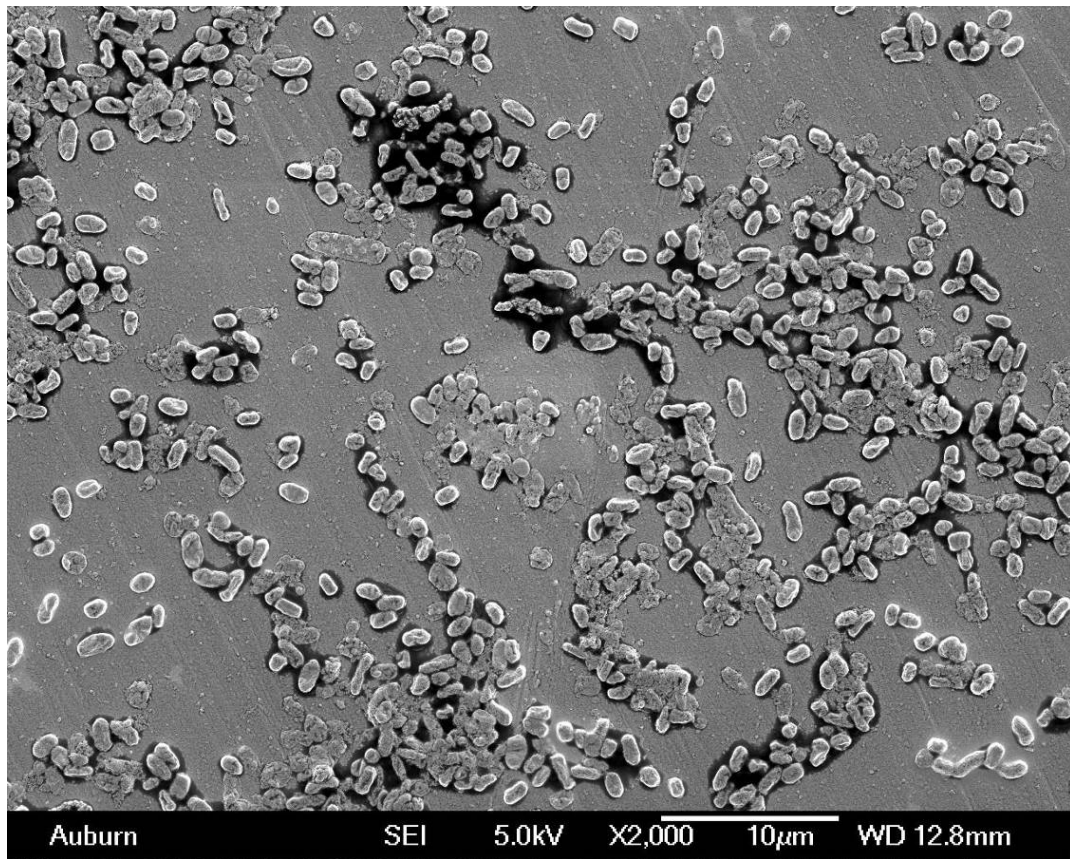
Figure 4-23: Typical SEM image of *S. typhimurium* bound to an antibody immobilized magnetoelastic sensor surface. *S. typhimurium* suspensions (5×10^8 cfu/ml) in apple juice.

Table 4-1: Comparison of bacterial cells counted from SEM images and theoretically expected number of cells calculated from equation (2) according to the measured frequency shifts.

	Number of cells from frequency shifts	Number of cells from SEM	% difference in cell counts
Water	64954	84424	29.97%
Fat free milk	57681	60293	4.53 %
Apple juice	66816	84098	25.87%

4.2.3   Discussion

The use of polyclonal antibody immobilized magnetoelastic biosensors for the detection of *S. typhimurium* in food products (water, fat free milk and apple juice) has been successfully established in this study.   The mass sensitivity of the biosensor increases with decreasing physical size of the sensor.   Detection limits of 5×10^3 and 10^3 cfu/ml were obtained for 15 μm thick sensors with sizes of 2×0.4mm and 1×0.2mm, respectively. Figure 4-18 shows the comparative responses of 2×0.4×0.015 mm sensors, when exposed to increasing concentrations of bacteria suspended in water, fat-free milk, and apple juice. As can be seen, the shift in the resonance frequency of all the sensors shows a similar trend in the different foods. The first detectable response due to the presence of bacteria occurs at a concentration of 5×10^3 cfu/ml. Dose response is linear over five decades of bacterial concentrations. The sensor sensitivity was measured as a slope of the linear portion of the dose response, is 139 Hz/ decade (R>0.99, P<0.001) for the samples tested in water, 127 Hz/decade (R>0.99, P<0.0001) and 129 Hz/ decade

(R>0.99, P<0.0001) in fat free milk and apple juice respectively. When the control sensor exposed to increasing concentration of *S. typhimurium*, a change in the resonance frequency (~ 50 Hz) was seen at very high concentration of 5×10^6 cfu/ml. This small change in the frequency can be associated to the very little non specific binding of bacterial cells to the sensor surface.

From the dose responses obtained, the Hill plot (shown in figure 4) was derived using the principles explained in the experimental procedure section. The dissociation constant, K_d and the binding valencies were calculated. Table 4-2 summarizes the Hill plot results obtained for the sensors when exposed to water, fat-free milk, and apple juice. All the tests conducted with different solutions showed a multi-valent binding, indicating that the bacteria in solution are binding to the immobilized antibody at more than one site. As compared to biosensors tested in water and apple juice samples, biosensors tested in fat free milk had a higher K_d value and smaller binding valency, which is also in agreement with the frequency shift data from the dose response curves. The lesser amount of binding in the fat free milk can be due to lesser number of antibody sites available for the bacteria binding caused by proteins in the fat free milk blocking few of the antibody sites. The lower K_d values obtained from the three samples indicated stronger and higher sensitivity of binding [165-167]. SEM images provided visual verification that the measured frequency shifts were in fact due to the attachment of bacteria to the sensor surface.

Table 4-2: Dissociation constants and binding valencies for magnetoelastic sensors in different liquid media.

	Hill Coefficient (n_H)	Binding valency	K_d (cfu/ml)
Water	0.43	2.33	435
Apple Juice	0.42	2.38	309
Milk	0.54	1.85	1389

Although sensitivity can be enhanced by using smaller sensors, this is likely to lead to difficulties in antibody immobilization. A study on antibody coated sensor size and bacterial density coverage indicated that the bacterial density coverage on the sensor decreased linearly with the physical dimensions of the sensor. This decrease in the bacterial densities is likely to be related to the decrease in the available number of antibodies on the sensor surface. The reduction in the antibody monolayer area may be due to two possible reasons, one of which is damage to the monolayer during sensor handling and the other that the monolayer was no adhering to (going around) the magnetoelastic particle.

4.3 Bionoise

The objective of the present study was to develop a culture-independent wireless, biosensor technology based upon antibody immobilized magnetoelastic biosensors. The specific detection potential of this biosensor technology was evaluated by detecting *S. typhimurium* in a cocktail of non specific bacterial suspensions such as *Escherichia coli*

O157:H7 and *Listeria monocytogenes*. 2×0.4×0.015mm sensors were used in these investigations. All the bionoise tests were performed at room temperature (25 ± 1^0C).

4.3.1 Response curves

Magnetoelastic biosensor performance was determined by exposure to increasing concentrations of *S. typhimurium* (5×10^1 to 5×10^8 cfu/ml) suspensions in a mixed microbial population of non specific biological analytes such as *E. coli* and/or *Listeria monocytogenes* (5×10^8 cfu/ml). 1 ml solution of each concentration (with biological interferents) was flown using a peristaltic pump at a flow rate of 100 μl/min for 10 minutes. After the antibody immobilized sensor achieved steady state response in water, sensor was exposed to a fixed concentration (5×10^8 cfu/ml) of biological interferents following increasing concentrations of *S. typhimurium* as cocktail in fixed concentrations of biological interferents. Figures 4-24 and 4-25 show the responses of the magnetoelastic biosensors, when exposed to *S. typhimurium* in the presence of *E. coli* (Figure 4-24), *E. coli* and *Listeria monocytogenes* (Figure 4-25).
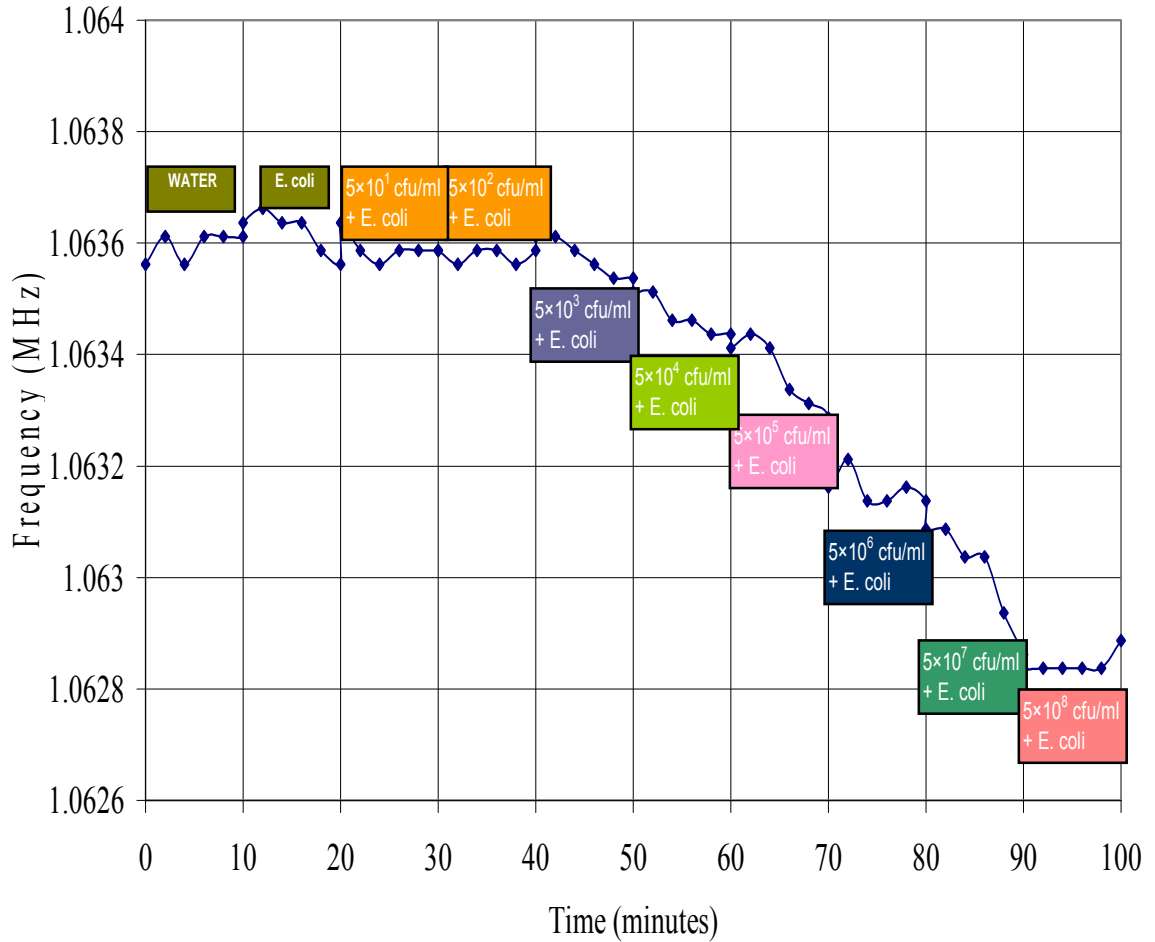
Figure 4-24: Magnetoelastic biosensor response for different concentrations (5×10^1 through 5×10^8 cfu/ml) of *S. typhimurium* suspensions in water, along with a fixed concentration (5×10^8 cfu/ml) of *E. coli* as an interferent. Data was recorded at two minute intervals. Each concentration of bacterial suspension was run for 10 minutes at a flow rate of 100 μl/min.
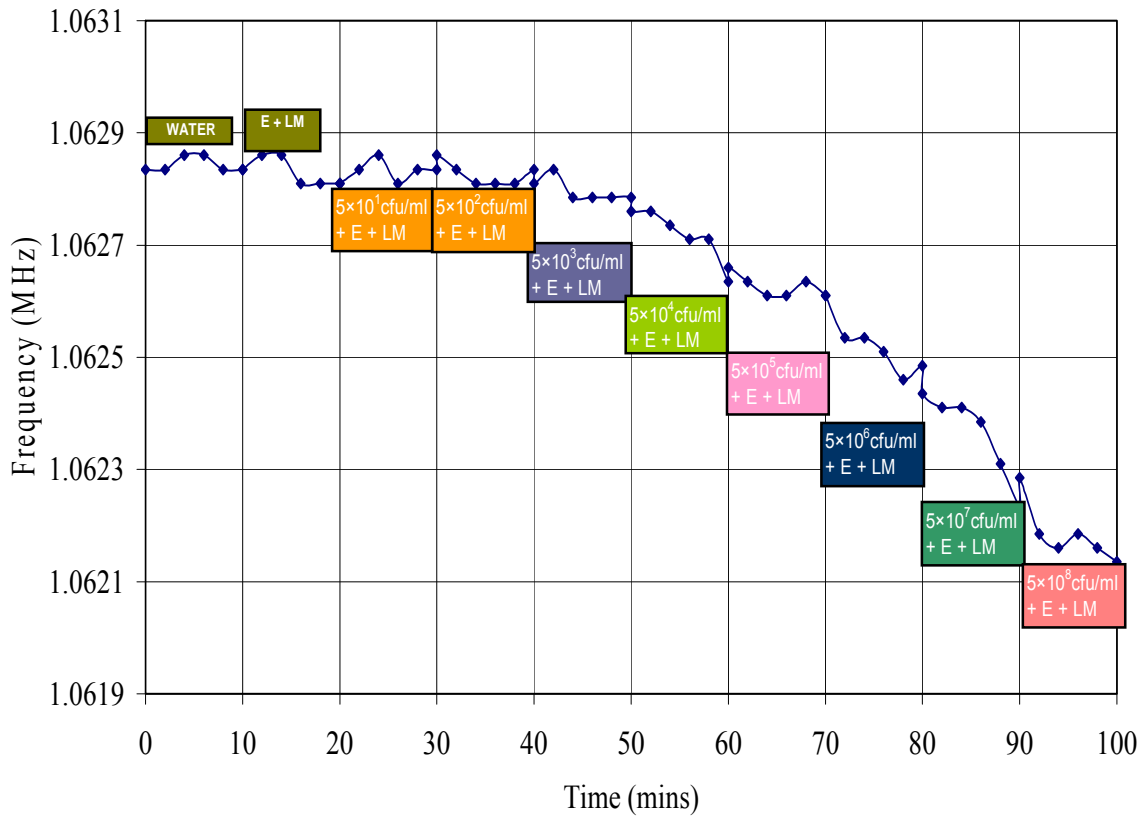
Figure 4-25: Magnetoelastic biosensor response for different concentrations (5×10^1 through 5×10^8 cfu/ml) of *S. typhimurium* suspensions in water, along with fixed concentrations (5×10^8 cfu/ml) of *E. coli* (E) and *Listeria monocytogenes* (LM) as biological interferents. Data was recorded at two minute intervals. Each concentration of bacterial suspension was run for 10 minutes at a flow rate of 100 μl/min.
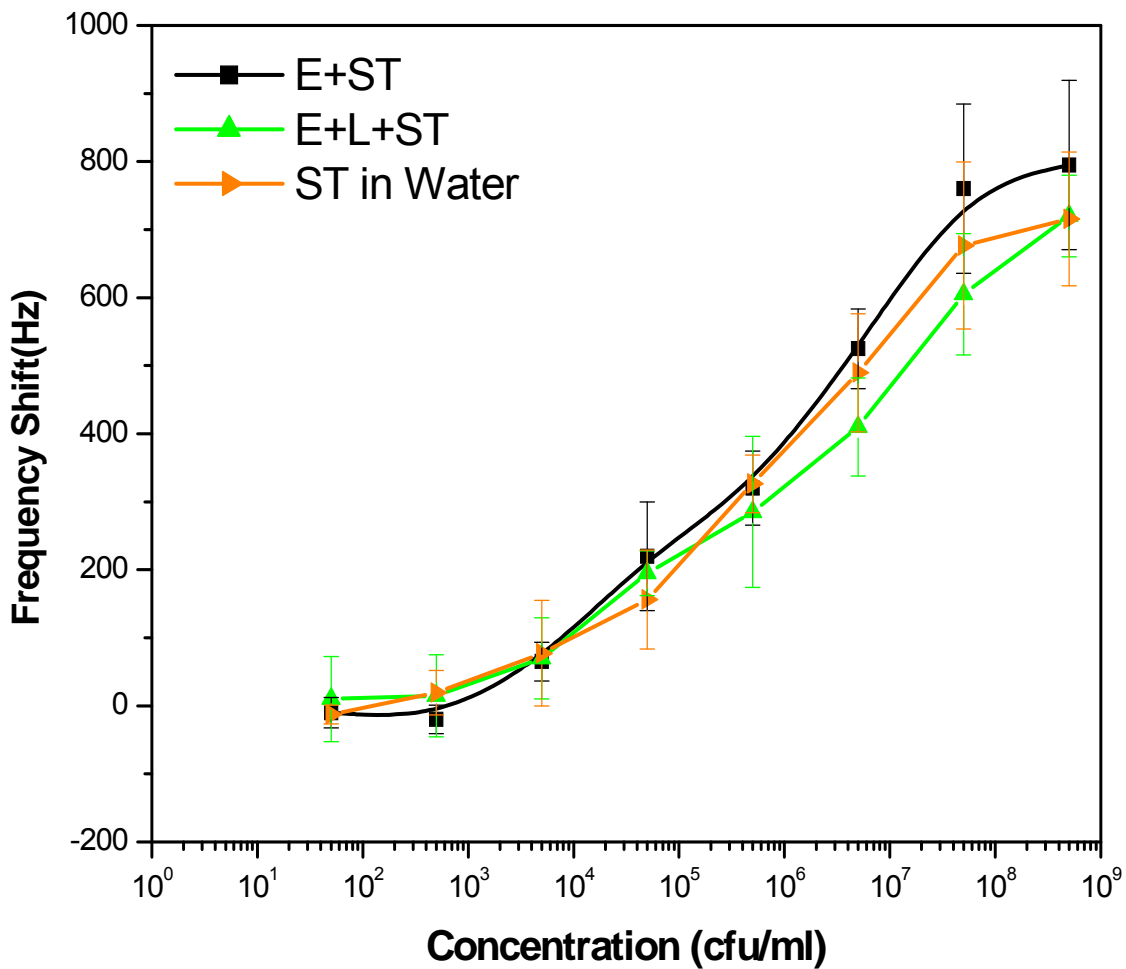
Figure 4-26: Magnetoelastic biosensor's (2×0.4×0.015mm) response for graded concentrations (5×10^1 through 5×10^8 cfu/ml) of *S. typhimurium* (ST) suspensions in water, with cocktails of *E. coli* (E) and *Listeria monocytogenes* (L). The noise due to biological interferants was deducted from the total frequency shifts at each concentration.
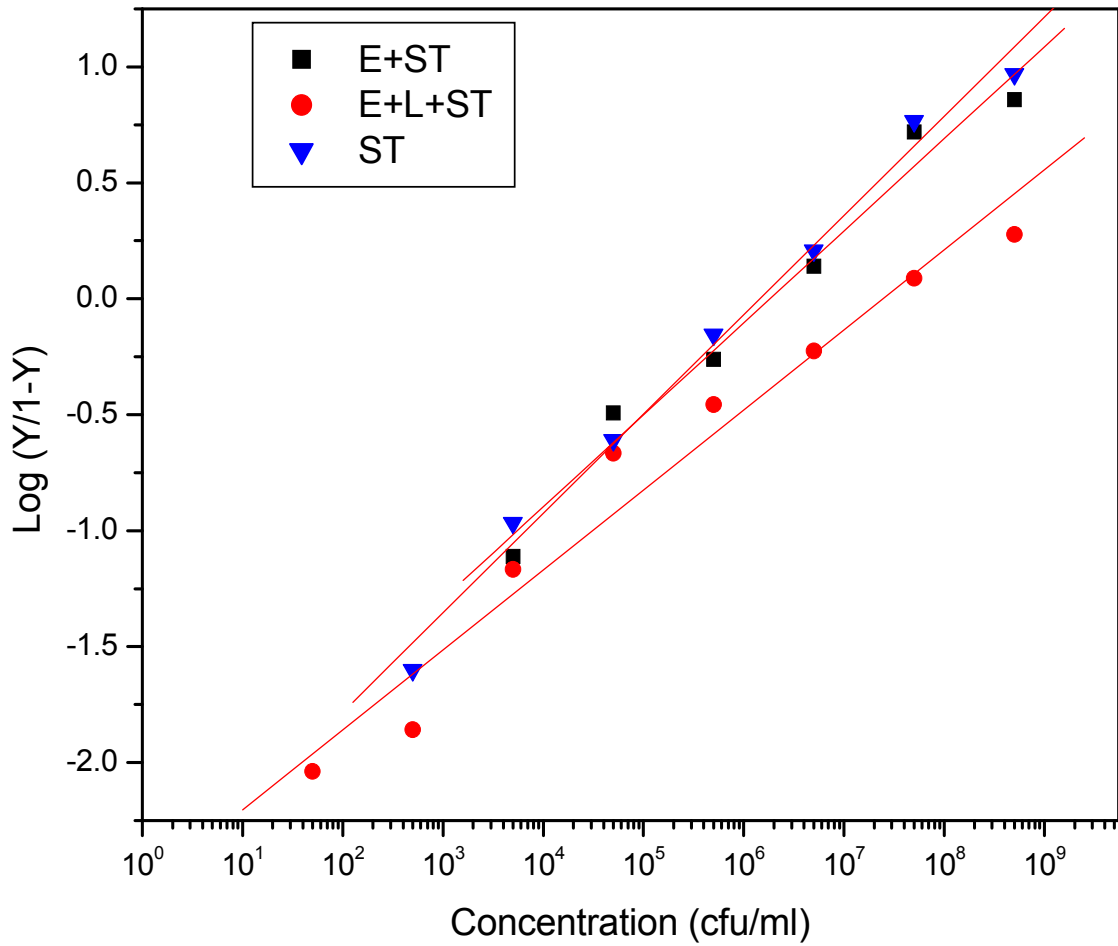
Figure 4-27: Hill plots of binding isotherms showing the ratio of occupied and free antibody sites as a function of bacterial concentrations spiked in cocktails of non specific bacteria. The straight line is the linear least squares fit to the data.

Table 4-3: Results of bio-noise experiments for antibody coated sensors exposed to different combinations of biological interferants in water. The results are each averages of five individual sensor measurements.

Interferants	Average Frequency shift (Bionoise) (Hz)
E. coli	7.6 (±) 15.2
E. coli and *Listeria monocytogenes*	11.6 (±) 22

Table 4-4: The dissociation constants and binding valencies of magnetoelastic biosensor in mixed microbial population.

	Hill Coefficient (n_H)	Binding valency	K_d (cfu/ml)
ST	0.43	2.33	435
E+ST	0.4	2.5	305
E+L+ST	0.35	2.86	287

4.3.2 Discussion

Figure 4-26 shows the comparative responses of a 2×0.4× 0.015 mm sensor, when exposed to increasing concentrations of *S. typhimurium* in water in the presence of mixed microbial population. It is evident from Figure 4-27; that no significant effect of biological interferants was observed on the magnetoelastic sensor performance. When a single biological interferants (*E. coli*) was used with highest concentration ($5×10^8$ cfu/ml) almost no effect was observed. A cocktail of two different interferants at high concentration ($5×10^8$ cfu/ml) contributed only about 6 % (11.6 (±) 22 Hz) of total sensor response. Hence, antibody immobilized magnetoelastic sensors can be used to monitor the bacterial contaminations even in the presence of non specific interferants.

As can be seen, the shift in the resonance frequency of all the sensors shows a similar trend, with a gentle log phase in the curve. From the dose responses obtained, the Hill plot was derived using the principles explained in the experimental procedures. The disassociation constant, K_d and the binding valences were calculated. All the tests conducted with different solutions showed a multi-valent binding, indicating that the bacteria in solution are binding to the immobilized antibody at more than one site. From table 4-4 it can be seen that the dissociation constant was smaller with increasing number of interferants, this may be due to the attachment of bacteria (*Salmonella* as well as other biological interferants) to the gold surface on the sensor (i.e. uncoated antibody sites). The non specific binding sites were shared between the different bacteria and the majority of the antibody sites were occupied by *S. typhimurium* cells.

4.4 Thermal stability of Polyclonal Antibody immobilized magnetoelastic biosensors

For all practical applications, it is essential for both major components (transducer and biorecognition element) to be robust enough to withstand the rigors they typically encounter in the field conditions. However, in most cases, the biorecognition element is relatively vulnerable to the vagaries of the field environment (e.g. in deserts temperatures can reach as high as 65 °C). Hence, it is of utmost importance to test the stability of the biosensor system at higher temperatures. It has been reported that the binding activity of mouse monoclonal antibodies become degraded within as little as two hours exposure to higher temperatures [168]. Another study found that there was a 15% loss of activity at 37 °C after 15 days when the monoclonal antibodies were stored in a buffer with pH 10 [169]. Specifically designed antibodies have been shown to have a greater stability at 4 °C for a period of 6 months, however their stability at higher temperatures was not studied [170]. A substantial quantity of literature exists that shows the relationship of temperature to the stability of monoclonal antibodies [171-173]. However most of the reported studies on antibodies' stability were performed on free antibodies instead of those immobilized on a sensor surface. Since the immobilization of antibodies on a sensor platform may alter their stability, the current study investigated the stability of polyclonal antibody immobilized on a magnetoelastic sensor platform at three different temperatures (25, 45 and 65 °C).

4.4.1 Long-term stability tests
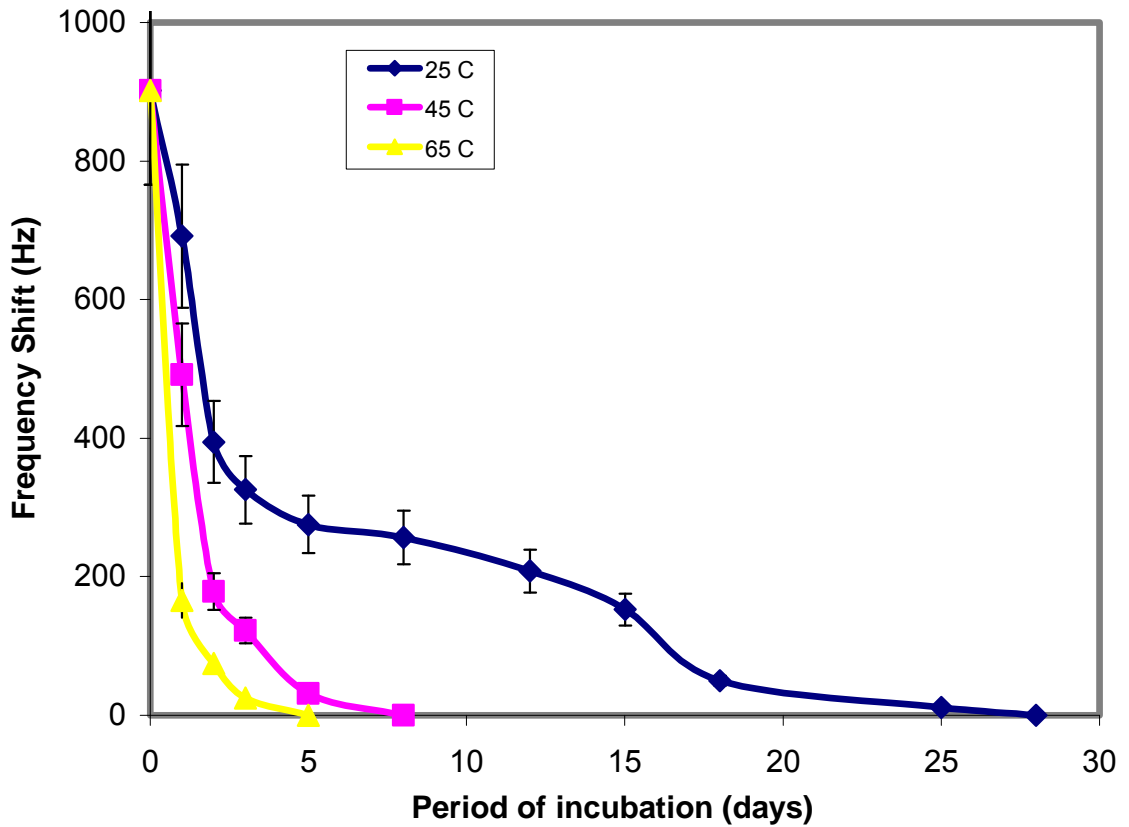
Figure 4-28: Magnitude of resonance frequency shifts caused by the binding of *S. typhimurium* to stored magnetoelastic biosensors. The biosensors stored at 25 °C, 45 °C, and 65 °C were removed from the incubators at various intervals, and tested in 1ml of water containing *S. typhimurium* at a concentration of 1×10^9 cfu/ml.

Figure 4-29 shows the resonance frequency shift responses of stored biosensors following exposure to 1 ml of water containing *S. typhimurium* (1×10^9 cfu/ml). The response of biosensor on day 0 at 25 °C was taken as reference (test control) to compare the change in binding activity at different temperatures with time. From the results obtained, it is evident that both storage temperature and time alter the biosensor performance. Biosensors stored at 25 °C, had a rapid decrease up to 3 days, followed by a more gradual decrease in the binding activity. The biosensors stored at higher temperatures show a steeper decrease in binding activity, with no shift (no binding) observed by day 8 and day 5 for the sensors stored at 45 and 65 °C, respectively.

4.4.2 Scanning Electron Microscopy (SEM)

In order to confirm that binding of *S. typhimurium* to the sensor surface was causing the measured frequency shifts, SEM photomicrographs were taken on all the stored and tested biosensors after exposure to *S. typhimurium*. Figure 4-29 to 4-32 show typical SEM images of the biosensors stored at different temperatures, after exposure to *S. typhimurium*. As can be seen, the bacterial coverage density decreased with time and increased temperature.

<center>(a)   (b)</center>
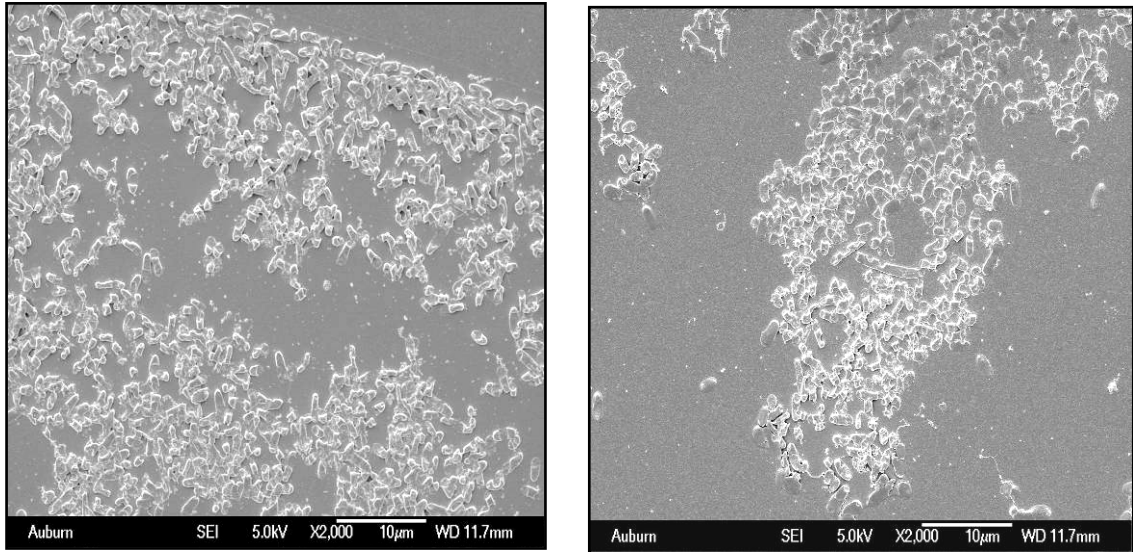
Figure 4-29: Typical SEM images of *S. typhimurium* bacterium bound to the polyclonal antibody immobilized biosensor surface with increasing time and temperature (a) Day 0 and (b) Day 1, at room temperature (25 ºC).
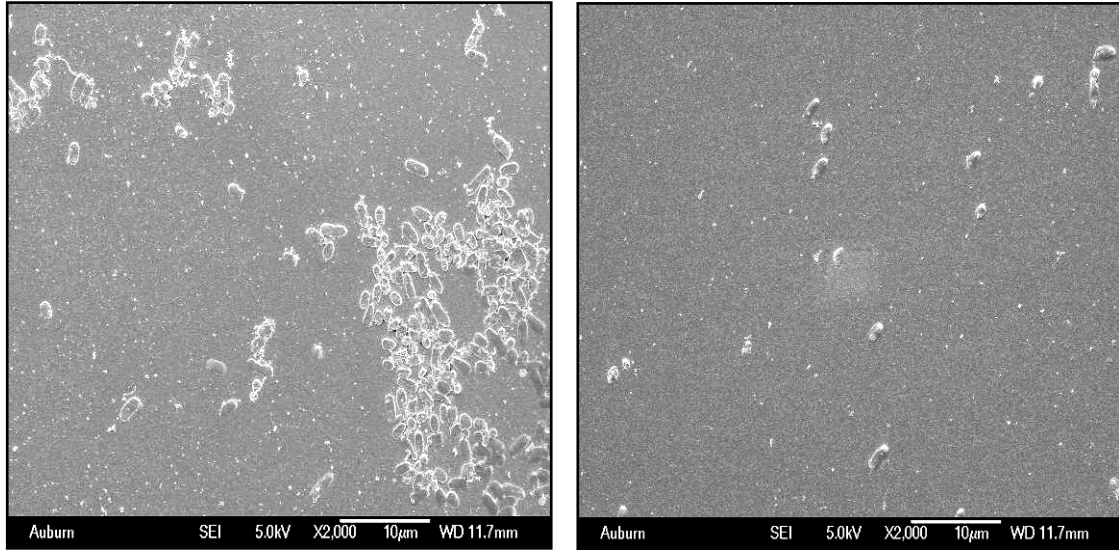
(c) **(d)**

Figure 4-30: Typical SEM images of *S. typhimurium* bacterium bound to the polyclonal antibody immobilized biosensor surface with increasing time and temperature (c) Day 5 and (d) Day 28, at room temperature (25 ºC).
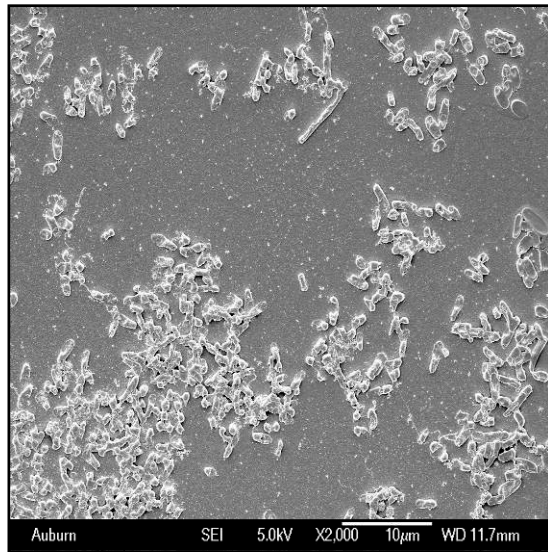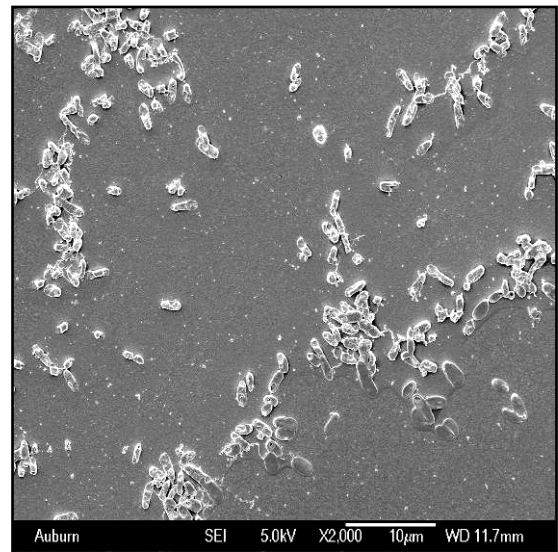
(e)   **(f)**

Figure 4-31: Typical SEM images of *S. typhimurium* bacterium bound to the polyclonal antibody immobilized biosensor surface with increasing time and temperature (e) Day 1 and (f) Day 5, at 45 ºC.

(g) **(h)**
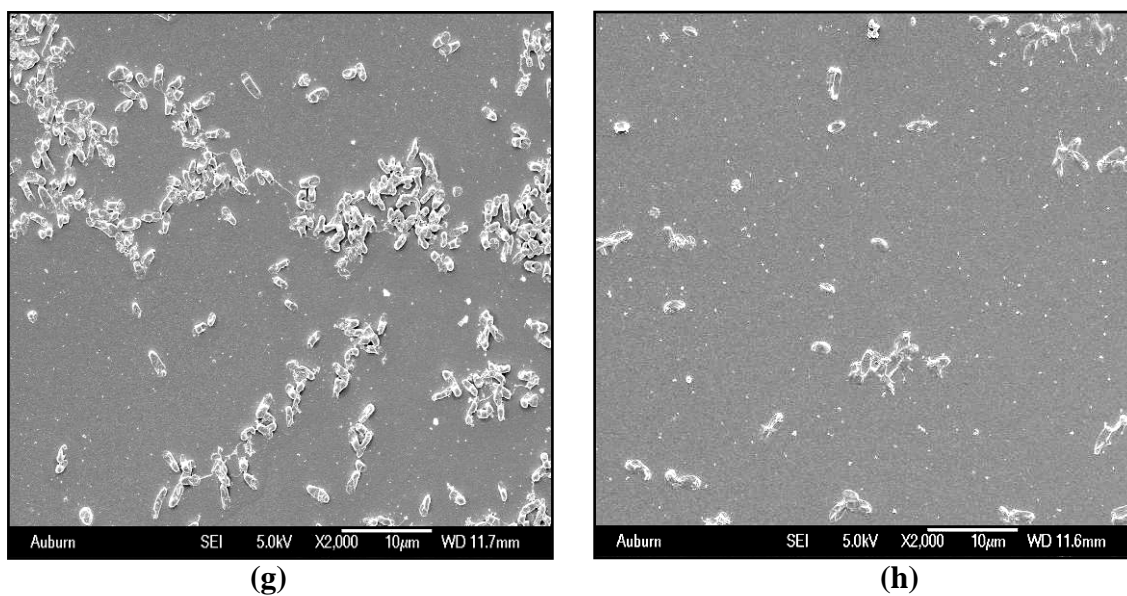
Figure 4-32: Typical SEM images of *S. typhimurium* bacterium bound to the polyclonal antibody immobilized biosensor surface with increasing time and temperature (e) Day 1 and (f) Day 3, at 65 ºC.

4.4.3 Bacterial density Calculations

SEM images were used to calculate the bacterial density on the sensor surfaces and a bacterial density versus time profile for antibody was generated. After counting the number of the bacteria bound to the sensor surfaces, the surface distribution density of bacteria was calculated for each sensor as described in the experimental procedures.

The changes in surface distribution density of the bacteria bound to the biosensor surface with time (in days) for the biosensors stored at different temperatures are shown in Figure 4-33. The results show a more rapid decrease in the density of bacteria captured on the biosensors stored at 45 and 65 °C. The biosensors stored at 25 °C show an initial rapid drop in density followed by a gradual. The decrease in the bacterial densities exhibited a trend similar to the frequency shift measurements.
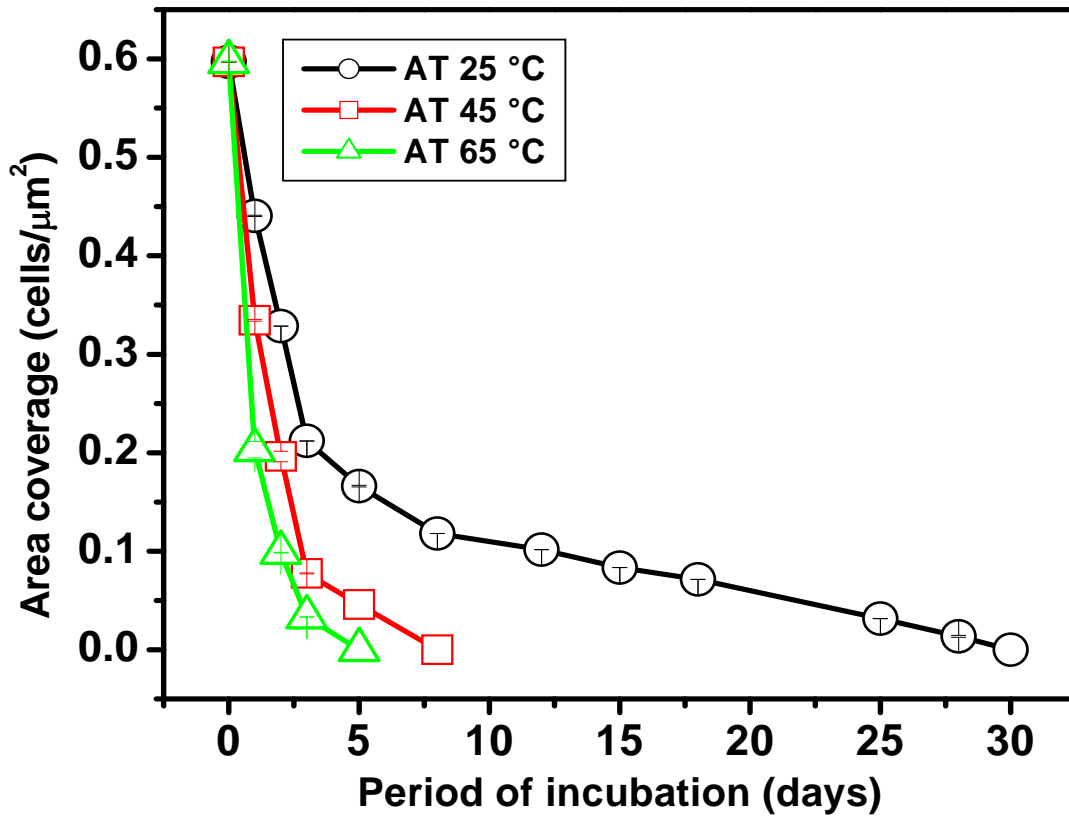
Figure 4-33: Surface coverage densities   (average number of cells/μm^2)

calculated from SEM micrographs of stored magnetoelastic biosensors (25 ºC, 45 ºC, and

65 ºC) after exposure to *S. typhimurium*.

4.4.4 Activation energy calculation

The activation energy was calculated assuming Arrhenius dependence [163] as below,

$$K = A * e^{(-E_a/RT)} \tag{4-1}$$

where K is the rate coefficient, A is a constant, E_a is the activation energy, R is the universal gas constant ($R = 1.987$ cal mol^{-1}K^{-1}), and T is the absolute temperature From equation (4-1), K equals

$$\ln K = \ln A - \frac{E_a}{RT} \tag{4-2}$$

Figure 4-35 shows the Arrhenius plot (lnK) versus 1000/T over a temperature range of 25 ° C to 65° C for the magnetoelastic biosensors. The activation energy can be derived from the slope of the curve:.

$$\text{Slope} = -\frac{E_a}{R} \tag{4-3}$$

$$E_a = - \text{Slope} * R \tag{4-4}$$

Thus, the activation energy Ea for this biosensor system was found to be:

$$Ea = - (-3.8882 * 1000 * 1.987) = 7725.8 \text{ cal/mol}$$

The low value for the activation energy suggests that the polyclonal antibodies are strongly dependent on the temperature and thus tend to degrade rapidly at higher temperatures. Consequently, the response of biosensors may be limited by the degradation of the bio recognition element immobilized on the sensor.
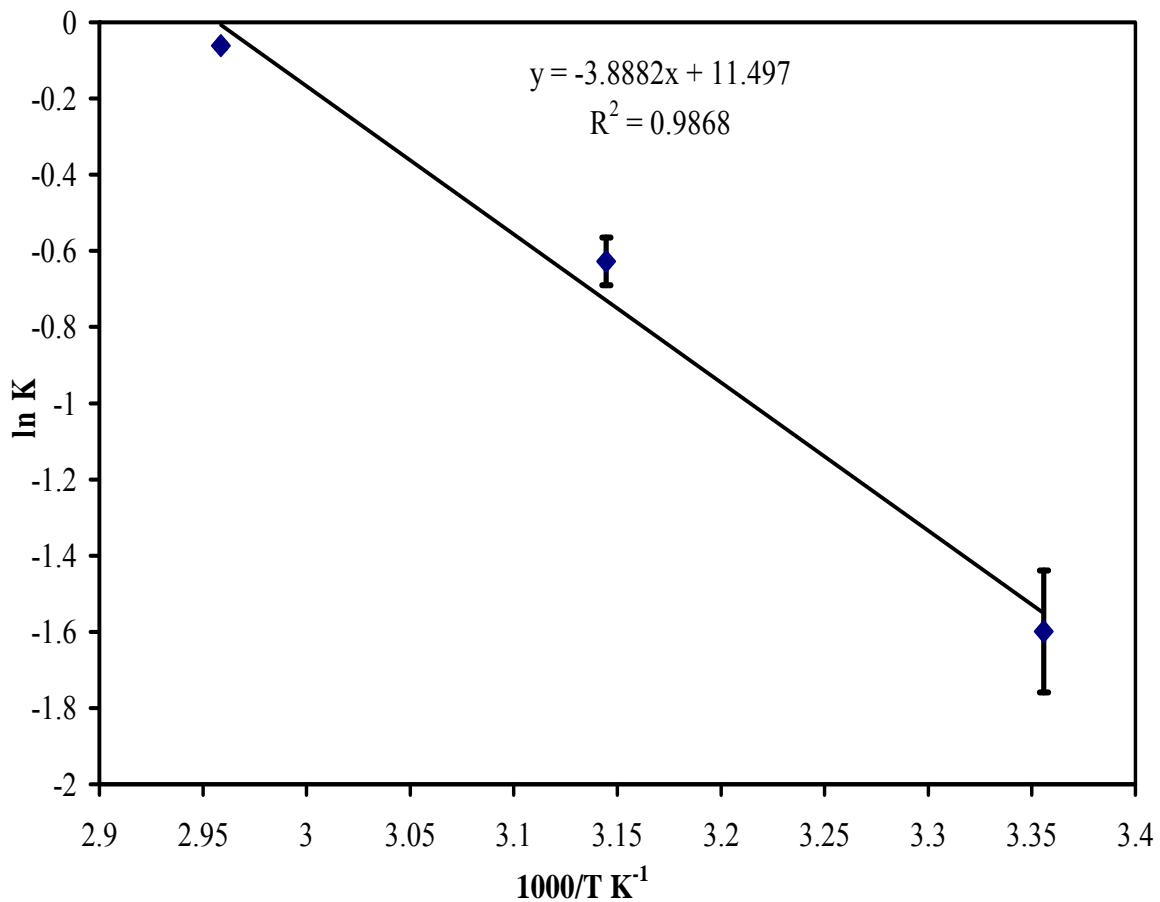
Figure 4-34: The effect of temperature on the longevity of the antibodies. The Activation energy of the antibodies was calculated from the slope of the plot.

4.4.5 Discussion

The results show a more rapid decrease in the density of bacteria on the biosensor surfaces for those sensors incubated at 45 and 65 °C, where as an initial rapid drop in density followed by a gradual drop exhibited by the biosensors maintained at 25 °C. The decrease in the bacterial densities exhibited trend similar to the frequency shift measurements.

Results from the SEM study also confirmed that the observed frequency shifts were a result of capture of *S. typhimurium* cells by the immobilized antibody. The change in resonance frequency generated by the sensors before and after being exposed to bacterial suspensions can be attributed to the increase in mass of the bound target species (*S. typhimurium*) to the sensor surface. The decrease in the bacterial densities can be attributed to the loss of activity of antibodies immobilized on the sensor platform. Thus, the response of biosensors may be limited by the degradation of the antibodies immobilized on the sensor.

To derive the activation energy of biosensor degradation, an Arrhenius plot was created using the gathered experimental data from the SEM analysis (bacterial density coverage). Activation energy was calculated assuming an Arrhenius dependence [174]. The activation energy (E_a) for this biosensor degradation was determined to be 7.7 kcal/mol (32.3 kJ/mol). The light chains of IgG molecules are vulnerable to thermal deterioration (E_a=5.5 kcal/mol) [175, 176], which suggests that the probable cause of biosensor degradation is the denaturing of light chains in the polyclonal antibodies. Other enzyme based amperometric sensors have reported activation energies of degradation of 27 -31 kJ/mol [177] and 29 kJ/mol [178] and 50 kJ/mol [179].

4.5 Specificity Tests

An essential test for the characterization of any biosensor is to investigate the specificity of the bioprobe (antibody). In this study, in order to test the specificity polyclonal antibody immobilized magnetoelastic biosensors were exposed to *Salmonella* species and also to different genus of bacteria such as *Escherichia coli* O157:H7, *Listeria monocytogenes* and *Staphylococcus aureus*. All the sensors were tested with different species of bacteria at a fixed concentration of 10^9 cfu/ml. Figure 4-35 shows the measured density of the bacterial cells attached to the polyclonal antibody immobilized sensor surface, calculated from the SEM images as described earlier in the experimental procedures. Figure 4-35 shows that the polyclonal antibodies used in this work specifically bound to the *Salmonella* species, and showed significantly lesser affinity to non specific species such as *Escherichia coli* O157:H7, *Listeria monocytogenes* and *Staphylococcus aureus*.
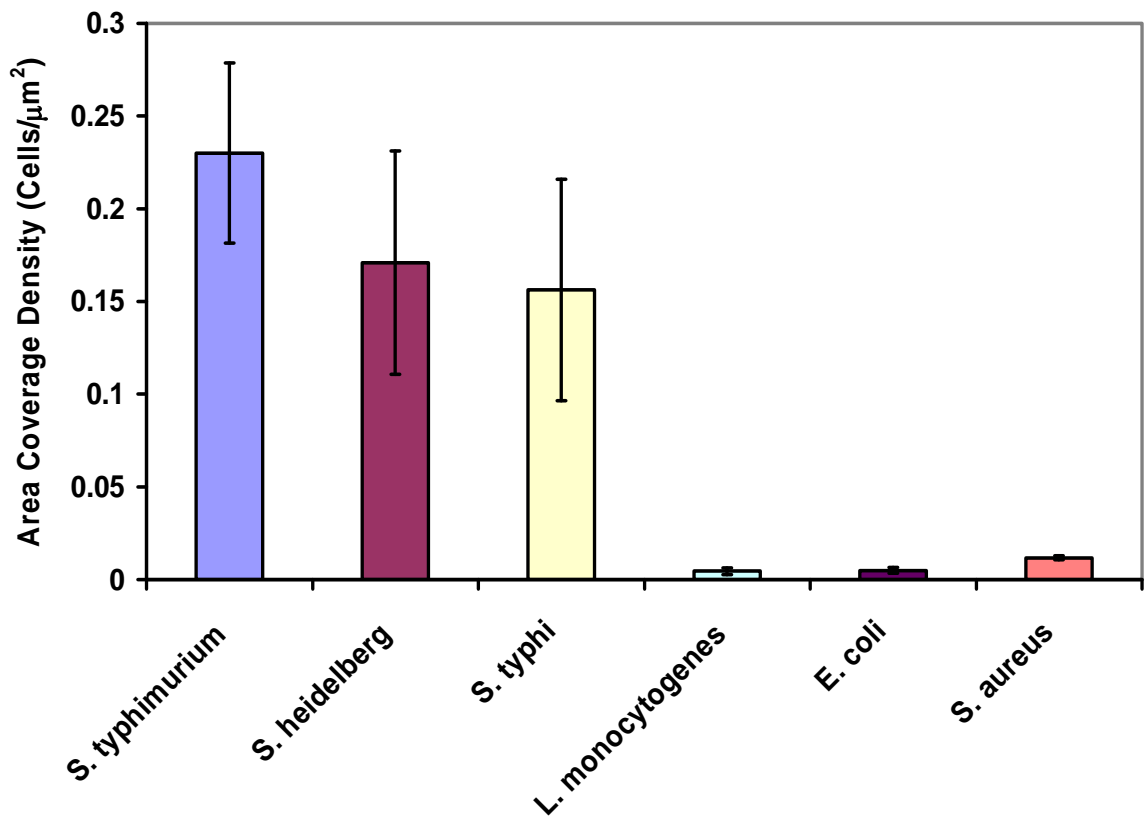
Figure 4-35: Average densities of different bacterial cells attached to the polyclonal antibody immobilized sensor surface.

5 CONCLUSIONS

The current research was conducted to study the application of a novel magnetoelastic material as a wireless biosensor for the specific detection of *Salmonella typhimurium* in contaminated food products. For this purpose, a sensor was prepared with a monolayer of target species specific antibody. Immobilization of the antibody was achieved through molecular assembly of the antibody using an LB film technique, which facilitates orientation of the antibody to ensure maximum affinity for the target analyte. The relationship of sensor size to the sensitivity of detection and the thermal stability of the immobilized antibody for the detection of *S. typhimurium* was investigated.

The application of polyclonal antibody immobilized magnetoelastic biosensors for the detection of *S. typhimurium* in food products (water, fat free milk and apple juice) was successfully established. A detection limit of 5×10^3 cfu/ml was obtained for a $2 \times 0.4 \times 0.015$ mm size sensor in all the three different food samples employed in this study.

An increase in the sensitivity was observed with smaller size sensors; a detection limit of 10^3 cfu/ml, with a sensitivity of 246 Hz/decade was obtained for $1 \times 0.2 \times 0.015$ mm sensors, as compared to a detection limit of 5×10^3 cfu/ml and a sensitivity of 139 Hz/decade for $2 \times 0.4 \times 0.015$ mm sensors.

The dose response studies in mixed microbial population clearly indicated a pronounced affinity for *S. typhimurium* even in the presence of other bacteria such as *Listeria monocytogenes* and *E. coli* O157:H7.

The binding activity of the polyclonal antibodies immobilized on the magnetoelastic sensor platform became zero (no binding) after a period of 30, 8 and 5 days at 25, 45 and 65 °C, respectively. Degradation energy of biosensor was obtained through Arrhenius equation and was determined as 7.7 kcal/mol. The reduction in activity of the magnetoelastic biosensor with increasing time and temperature may be attributed to the denaturing of light chains of the antibodies.

The binding of *S. typhimurium* to the immobilized antibody was confirmed by SEM studies. The enumeration of bacterial cells on the antibody immobilized sensor confirmed that the shift in the resonance frequency of the magnetoelastic sensor was due to the binding of *S. typhimurium* to the antibody immobilized sensor.

6 RECOMMENDATIONS FOR FUTURE WORK

Smaller size magnetoelastic sensors proved to have better sensitivity, but antibody immobilization using Langmuir-Blodgett (LB) method had difficulties, particularly with smaller size sensors, so it would be interesting to study different biorecognition elements and also new immobilization techniques. As magnetostrictive sensors are beginning to find new applications in the field of biosensing, it would be advantageous to be able to utilize a regenerative biorecognition layer, which would enable the sensors to be used for the continuous monitoring of bacterial contaminations. Array biosensors are also likely to be useful in the multi analyte detection systems. The application of a reference sensor alongside the antibody coated sensor should address the intrusion of unwanted effects such as false signals due to non specific binding and also environmental perturbations.

REFERENCES

1. Thevenot, D.R., et al., *Electrochemical biosensors: recommended definitions and classfication.* Biosens. Bioelectron., 2001. **16**(1-2): p. 121-131.

2. Turner, A.P.F., *Current Trends in Biosensor Research and Development.* Sensors Actuators, 1989. **17**: p. 433-450.

3. Rogers, K.R., *Biosensors for Environmental Applications.* Biosensors Bioelectronics, 1995. **10**: p. 533-541.

4. Lowe, C.R., *An Introduction to the Concepts and Technology of Biosensors.* Biosensors, 1985. **1**: p. 4.

5. Landry, D., *Immunoglobulin Structure.* 2000.

6. Elizabeth, A.H.H., *Biosensors.* 1991, New York: Printice Hall.

7. Diamond, D., *Principles of Chemical and Biological Sensors.* Vol. 150. 1998, New York: John Wiley & Sons.

8. Dewa, A.S., Ko, W. H., *Biosensors, Semiconductor Sensors.* 1994, New York: Wiley Interscience. 415.

9. http://www.biology.arizona.edu/immunology/tutorials/antibody/structure.html, The University of Arizona, 2006.

10. Sigma-Aldrich, A.E., *http://www.sigmaaldrich.com.* 2006.

11. Miyashita, M., Shimada, T., Miyagawa, H., Akamatsu, M., *Surface plasmon resonance-based immunoassay for 17beta-estradiol and its application to the measurement of estrogen receptor-binding activity.* Anal Bioanal Chem., 2005. **381**(3): p. 667-673.

12. Hock, B., Seifert, M., Kramer, K., *Engineering receptors and antibodies for biosensors.* Biosensors and Bioelectronics, 2002. **17**(3): p. 239-249.

13. Fiebor, B., *Detection of Salmonella typhimurium in phosphate buffered saline solution and fat free milk*, in *Materials Engineering*. 2003, Auburn University: Auburn.

14. Bailey, C.A., *A theoretical interpretation of the antibody-antigen interactions between Salmonella and a thickness shear mode (TSM) quartz resonator*, in *Materials Engineering*. 2003, Auburn University: Auburn.

15. *National Institute of Allergy and Infectious Diseases Fact sheet.* 2005.

16. Wagner, J.A.B., *Bacterial Food Poisoning: Extension Food Technologist Texas Agricultural Extension Service*. 2006.

17. *Preliminary FoodNet Data on the Incidence of Infection with Pathogens Transmitted Commonly Through Food --- 10 States, United States, 2005*, in *MMWR*. 2006. p. 392-395.

18. D'Aoust, J.-Y., *Salmonella. In Foodborne Bacterial Pathogens, M.P.Doyle, ed. Marcel Dekker, New York.* 1989: p. 327-445.

19. Hui, Y.H., Richard Gorham, J., Murrell, K. D., Cliver, D. O., *Foodborne Disease Handbook Diseases Caused by Bacteria*. Vol. 1. 1994, New York: Marcel Dekker. 215-252.

20. Babacan, S., Pivarnik, P., Letcher, S., Rand, A., *Piezoelectric flow injection analysis biosensor for the detection of Salmonella typhimurium.* Food Sci, 2002. **67**: p. 314-320.

21. Tims, T.B., Lim, D. V., *Rapid detection of Bacillus anthracis spores directly from powders with an evanescent wave fiber-optic biosensor.* Journal of Microbiol Methods., 2004. **59**(1): p. 127-130.

22. Taitt, C.R., Shubin, Y. S., Angel, R., Ligler, F. S., *Detection of Salmonella enterica serovar typhimurium by using a rapid, array-based immunosensor.* Appl Environ Microbiol., 2004. **70**(1): p. 152-158.

23. Olsen, E.V., Pathirana, S. T., Samoylov, A. M., Barbaree, J. M., Chin. B. A., Neely, W. C., Vodyanoy, V., *Specific and selective biosensor for Salmonella and its detection in the environment.* Journal of Microbiol Methods., 2003. **53**(2): p. 273-285.

24. Grimes, C.A., Kouzoudis, D., *Remote Query Measurement of Pressure, Fluid-Flow Velocity, and Humidity Using Magnetoelastic Thick-Film Sensors.* Sensors and Actuators, 2000. **84**: p. 205-212.

25. Kouzoudis, D., Grimes, C. A., *The Frequency Response of Magnetoelastic Sensors to Stress and Atmospheric Pressure. Smart Materials and Structures.* Smart Materials and Structures, 2000. **8**: p. 885-889.

26. Jain, M.K., Schmidt, S., Ong, K. G., Mungle, C., Grimes, C. A., *Magnetoacoustic Remote Query Temperature and Humidity Sensors.* Smart Materials and Structures, 2000. **9**: p. 502-510.

27. Landau, L.D., Lifshitz, E. M., *Theory of elasticity.* 3 ed. 1986: Pergamon Press.

28. http://www.gmotesting.com/elisa_app.shtml, *Applicability of ELISA Testing.*

29. Jean C. Buzby., T.R., C. T. Jordan Lin., James M. MacDonald., *Bacterial Foodborne Disease: Medical Costs and Productivity Losses*, in *Agriculture Economic Report,*. 1996. p. (AER 741): p iv-2).

30. Paul S. Mead., L.S., Vance D. Dietz., Linda F. McCaig., Joseph S.Breese., Craig Shapiro., Patricia M.Griffin and Robert V Tauxe., *Food-Related Inllness and Death in the United States.* Emerging Infectious Diseases, 1999. **5**(5): p. 607-625.

31. Potter, M.E., Gonzalez-Ayala, S., Silarug, N., *Epidemiology of foodborne diseases. In: Doyle, M. P., Beuchat, L. R., Montville, T. J.* Food Microbiology: Fundamentals and Frontiers. ASM Press, Washington, DC., 1997.

32. Beran, G.W., Shoeman, H. P., Anderson, K. F., *Food Safety: an overview of problems.* Dairy Food Environ. Sanit., 1991. **11**: p. 189-194.

33. Swaminathan, B., Feng, P., *Rapid detection of food-borne pathogenic bacteria.* Annu. Rev. Microbiol, 1994. **48**: p. 401-426.

34. Ackers, M.L., Schoenfeld, S., Markman, J., Smith, M. G., Nicholson, M. A., DeWitt, W., et al., *An outbreak of Yersinia enterocolitica O:8 infections associated with pasteurized milk.* J Infect Dis, 2000. **181**: p. 1834-7.

35. Ryan, C.A., Nickels, M. K., Hargrett-Bean, N. T., Potter, M. E., Endo, T., Mayer, L., et al., *Massive outbreak of antimicrobial-resistant Salmonellosis traced to pasteurized milk.* JAMA, 1987. **258**: p. 3269-74.

36. Dalton, C.B., Austin, C. C., Sobel, J., Hayes, P. S., Bibb, W. F., Graves, L. M., et al., *An outbreak of gastroenteritis and fever due to Listeria monocytogenes in milk.* N Engl J Med, 1997. **336**: p. 100-5.

37. *Outbreaks of Salmonella Infections Associated with Eating Roma Tomatoes --- United States and Canada, 2004.* MMWR, 2005. **54**(13): p. 325-328.

38. Jones, F., Rives D, Carey., *Salmonella contamination in commercial eggs and an egg production facility.* J. Poult Sci, 1995. **74**(753-7).

39. Carl M. Schroeder., A.L.N., Wayne D. Schlosser, Allan T. Hogue, Frederick J.Angulo, Jonathon S. Rose, Eric D. Ebel, W. Terry Disney, Kristin G. Holt, and David P. Goldman., *Estimate of Illnesses from Salmonella Enteritidis in Eggs, United States, 2000.* Emerging Infectious Diseases, 2005. **11**: p. 113-115.

40. *Outbreak of Salmonella Serotype Muenchen Infections Associated with Unpasteurized Orange Juice -- United States and Canada, June 1999.* MMWR, 1999. **48**(27): p. 582-585.

41. *Centers for Disease Control and Prevention. A common-source outbreak of Salmonella newport-Louisiana.* MMWR Morb Mortal Wkly Rep, 1975. **24**: p. 413-4.

42. *Centers for Disease Control and Prevention. Salmonella gastroenteritis associated with milk-Arizona.* MMWR Morb Mortal Wkly Rep, 1979. **28**: p. 117-20.

43. *Centers for Disease Control and Prevention. Salmonellosis from inadequately pasteurized milk-Kentucky.* MMWR Morb Mortal Wkly Rep, 1984. **33**: p. 505-6.

44. Layton, M., Calliste, S., Gomez, T., Patton, C., Brooks, S., *A mixed foodborne outbreak with Salmonella Heidelberg and Campylobacter jejuni in a nursing home.* Infect Control Hosp Epidemiol, 1997. **18**: p. 115-21.

45.   Mahony, M., Barnes, H., Stanwell-Smith R., Dickens, T., Jephcott, A., *An outbreak of Salmonella Heidelberg infection associated with a long incubation period.* J Public Health Med, 1990. **12**: p. 19-21.

46.   Snoeyenbos, G.H., Smyser, C. F., Van Roekel, H., *Salmonella infection of the ovary and peritoneum of chickens.* Avian Dis, 1969. **13**: p. 668-70.

47.   Bokanyi, R., Stephens, J., Foster, D., *Isolation and characterization of Salmonella from broiler carcasses or parts.* Poult Sci, 1990. **69**: p. 592-8.

48.   *Multistate Outbreak of Salmonella Typhimurium Infections Associated with Eating Ground Beef - United States, 2004.* MMWR, 2006. **55**(7): p. 180-182.

49.   Fontaine, R., Cohen, M., Martin, W., Vernon, T., *Epidemic Salmonellosis from cheddar cheese: surveillance and prevention.* Am J Epidemiol, 1980. **111**: p. 247-53.

50.   Cernosek, R.W., Chin, B. A., Barbaree, J. M., Vodyanoy, V., Conner, D. E., Hsieh, Y-H. P., *A Rapid Biosensing System for Detecting Food-Borne Pathogens.* Proc. Sensors Expo, 2001.

51.   Tietjen, M., Fung, D. Y. C., *Salmonella and food safety.* Crit. Rev. Microb, 1995. **21**: p. 53-83.

52.   Hobson, N.S., Tothill, I., Turner, A. P. F., *Microbial Detection.* Biosensors Bioelectron, 1996. **11**(5): p. 455-477.

53.   Helrich, K., *Official Methods of Analysis of the Association of Official Analytical Chemists, Microbiological Methods, 2, 15 ed.* 1990: Arlington, VA. p. 425-497 (Chapter17).

54. Kasper, C.W., tartera, C., *Methods for detecting microbial pathogens in food and water.* Methods Microbiol, 1990. **22**: p. 497-530.

55. Meng, J.H., Zhao, S. H., Doyle, M. P., Kresovich, S., *Polymerase chain-reaction for detecting E. coli 0157:H7.* Intl. J. Food Microbiol, 1996. **32**(1-2): p. 103-113.

56. Sperveslage, J., Stackebrandt, E., Lembke, F. W., Koch, C., *Detection of bacterial contamination, including bacillus spores, in dry growth media and in milk by identification of their 16SRDNA by polymerase chian-reaction.* J. Microbiol. Methods, 1996. **26**(3): p. 219-224.

57. Cordek, J., Wang, X. W., Tan, W. H., *Direct immobilization of glutamate dehydrogenase on opticalfiber probes for ultrasensitive glutamate detection.* Anal. Chem., 1999. **71**(8): p. 1529-1533.

58. Opitz, N., Graf, H. J., Lubbers, D. W., *Oxygen Sensor for the Temperature-Range 300-K to 500-KBasedon Fluorescence Quenching of Indicator-Treated Silicone-Rubber Membranes.* Sens. Actuators, 1988. **13**(2): p. 159-163.

59. Peterson, J.I., Fitzgerald, R. V., Buckhold, D. K., *Fiber-Optic Probe for Invivo Measurement of Oxygen Partial-Pressure.* Anal. Chem., 1984. **56**(1): p. 62-67.

60. Woltheis, O.S., et al., *Fluorimetric Analysis. A Fast Responding Fluorescence Sensor for Oxygen.* Mikrochim. Acta,, 1984. **1**(1-2): p. 153-158.

61. Potyrailo, R.A., Hiefije, G. M., *Oxygen detection by fluorescence quenching of tetraphenylporphyrin immobilized in the original cladding of an opticalfiber.* Anal. Chim. Acta, 1998. **370**(1): p. 1-8.

62.   Xu, W.Y., et al., *Oxygen sensors based on luminescence quenching of metal complexes. Osmium complexes suitable for laser diode excitation.* Anal. Chem., 1996. **68**(15): p. 2605-2609.

63.   Liu, Y.M., et al., *Evaluation of Some Immobilized Room-Temperature Phosphorescent Metal-Chelates as Sensing Materials for Oxygen.* Anal. Chem., 1994. **66**(6): p. 836-840.

64.   Mills, A., Thomas, M. D., *Effect ofplasticizer viscosity on the sensitivity of an [R U(bpy) (3) (2 +) (Ph4B-) (2)1-based optical oxygen sensor.* Analyst, 1998. **123**(5): p. 1135-1140.

65.   Muller, C., et al., *Optical chemo- and biosensors for use in clinical applications.* Sens. Actuators B Chem., 1997. **40**(1): p. 71-77.

66.   Kuswandi, B., *Simple opticalfibre biosensor based on immobilised enzyme for monitoring of trace heavy metal ions.* Anal. Bioanal. Chem., 2003. **376**(7): p. 1104-1110.

67.   Andreou, V.G., Clonis, Y. D., *Novelfiber-optic biosensor based on immobilized glutathione 5-transferase and sol-gel entrapped bromcresol green for the determination of atrazine.* Anal. Chim. Acta, 2002. **460**(2): p. 151-161.

68.   Brecht, A., et al., *A Direct Optical Immunosensor for Atrazine Detection.* Anal. Chim. Acta, 1995. **311**(3): p. 289-299.

69.   Anderson, G.P., Nerurkar, N. L., *Improvedfluoroimmunoassays using the dye Alexa Fluor 647 with the RAPTOR, afiber optic biosensor.* J. Immunol. Methods, 2002. **271**(1-2): p. 17-24.

70. Nath, N., et al., *A rapid reusable fiber optic biosensor for detecting cocaine metabolites in urine.* J. Anal. Toxicol., 1999. **23**(6): p. 460-467.

71. Toppozada, A.R., et al., *Evaluation of a fiber optic immunosensor for quantitating cocaine in coca leaf extracts.* Biosens. Bioelectron, 1997. **12**(2): p. 113-124.

72. Bakaltcheva, I.B., et al., *Multi-analyte explosive detection using afiber optic biosensor.* Anal. Chim. Acta, 1999. **399**(1-2): p. 13-20.

73. Brecht, A., et al., *Optical immunoprobe development for multiresidue monitoring in water.* Anal. Chim. Acta, 1998. **362**(1): p. 69-79.

74. Mouvet, C., et al., *Determination ofsimazine in water samples by waveguide surface plasmon resonance.* Anal. Chim. Acta, 1997. **338**(1-2): p. 109-117.

75. Kwon, H.J., Balcer, H. I., Kang, K. A., *Sensing performance ofprotein C immuno-biosensor for biological samples and sensor minimization.* Comp. Biochem. Physiol. A. Mol. Integr. Physiol., 2002. **132**(1): p. 231-238.

76. Wang, X.F., Krull, U. J., *Tethered thiazole orange intercalating dye for development offibre-optic nucleic acid biosensors.* Anal. Chim. Acta, 2002. **470**(1): p. 57-70.

77. Almadidy, A., et al., *Direct selective detection of genomic DNA from colform using afiber optic biosensor.* Anal. Chim. Acta, 2002. **461**(1): p. 37-47.

78. Almadidy, A., et al., *A fibre-optic biosensor for detection of microbial contamination.* Can. J. Chem., 2003. **81**(5): p. 339-349.

79. Ignatov, S.G., Ferguson, J. A., Walt, D. R., *A fiber-optic lactate sensor based on bacterial cytoplasmic membranes.* Biosens. Bioelectron., 2001. **16**(1-2): p. 109-113.

80.   Corbisier, P., et al., *Whole cell- and protein-based biosensors for the detection of bioavailable heavy metals in environmental samples.* Anal. Chim. Acta, 1999. **387**(3): p. 235-244.

81.   Mulchandani, A., Mulchandani, P., Kaneva, I., Chen. W., *Biosensor for direct determination of organophosphate nerve agents using recombinant Escherichia coli with surface- expressed organophosphorus hydrolase. 2. Fiber optic microbial biosensor.* Anal. Chem., 1998. **70**(23): p. 5042-5046.

82.   Pancrazio, J.J., Whelan, J. P., Borkholder, D. A., Ma, W., Stenger, D. A., *Development and Application of Cell-Based Biosensors.* Annals of Biomedical Engineering, 1999. **27**: p. 697-711.

83.   Gray, S.A., et al., *Design and demonstration of an automated cell-based biosensor.* Biosensors and Bioelectronics, 2001. **16**: p. 534-542.

84.   Liu, Z.H., Wen, M. L., Yao, Y., Shi, N. H., Liu, S. Q., Qiao, M., *Bacteria based sensor for monitoring glycerol.* Collection of Czechoslovak Chemical Communications, 1999. **64**: p. 1412-1418.

85.   Ziegler, C., *Cell-based biosensors.* Fresenius J Anal Chem, 2000. **366**: p. 552–559.

86.   Simonian, A.L., Rainina, E. I., Wild, J. R. in: A. Mulchandani, K. R. Rogers (Eds.), *Enzyme and Microbial Biosensors: Techniques and Protocols*. 1998, Totowa, NJ: Humana Press.

87.   Mulchandani, A., Rogers, K. R., *Enzyme and Micriobial Biosensors: Techniques and Protocols*. 1998, Totowa, NJ: Humana Press.

88.   Tran, M.C., *Biosensors*. 1993, Paris: Chapman hall and Masson.

89. Koncki, R., Hulanicki, A., Glab, S., *Biochemical Modifications of Membrane Ion Selective Electrodes.* Trends Anal. Chem., 1997. **16**: p. 528.

90. Mulchandani, A., Chauhan, S., Kaneva, I., Mulchandani, P., Chen, W., *A potentiometric microbial biosensor for direct determination of organophosphate nerve agents.* Electroanalysis, 1998. **10**: p. 733-737.

91. Gaberlein, S., Spener, F., Zaborosch, C., *Microbial and cytoplasmic membrane-based potentiometric biosensors for direct determination of organophosphorus insecticides.* Appl. Microbiol. Biotechnol, 2000. **54**(5): p. 652-8.

92. Shi, R.B., Stein, K., Schwedt, G., *Determination of Mercury(II) Traces in Drinking Water by Inhibition of an Urease Reactor in a Flow Injection Analysis (FIA) System.* Fresenius J. Anal. Chem, 1997. **357**: p. 752-755.

93. Verma, N., Singh, M., *A disposable microbial based biosensor for quality control in milk.* Biosens. Bioelectron., 2003. **18**(10): p. 1219-1224.

94. Dill, K., Song, J. H., Blomdahl, J. A., Olson, J. D., *Rapid, sensitive and specific detection of whole cells and spores using the lightaddressable potentiometric sensor.* J Biochem Biophys Methods, 1997. **34**: p. 161-6.

95. Dill, K., Stanker, L. H., Young, C. R., *Detection of salmonella in poultry using a silicon chip-based biosensor.* J Biochem Biophys Methods, 1999. **41**: p. 61-7.

96. Palchetti, I., Cagnini, A., Del Carlo, M., Coppi, C., Mascini, M. and Turner, A. P. F., *Determination of Anticholinesterase Pesticides in Real Samples Using a Disposable Biosensor.* Anal. Chim. Acta, 1997. **337**: p. 315-321.

97. Marrazza, G., Chianella, I. and Mascini, M., *Disposable DNA Electrochemical Biosensors for Environmental Monitoring.* Anal. Chim. Acta.

98.   Ivnitski, D., Wilkins, E., Tien, H. T., Ottova, A., *Electrochemical biosensor based on supported planar lipid bilayers for fast detection of pathogenic bacteria.* Elecom, 2000. **2**: p. 457–60.

99.   Rishpon, J., Ivnitski, D., *An amperometric enzyme-channeling immunosensor.* Biosens Bioelectron, 1997. **12**(2): p. 195-204.

100.   Pérez, F.G., Mascini, M., *Immunomagnetic separation with mediated flow injection analysis amperometric detection of viable Escherichia coli 0157.* Anal Chem, 1998. **70**: p. 2380-6.

101.   Brewster, J.D., Mazenko, R. S., *Filtration capture and immunoelectrochemical detection for rapid assay of Escherichia coli 0157:H7.* J Immunol Methods, 1998. **211**: p. 1-8.

102.   Gehring, A.G., Crawford, C. G., Mazenko, R. S., Van Houten, L. J., Brewster, J. D., *Enzyme-linked immunomagnetic electrochemical detection of Salmonella typhimurium.* J Immunol Methods, 1996. **195**: p. 15-25.

103.   Soldatkin, A.P., Korpan, Y. I., Zhylyak; G. A., Martelet, C. and El'Skaya, A. V., *Selective Determination of Heavy Metal Ions with Sensors Coupled to Immobilised Enzymes" Biosensors for Direct Monitoring of Environmental Pollutants in Field*, ed. D.P. Nikolelis, Krull, U. J., Wang, J. and Mascini, M. 1998, Boston: Kluwer Publishers. 281-288.

104.   Zhylyak, G.A., Dzyadevich, S. V., Korpan, Y. I., Soldatkin, A.P. and El'Skaya, A. V., *Application of Urease Conductometric Biosensor for Heavy Metal Ion Determination.* Sensors Actuators B, 1995. **24**: p. 145-148.

105.   Bhatia, R., Dilleen, J. W., Atkinson, A. L., Rawson, D. M., *Combined physico-chemical and biological sensing in environmental monitoring*. Biosens. Bioelectron, 2003. **18**(5-6): p. 667-674.

106.   Caliendo, V.I.A., Fedososv, C., Koelyanskii, V. I., Verardi, I. M. and Verona, E. *Characterization of Pd and Pd:Ni films for SAW hydrogen sensors*. in *190th Meeting Acoustic Wave Based Sensor Symp*. 1996. SanAntonio, TX.

107.   Caliendo, C.D.A., A.; Varadi, P.; Verona, E. *Surface acoustic wave H2 sensor on silicon substrate*. in *Ultrasonics Symposium, Proceedings. IEEE 1988*. 1988. Chicago, IL: New York: IEEE.

108.   Ippolito, S.J., et al., *Layered WO3/ZnO/36[deg] LiTaO3 SAW gas sensor sensitive towards ethanol vapour and humidity*. Sensors and Actuators B: Chemical, 2006. **In Press, Corrected Proof**.

109.   Penza, M., Anisimkin, V. I., *Surface acoustic wave humidity sensor using polyvinyl-alcohol film*. Sensors and Actuators A: Physical, 1999. **76**(1-3): p. 162-166.

110.   Shen, C.-Y., Huang, Chun-Pu., Huang, Wang-Tsung., *Gas-detecting properties of surface acoustic wave ammonia sensors*. Sensors and Actuators B: Chemical, 2004. **101**(1-2): p. 1-7.

111.   Korsah, K., C.L. Ma, and B. Dress, *Harmonic frequency analysis of SAW resonator chemical sensors: application to the detection of carbon dioxide and humidity*. Sensors and Actuators B: Chemical, 1998. **50**(2): p. 110-116.

112. Chang, H.-W. and J.-S. Shih, *Surface acoustic wave immunosensors based on immobilized C60-proteins.* Sensors and Actuators B: Chemical, 2006. **In Press, Corrected Proof**.

113. Kostial, P., *Surface acoustic wave control of the ion concentration in water.* Applied Acoustics, 1994. **41**(2): p. 187-193.

114. Cai, Q., et al., *Surface Acoustic Wave (SAW)-Impedance Sensor for Kinetic Assay of Trypsin.* Microchemical Journal, 1997. **55**(3): p. 367-374.

115. Ballantine, D.S., White, R.M., Martin, S.J., Ricco, A.J., Frye, G.C., Zellers, E.T., and Wohltjen, H. : . *Acoustic Wave Sensors: Theory, Design, and Physico-Chemical Applications*. 1997, San Diego: Academic Press.

116. Welsch, W.K., C. Von Schickfus, M. and Hunklinger, S., *Development of a surface acoustic wave immunosensor.* Anal. Chem, 1996. **68**: p. 2000-2004.

117. Bender, F.C., R. W. and Josse, F., *Lovewave biosensors using cross-linked polymer waveguides on LiTaO3 substrates.* Electronics Letters, 2000. **36**(19).

118. Fabrice Martin, M.I.N., Glen McHale, Kathryn A. Melzak, Electra Gizeli, *Pulse mode shear horizontal-surface acoustic wave (SH-SAW) system for liquid based sensing applications.* Biosensors and Bioelectronics, 2004. **19**: p. 627-632.

119. Bhide, T.M., Yamarthy, C. S., Ellis, C. D. and Cernosek, R. W., *Shear Horizontal Surface Acoustic Wave Sensor Platform Development For Chemical And Biological Detection*. 2001, Auburn University: Auburn.

120. Lee, D.L., *Analysis of energy trapping effects for SH-type waves on rotated Y-cut quartz.* IEEE Trans. Sonics Ultrason, 1981. **28**: p. 330-341.

121.   Ricco, A.J., *SAW Chemical Sensors (Invited).* The Electrochemical Society Interface, 1994. **3**(38).

122.   Ricco, A.J. and S.J. Martin, *Thin metal film characterization and chemical sensors: monitoring electronic conductivity, mass loading and mechanical properties with surface acoustic wave devices.* Thin Solid Films, 1991. **206**(1-2): p. 94-101.

123.   Bandey, H.L., et al., *Blood rheological characterization using the thickness-shear mode resonator.* Biosensors and Bioelectronics, 2004. **19**(12): p. 1657-1665.

124.   Helle, H., et al., *Monitoring of biofilm growth with thickness-shear mode quartz resonators in different flow and nutrition conditions.* Sensors and Actuators B: Chemical, 2000. **71**(1-2): p. 47-54.

125.   Holloway, A.F., et al., *Impedance analysis of the thickness shear mode resonator for organic vapour sensing.* Sensors and Actuators B: Chemical, 2004. **99**(2-3): p. 355-360.

126.   Martin, S.J., G.C. Frye, and K.O. Wessendorf, *Sensing liquid properties with thickness-shear mode resonators.* Sensors and Actuators A: Physical, 1994. **44**(3): p. 209-218.

127.   Zhang, C., S. Schranz, and P. Hauptmann, *Surface microstructures of TSM resonators and liquid properties measurement.* Sensors and Actuators B: Chemical, 2000. **65**(1-3): p. 296-298.

128.   Adanyi, N., Varadi, Maria., Kim, Namsoo., Szendro, Istvan., *Development of new immunosensors for determination of contaminants in food.* Current Applied

Physics Engineering Aspects of Nanomaterials and Technologies, 2006. **6**(2): p. 279-286.

129. Su, X.-L. and Y. Li, *A self-assembled monolayer-based piezoelectric immunosensor for rapid detection of Escherichia coli O157:H7.* Biosensors and Bioelectronics, 2004. **19**(6): p. 563-574.

130. Caton, P.F., *Microfiltration and flexural plate wave devices.* 2001, University of California: Berkeley.

131. Lee, C.S., No, K., Wee, D. M., Lee, J. H. and Choi, C. A., *A novel angular rate sensor employing flexural plate wave.* IEEE Ultrason. Symp, 1999: p. 493-496.

132. Nguyen, N.T., White, R. M., *Acoustic streaming in micromachined flexural plate wave devices: numerical simulation and experimental verification.* IEEE Trans. Ultrason., Ferroelect., Freq. Contr., 2000: p. 1463-1471.

133. Butler, M.A., Hill, M. K. Spates, J. J. and Martin, S. J., *Pressure sensing with a flexural plate wave resonator.* J. Appl. Phys, 1999. **85**(3): p. 1998-2000.

134. Costello, B.J., Martin, B. A. and White, R. M., *Ultrasonic plate waves for biochemical measurements.* IEEE Ultrason. Symp, 1989: p. 977-981.

135. Black, J.P., Chen, B., Quinn, R., Madou, M. and White, R. M., *Comparison of the performances of flexural plate wave and surface acoustic wave devices as the detector in gas chromatography.* IEEE Ultrason. Symp., 2000: p. 435-440.

136. White, R.M., Wenzel, S. W., *Fuild loading of a Lamb-wave sensor.* Appl. Phys. Lett., 1988. **52**(20): p. 1653-1655.

137. Wenzel, S.W., White, R. M., *Analytical comparison of the sensitivities of bulk-wave surfacewave and flexural plate-wave ultrasonic gravimetric sensors.* Appl. Phys. Lett., 1989. **54**: p. 1976.

138. Aizawa, M., *Immunosensors for Chemical Analysis.* Advances in Clinical Chemistry, 1994. **31**: p. 247-275.

139. Lukosz, W., Clerc, D., Nellen, P.M., Stamm, C., Weiss, P., *Output grating couplers on planar optical wave-guides as direct immunosensors.* Biosensors and Bioelectronics, 1991. **6**: p. 227-232.

140. Sloper, A.N., Deacon, J.K., Flannagan, M.T., *A planar indium phosphate monomode wave-guide evanescent field immunosensor.* Sensors Actuators B, 1990. **1**: p. 285-297.

141. Frat Amico, P.M., Strobaugh, T. P., Medina, M. B., Gehring, A. G., *Detection of E. coli O157:H7 using a surface-plasmon resonance biosensor.* Biotechnol. Techn., 1998. **12**(7): p. 571-576.

142. Bringham-Burke, M., Edwards, J.R., O'Shannessy, D.J., *Detection of receptor ligand interactions using surface plasmon resonance:model studies employing the HIV-1 GP120:CD4 interactions.* J. Anal. Biochem., 1992. **205**: p. 125-131.

143. Medina, M.B., Houten, L. V., Cooke, P. H., Tu, S. I., *Real-time analysis of antibody binding interactions with immobilized E. coli 0157:H7 cells using the BIAcore.* Biotechnol. Techn., 1997. **11**(3): p. 173-176.

144. Pollard-Knight, D.V., Hawkins, E., Yeung, D., Pashby, D.P., Simpson, M., McDougall, A., Buckle, P., Charles, S.A., *Immunoassays and nucleic-acid*

detection with a biosensor based on surface plasmon resonance. Ann. Biol. Clin, 1990. **48**: p. 642-646.

145. Karlsson, R., Michaelsson, A., Mattsson, L., *Kinetic-analysis of monoclonal antibody-antigen interactions with a new biosensor based analytical system.* J. Immunol. Methods, 1991. **145**: p. 229-240.

146. Swenson, F.J., *Development and evaluation of optical sensors for the detection of bacteria.* Sensors Actuators B, 1993. **11**: p. 315-321.

147. Nakamura, N., Shigematsu, A., Matsunaga, T., *Electrochemical detection of viable bacteria in urine and antibiotic selection.* Biosensors Bioelectron., 1991. **6**(7): p. 575-580.

148. Watts, H.J., Lowe, C.R., Pollard-Knight, D.V., *Optical biosensor for monitoring microbial cells.* Anal. Chem., 1994. **66**: p. 2465-2470.

149. Schneider, B.H., Edwards, J. G., Hartman, N. F., *Hartman interferometer: versatile integrated optic sensor for label-free, real-time quantification of nucleic acids, proteins, and pathogens.* Clin. Chem., 1997. **43**(9): p. 1757–1763.

150. Paddle, B.M., *Biosensors for Chemical and Biological Agents in Defence Interest.* Biosensors and Bioelectronics, 1996. **11**(11): p. 1079-1113.

151. BIACORE, A., *BIACORE Technology Handbook.* 1998.

152. Rogers, K.R., Cao, C. J., Valdes, J. J., Eldefrawi, A. T. and Eldefrawi, M. E., *Acetylcholinesterase Fiber-Optic Biosensor for Detection of Anticholinesterases.* Fundam. Applied Toxicol, 1991. **16**: p. 810-820.

153. Wikipedia, *http://en.wikipedia.org/wiki/Magnetostriction*. Retrieved July4, 2006.

154.   Cai, Q.Y., Jain, M. K., Grimes, C. A., *A wireless, remote query ammonia sensor.* Sensors and Actuators B: Chemical, 2001. **77**: p. 614-619.

155.   Cai, Q.Y., Arthur Cammers-Goodwin., Grimes, C. A., *A Wireless, Remote Query Magnetoelastic CO2 Sensor.* Journal of Environmental Monitoring, 2000. **2**: p. 556-560.

156.   Cai, Q.Y., Grimes, C. A., *A salt independent pH sensor.* Sensors and Actuators B: Chemical, 2001. **79**: p. 144-149.

157.   Jain, M.K., Schmidt, S., Mungle, C., Loiselle, K., Grimes, C. A., *Measurement of temperature and liquid viscosity using magneto-acoustic/magneto-optical sensors.* IEEE. Trans. on Magnetics, 2001. **37**(4): p. 2767-2769.

158.   Jain, M.K., Grimes, C. A., *A wireless magnetoelastic micro-sensor array for simultaneous measurement of temperature and pressure.* IEEE Trans. Magnetics, 2001. **37**(4): p. 2022-2024.

159.   Jain, M.K., Schmidt, S., Grimes, C. A., *Magneto-acoustic sensors for measurement of liquid temperature, viscosity, and density.* Applied Acoustics, 2001. **62**: p. 1001-1011.

160.   Schmidt, S., Grimes, C. A., *Elastic modulus measurement of thin films coated on magnetoelastic ribbons.* IEEE. Trans. on Magnetics, 2001. **37**(4): p. 2731-2733.

161.   http://metglas.com/products/page5_1_2_7.htm, *Magnetic Alloy 2826MB; Technical Bulletin.* September, 2006.

162.   Pathirana, S.T., Barbaree, J., Chin, B. A., Hartell, M. G., Neely, W. C., Vodyanoy, V., *Rapid and sensitive biosensor for Salmonella.* Biosens. Bioelectron, 2000. **15**: p. 135-141.

163.   Segel, I.H., Segel, A. H., *Biochemical Calculations*. 1976, New York: Wiley.

164.   Petrenko, V.A., Vodyanoy, V. J., *Phage display for detection of biological threat agents.* J. Microbiol. Methods, 2003. **53**: p. 253.

165.   Ye, L., Letcher, S. V., Rand, A. G., *Piezoelectric biosensor for detection of Salmonella typhimurium.* J. Food Sci, 1997. **62**: p. 1067-1086.

166.   Pyun, J.C., Beutel, H., Meyer, J. U., Ruf, H. H., *Development of a biosensor for E. coli based on a flexural plate wave (FPW) transducer.* Biosens. Bioelectron, 1998. **13**: p. 839-845.

167.   Park, I.S., Kim, N., *Thiolated Salmonella antibody immobilization onto the gold surface of piezoelectric quartz crystal.* Biosens. Bioelectron, 1998. **13**: p. 1091-1097.

168.   R. H. Van der Linden, L.G.F., B. de Geus, M. M. Harmsen, R. C. Ruuls, W. Stok, L. de Ron, S. Wilson, P. Davis, C. T. Verrips, *Comparison of physical chemical properties llamma VHH antibody fragments and mouse monoclonal antibodies.* Biochim. Biophys. Acta1431, 1999: p. 37-46.

169.   A. Usami, A.O., S. Takahama, T. Fujii, *The effect of pH, hydrogen peroxide and temparature on the stability of human monoclonal antibody.* J. Pharm. Biomed. Anal, 1996. **14**: p. 1133-40.

170.   C. Steinhauer, C.W., A. C. Hager, C. A. Borrebaeck, *Single framework recombinant antibody fragments designed for protein chip applications.* Biotechniques Suppl, 2002: p. 38-45.

171.   Y. Reiter, U.B., K. O. Webber, S. H. Jung, B. Lee, I. Pastan, *Engineering interchain disulfide bonds into conserved framework regions of Fv fragments:*

improved biochemical characteristics of recombinant immunotoxins containing disulfide-stabilized Fv. Protein Eng, 1994. **7**: p. 697-704.

172. K. Kramer, M.F., A. Skerra, B. Hock, *A generic strategy for subcloning antibody variable regions from the scFv phage display vector pCANTAB 5 E into pASK85 permits the economical production of F(ab) fragments and leads to improved recombinant immunoglobulin stability.* Biosensors Bioelectron, 2002. **17**: p. 305-13.

173. H. Dooley, S.D.G., W. J. Harris, A. J. Porter, *Stabilization of antibody fragments in adverse environments.* Biotechnol. Appl. Biochem, 1998. **28**: p. 77-83.

174. Segal, I.H., *Biochemical Calculations.* 1976, New York: John Wiley & Sons.

175. Connie M. Chung, J.D.C., Lawreen H. Connors,yz Olga Gursky, Amareth Lim, Andrew B. Dykstra, Juris Liepnieks, Merrill D. Benson, Catherine E. Costello, Martha Skinner,and Mary T. Walsh, *Thermodynamic Stability of a kI Immunoglobulin Light Chain: Relevance to Multiple Myeloma.* Biophysical, 2005. **88**: p. 4232-4242.

176. Rowe, S.E., Tanford, C, *Equilibrium and Kinetics of the Denaturation of a Homogeneous Human Immunoglobulin Light Chain.* Biochemistry, 1973. **12**(24): p. 4822.

177. Serban F. Peteu, D.E., R. Mark Worden, *A Clark-type oxidase enzyme-based amperometric microbiosensor for sensing glucose, galactose, or choline.* Biosensors & Bioelectronics, 1996. **11**(10): p. 1059-1071.

178. Sakura, S.B., R. P., *Amperometric processes with glucose oxidase embedded in the electrode.* Bioelectrochem. Bioenergetics,, 1992. **343**: p. 387-400.

179. Cass, A.E.G., Davis, G., Francis, G. D., Hill, H. A. O., Aston, W. J., Higgins, I. J., Plotkin, E. V., Scott, L. D. L. & Turner, A. P. F., *Ferrocene-mediated enzyme electrode for amperometric determination of glucose.* Anal. Chem, 1994. **56**: p. 667-671.